Sandia National Laboratories
Operated for the U.S. Department of Energy by
Sandia Corporation
Albuquerque, New Mexico 87185-1147

date: November 13, 1997

to: Warren Cox, MS-1147 (6132)

Sue Collins

from: Sue Collins, MS-1147 (6133)

subject: SWHC Report

The purpose of this memorandum is to:

1. Transmit the final report on the Site-Wide Hydrogeologic Characterization Project (SWHC) flow model as well as a short letter report on effects from the faults, and

2. Request your management review (by the first week of January) since they will be attachments to the "final" SWHC report to the regulators.

Just a couple of notes:

1. "Final" is in quotations since we still have not received an official Notice of Deficiency or other regulatory driver for this deliverable.

2. You should expect to receive a copy of the "final" SWHC report shortly after your review of this report.

Copy to:
MS 1147 Sue Collins (6133)
Greg Ruskauff (Intera, Inc.)
MS 1147 ER/Records Center 1330/QUA REP

Copy to w/o attachment:
MS 1147 Fran Nimick (6133)
John McCord (Intera, Inc)

Sandia National Laboratories

EVALUATION OF GROUNDWATER FLOW AND HYDROGEOLOGIC CONCEPTUAL MODEL KIRTLAND AIR FORCE BASE ALBUQUERQUE, NEW MEXICO

NOVEMBER 1997

Environmental Restoration Project

United States Department of Energy
Albuquerque Operations Office

TABLE OF CONTENTS

SECTION **PAGE**

TABLE OF CONTENTS continued

SECTION **PAGE**

LIST OF FIGURES

FIGURE **PAGE**

LIST OF FIGURES continued

LIST OF TABLES

LIST OF APPENDICES

Appendix A: Hydrographs from Calibrated Model

LIST OF APPENDICES continued

LIST OF PLATES

This page intentionally left blank.

EXECUTIVE SUMMARY

A deterministic, numerical groundwater flow model of the Kirtland Air Force Base (KAFB) area was used to explore and test quantitatively the conceptual model of the hydrogeology developed by the Sandia National Laboratories (SNL) Site-Wide Hydrogeologic Characterization Project (SWHC). Information from the U.S. Geological Survey (USGS), the New Mexico Bureau of Mines and Mineral Resources, other public sources, and the SNL SWHC Project was used to develop the conceptual model of the hydrogeology in the vicinity of the site. The SNL/KAFB model builds upon the work presented in the SWHC 1993, 1994, and 1995 annual reports (SNL/NM 1994, 1995, 1996) and is consistent with the U.S. Environmental Protection Agency modeling recommendations noted in their review of the 1994 SWHC annual report. The conceptual model separated the sediments into alluvial fan and ancestral Rio Grande fluvial deposits, arranged in complex intergradational architectures. Pumping test results, water level measurements, and geological mapping from the SWHC were used to determine the distribution of facies and their hydraulic properties in the model.

The computer code MODFLOW, written by the USGS, was used to simulate the three-dimensional flow of groundwater beneath KAFB. MODFLOW is the most widely used groundwater flow model in the world and has been successfully used in analyses performed in the area by the U.S. Geological Survey and others to construct and calibrate both steady-state and transient models. The Albuquerque Basin Model (ABM), constructed by the USGS (Kernodle et al., 1995), was used as the starting point for the KAFB model. Groundwater levels have been declining since the 1960's in the KAFB area, and it was necessary to consider large-scale trends in water levels, which the ABM does. The SNL/KAFB portion of the basin model was removed by using a modified telescopic mesh refinement approach in which the flows across the boundaries and the aquifer properties were used to create a smaller, more expeditious model. The submodel grid remained the same as the ABM grid.

The fit of the USGS model to the SNL/KAFB potentiometric data was fair to poor and did not adequately replicate the major features observed in the area. Incorporating geologic data collected during the SWHC Project largely resolved these discrepancies. The model was calibrated to conditions from January 1980 to March 1995. The quantitative calibration goals that were established for this analysis were met.

The model of the SNL/KAFB domain was substantially modified over the initial configuration constructed by the USGS. Modifications made to the USGS ABM included the addition of a long, north-south strip of axial channel deposits, extending much farther than in the ABM. In addition, SWHC Project estimates of hydraulic conductivity of alluvial fan material along the mountains were much lower than in the ABM, as was recharge from infiltration along Tijeras Arroyo. In the ABM, recharge along Tijeras Arroyo is over an order of magnitude higher than that estimated by the SWHC Project, and two models were calibrated to bracket the conceptual uncertainty caused by this difference. In the first, the recharge rate specified by the USGS was maintained and the model modified to reflect the SNL/KAFB conceptual model. For the second model, recharge along Tijeras Arroyo was reduced to the value estimated by the SWHC Project. The high recharge case required high hydraulic conductivities in the alluvial fan material where Tijeras Arroyo enters SNL/KAFB. The values were not unreasonable when compared with SWHC data from Technical Area 2, but the model still exhibited a pronounced overprediction (too much water) in the area, which suggested that the Tijeras Arroyo flow rate in the ABM may be too high. In the low recharge case, hydraulic conductivities in the area where Tijeras Arroyo enters SNL/KAFB were very low.

Advective particle tracking, which represents the motion of a parcel of water, was done to estimate ultimate discharge points and associated travel times of groundwater in the SNL/KAFB area.

Sensitivity coefficient and Monte Carlo approaches were used to assess the sensitivity of the model to parameters which represent facets of the SWHC conceptual model. This allows the assessment of the adequacy of the conceptual model and determination of the most important features, which can be used to guide any further detailed investigation. The most sensitive parameters included initial heads, specific yield, specific storage, alluvial hydraulic conductivity, axial channel deposit hydraulic conductivity, and alluvial fan leakance.

Of the hydraulic parameters in the model, specific yield was most sensitive. This is consistent with the conceptual model, which holds that a large portion of the water pumped from the basin is derived from storage, and more water is released from storage per unit decline of the potentiometric surface under water table than confined conditions. Specific yield is not well characterized on SNL/KAFB or in the basin in general, which can result in compensating errors with respect to transmissivity and water budget (i.e. an error in the water budget can be compensated for by changes in hydraulic parameters).

The sensitivity of the model to two relatively poorly known parameters, initial head and specific yield, has a deleterious effect on the predictive capability of any model of the basin because it is possible to have compensating errors in parameter values. In the case of initial heads, it is simply not possible to overcome the data deficiency from earlier in this century. However, the purpose of this analysis was comparative, and the difference in representations the important result. The numerical representation of the conceptual model developed by the SWHC Project appears to adequately represent reality.

1.0 INTRODUCTION

1.1 Background

The Sandia National Laboratories/Kirtland Air Force Base (SNL/KAFB) area encompasses 52,223 acres (ac) bounded on the north and northwest by the City of Albuquerque, New Mexico; on the east by Cibola National Forest; on the south by Isleta Pueblo; and on the west by land owned by the State of New Mexico, KAFB (buffer zones), and the Albuquerque International Airport. SNL occupies 2,820 ac within KAFB and consists of five main work areas, called technical areas, and additional test areas, such as Thunder Range south of Technical Area III (TA-III) and Coyote Canyon Test Field in the canyons on the east side of the Manzano Mountains (also called the Manzano Base). See Figure 1.1 for the location map.

1.2 Project Objectives

In order to have a successful modeling project, it is crucial that the project objectives be defined before the project starts. The overall goal of this project was to construct a model to be used to assess the Site-Wide Hydrogeologic Characterization (SWHC) Project conceptual model and develop a quantitative understanding of groundwater flow paths in the SNL/KAFB area. The modeling analysis also includes discussions of potential limitations of the model and an assessment of its accuracy.

1.3 Previous Groundwater Modeling Analyses

Two large regional-scale analyses have been conducted for the Albuquerque Basin (Kernodle and Scott, 1986; Kernodle et al., 1987; Kernodle et al., 1995) and will be reviewed briefly. Site-specific models have also been developed (e.g. for the Chemical Waste Landfill [CWL]) that will not be discussed here because they do not attempt to provide a site-wide interpretive perspective. Kernodle and Scott (1986) developed a three-dimensional model of steady-state flow in the Albuquerque Basin. Kernodle et al. (1987) present the extension of Kernodle and Scott's model to simulation of transient groundwater flow in the Albuquerque Basin. Both the previous models used the conceptual model developed in the 1960's, which had the highly productive aquifer (Santa Fe Group sediments) being much thicker and extensive than recent data has revealed. These (1986 and 1987) models do not adequately represent the current understanding of the Albuquerque Basin and will not be discussed further.

Rapid water level declines in the late 1980's and early 1990's suggested that the early conceptual model of the Albuquerque Basin was incorrect, and a series of investigations was undertaken to better define the hydrogeology of the basin. The results of the first phase, development of a detailed geologic framework, are summarized in Hawley and Haase (1992). This investigation revealed that the productive part of the Santa Fe Group was primarily associated with axial channel deposits of the ancestral Rio Grande. Thorn et al. (1993) performed a detailed assessment of hydrologic conditions as the second phase of the assessment, and Kernodle et al. (1995) translated the conceptual model developed by Hawley and Haase and Thorn et al. into a numerical model of the Albuquerque Basin to be used for water resource management. A more detailed discussion of the portion of the U.S. Geological Survey (USGS) model that covers the SNL/KAFB area is provided in section 4.2.1.

A two-dimensional, steady-state MODFLOW model was used to perform a reconnaissance of possible conceptual models for the SNL/KAFB area (SWHC 1995). An inverse technique was used to estimate model parameters. The results suggested that recharge was higher underneath arroyos, transmissivity is lower on the east than transmissivity to the west. The change from lower to higher hydraulic conductivity from east to west is generally consistent with the depositional model, which has alluvial fan deposits near the mountain front and axial channel deposits to the west. The use of a two-dimensional and steady-state approach was a simplification that limited the further extension of the model.

1.4 Report Organization

This report is organized into six chapters; tables will appear at the end of individual chapters, and all figures will appear at the end of the report. Chapter 1, the introduction to the report, summarizes the analysis and puts the work into perspective relative to past groundwater modeling analyses done in the area.

Chapter 2 discusses the hydrogeologic framework upon which a conceptual model of groundwater flow and transport in the area is based. Local and regional geology, hydrology, and groundwater flow are discussed in this chapter.

Chapter 3 presents the computer code selected for the analysis and how the model was constructed. Representation of the Rio Grande, pumping wells and recharge, and the general implementation of the conceptual model in the computer program is also described.

Chapter 4 describes the calibration methodology, procedures, and results. Final model parameterization is also presented. Chapter 5 discusses the analysis results and presents its conclusions, and Chapter 6 presents the references.

1.0 INTRODUCTION

1.1 Background

The Sandia National Laboratories/Kirtland Air Force Base (SNL/KAFB) area encompasses 52,223 acres (ac) bounded on the north and northwest by the City of Albuquerque, New Mexico; on the east by Cibola National Forest; on the south by Isleta Pueblo; and on the west by land owned by the State of New Mexico, KAFB (buffer zones), and the Albuquerque International Airport. SNL occupies 2820 ac within KAFB and consists of five main work areas, called technical areas, and additional test areas, such as Thunder Range south of Technical Area III (TA-III) and Coyote Canyon Test Field in the canyons on the east side of the Manzano Mountains (also called the Manzano Base). See Figure 1.1 for the location map.

1.2 Project Objectives

In order to have a successful modeling project, it is crucial that the project objectives be defined before the project starts. The overall goal of this project was to construct a model to be used to assess the Site-Wide Hydrogeologic Characterization (SWHC) Project conceptual model and develop a quantitative understanding of groundwater flow paths in the SNL/KAFB area. The modeling analysis also includes discussions of potential limitations of the model and an assessment of its accuracy.

1.3 Previous Groundwater Modeling Analyses

Two large regional-scale analyses have been conducted for the Albuquerque Basin (Kernodle and Scott, 1986; Kernodle et al., 1987; Kernodle et al., 1995) and will be reviewed briefly. Site-specific models have also been developed (e.g. for the Chemical Waste Landfill [CWL]) that will not be discussed here because they do not attempt to provide a site-wide interpretive perspective. Kernodle and Scott (1986) developed a three-dimensional model of steady-state flow in the Albuquerque Basin. Kernodle et al. (1987) present the extension of Kernodle and Scott's model to simulation of transient groundwater flow in the Albuquerque Basin. Both the previous models used the conceptual model developed in the 1960's, which had the highly productive aquifer (Santa Fe Group sediments) being much thicker and extensive than recent data has revealed. These (1986 and 1987) models do not adequately represent the current understanding of the Albuquerque Basin and will not be discussed further.

Rapid water level declines in the late 1980's and early 1990's suggested that the early conceptual model of the Albuquerque Basin was incorrect, and a series of investigations was undertaken to better define the hydrogeology of the basin. The results of the first phase, development of a detailed geologic framework, are summarized in Hawley and Haase (1992). This investigation revealed that the productive part of the Santa Fe Group was primarily associated with axial channel deposits of the ancestral Rio Grande. Thorn et al. (1993) performed a detailed assessment of hydrologic conditions as the second phase of the assessment, and Kernodle et al. (1995) translated the conceptual model developed by Hawley and Haase and Thorn et al. into a numerical model of the Albuquerque Basin to be used for water resource management. A more detailed discussion of the portion of the U.S. Geological Survey (USGS) model that covers the SNL/KAFB area is provided in section 4.2.1.

A two-dimensional, steady-state MODFLOW model was used to perform a reconnaissance of possible conceptual models for the SNL/KAFB area (SWHC 1995). An inverse technique was used to estimate model parameters. The results suggested that recharge was higher underneath arroyos, transmissivity is lower on the east than transmissivity to the west. The change from lower to higher hydraulic conductivity from east to west is generally consistent with the depositional model, which has alluvial fan deposits near the mountain front and axial channel deposits to the west. The use of a two-dimensional and steady-state approach was a simplification that limited the further extension of the model.

1.4 Report Organization

This report is organized into six chapters; tables will appear at the end of individual chapters, and all figures will appear at the end of the report. Chapter 1, the introduction to the report, summarizes the analysis and puts the work into perspective relative to past groundwater modeling analyses done in the area.

Chapter 2 discusses the hydrogeologic framework upon which a conceptual model of groundwater flow and transport in the area is based. Local and regional geology, hydrology, and groundwater flow are discussed in this chapter.

Chapter 3 presents the computer code selected for the analysis and how the model was constructed. Representation of the Rio Grande, pumping wells and recharge, and the general implementation of the conceptual model in the computer program is also described.

Chapter 4 describes the calibration methodology, procedures, and results. Final model parameterization is also presented. Chapter 5 discusses the analysis results and presents its conclusions, and Chapter 6 presents the references.

2.0 CONCEPTUAL MODEL

A conceptual model is a concise description of the components of the groundwater flow system and is developed from regional, local, and site-specific data. A conceptual model is a precursor to the development of a mathematical model and identifies groundwater sources and sinks, geologic origin and configuration of the aquifers, aquifer properties, and general flow system behavior. The conceptual model guides the construction and calibration of the numerical model and aids in interpretation of model results by presenting a general understanding of the groundwater flow system.

2.1 Regional Hydrogeology

The Albuquerque Basin is located in the Rio Grande Valley (Figure 2.1). Low topographic relief characterizes the floor of the basin (elevation 4,900 ft msl), the Sandia and Manzano Mountains (elevation 10,000 ft) are the eastern basin boundary, and a gentle rise to the plains forms the western boundary (elevation 6,500 ft). The Albuquerque Basin has no distinct north and south boundaries; rather, the northern limit is generally established where the Sandia and Jemez Mountains created a narrowing of the alluvial deposits. Over the last 30 million years, the deep valley has been filled in by erosion of the mountains around the basin and by sediment brought into the basin and deposited by rivers. These deposits are comprised, in part, of the late Oligocene to middle Pleistocene Age Santa Fe Group sediments, which range in thickness from 2,400 to 13,800 ft in the Albuquerque area (Hawley and Haase, 1992). The Santa Fe Group (SFG) is subdivided into Lower, Middle, and Upper units (Hawley and Haase, 1992). The Upper Santa Fe Group (USF) is the formation used almost exclusively for groundwater supply in the Albuquerque Basin.

During the time that the lower part of SFG was deposited, the basin was closed, and sediments that collected were fine grained from the then still low relief rift margins and playa-lake evaporitic deposits. Rifting accelerated during the deposition of the middle and upper SFG, and a through-flowing drainage system developed from the north (Thorn et al. 1993). Either the energy of the fluvial system was lower during deposition of the middle part of the SFG, or there was an influx of fine sediments into the active rift, since the middle SFG sediments are generally finer and less permeable than those of the upper part of the SFG. An ancestral river system was guided to the eastern side of the rift by rapid subsidence of the eastern part of the area during the time of the deposition of the middle and upper SFG. During deposition of the upper SFG, the fluvial depositional environment for axial channel deposits was especially energetic, and the deposits were coarse and well sorted. The position of the interface between the fluvial deposits (laid down in a north-south direction) and the alluvial fan sediments (directed east-west) remained sharp and stable for millions of years. Thorn et al. (1993) and Ruskauff (1996) both show mappings of the hydraulic conductivity of the USF.

The USF is characterized by intertonguing piedmont-slope alluvial fan and fluvial basin-floor deposits. Piedmont-slope deposits consist of poorly sorted, weakly stratified sand and conglomerate with a silt-clay matrix. Basin-floor deposits include cross-stratified ancestral river sediments characterized by thick zones of clean sand and gravel. Fine- to medium-grained overbank sediments were deposited in areas where major river systems were merging and in basin-flow and piedmont-slope transition zones. The thickness of the USF can be as much as 400 m, but is usually less than 300 m. Three hydrostratigraphic units are distinguished within the USF, including a coarse-grained alluvial fan pediment veneer facies in the eastern part of the basin, fluvial deposits of the ancestral Rio Grande, and alluvial and minor eolian deposits in the western part of the basin (Hawley and Haase, 1992). A generalized stratigraphic column is shown in Figure 2.2, and the general conceptual arrangement of facies is shown in Figure 2.3.

Barriers and preferential groundwater flow paths both exist within the SFG. Barriers include pinch out of productive material, for instance, as channel deposits grade and abut into distal alluvial deposits. The width of the most productive aquifer material, the axial channel deposits, is from about 2 to 6 miles. Faults are also barriers to groundwater flow within the basin. Faulting within the basin can juxatapose productive aquifer units against unproductive units, abruptly terminating high hydraulic conductivity material and creating a barrier to groundwater flow. It is believed that cementation of faults has further restricted flow (Thorn et al. 1993). Preferential flow paths occur within the braided-stream deposits associated with channel deposits and as gravel and sand deposit within alluvial fan deposits.

The Rio Grande extends the length of the Albuquerque Basin and is the only perennial stream in the basin. Water is diverted from the Rio Grande into a series of canals for irrigation of land in the inner valley. Drains, which intercept groundwater and receive return flow from canals, return water to the Rio Grande. Groundwater is the primary source of water for urban, rural, commercial, and industrial uses in the Albuquerque Basin. Groundwater in the Albuquerque Basin comes from three sources: depletion of aquifer storage, capture of mountain-front and tributary recharge, and induced recharge from the Rio Grande surface-water system. The effects of faults as barriers to flow was noted by Thorn et al. (1993).

The Albuquerque Basin has been extensively studied, and the reader is referred to Theis (1938), Theis and Taylor (1939), Bjorkland and Maxwell (1961), Reeder et al. (1967), Lambert (1968), U.S. Army Corps of Engineers (1979), Hudson (1982), Kelley (1977); Kelly (1982), Kues (1986; 1987), Anderholm and Bullard (1987), Lozinsky (1988), Kaehler (1990), Hawley and Haase (1992), Haywood (1992), Summers (1992), Thorn et al. (1993), and Hawley and Whitworth (1996) for more detail.

2.2 Site-Specific Hydrogeology

SNL/KAFB is located along the eastern margin of the Albuquerque Basin. The fault system that forms the eastern boundary of the basin bisects the area occupied by SNL/KAFB (Figure 2.4). The north to south striking Sandia fault enters the base from the north; almost colinearly the Hubbell Springs fault extends from the south; and the Tijeras fault cuts the base diagonally from the northeast. The topography is characterized by a series of alluvial fans that extend from the base of the mountains on the east to terraces along the river (Figure 2.5). The north- to south-trending fault complex divides the local groundwater flow system into three distinct hydrogeologic regions. The region west of the fault system is identified as Hydrogeologic Region 1 (HR-1). Hydrogeologic Region 2 (HR-2) is associated with the fault system, and Hydrogeologic Region 3 (HR-3) is located east of the fault system. Figure 2.6 shows the locations of these three hydrogeologic regions. HR-1 is part of the Albuquerque Basin and is of principal concern in the modeling analysis since HR-1 contains most of the SNL sites that may have been impacted by past SNL operations. Only HR-1 will be discussed further; for information on the other regions, the reader is referred to the SWHC Project reports (SNL/NM 1994, 1995, 1996). HR-1 and HR-2 are not incorporated in this groundwater flow model.

2.2.1 Stratigraphy

The sediments in the SNL/KAFB area are derived from two depositional processes: an alluvial-fan system with sediment sources located in the mountains to the east and a through-flowing north-to-south fluvial system. From SWHC Project geologic investigations, it is possible to recognize four mappable lithofacies: (1) coarse, proximal to medial alluvial-fan dominated by gravel and coarse sand, (2) fine, medial to distal alluvial-fan dominated by fine sand, silt, and clay, (3) fine fan and eolian, and (4) ancestral Rio Grande fluvial, ranging from coarse to fine-grained units. Seven geologic cross sections show the distribution of the four lithofacies (Figure 2.7 to 2.14).

In addition to the general basin geologic conceptual model developed by Hawley and Haase (1992), an analog for the SNL/KAFB portion of the basin is provided by the depositional model of the Palomas and Northern Mesilla Basins of the southern Rio Grande rift (Mack and Seager, 1990). These basins and the SNL/KAFB portion of the Albuquerque Basin share the same asymmetry, with an upfaulted mountain range on one side, a rapidly subsiding basin adjacent to the uplift, and a basin floor rotating downward along the bounding, normal fault. Mack and Seager (1990) argue that the areal distribution of alluvial-fan vs. axial fluvial lithofacies is tectonically controlled by this asymmetry and the distribution occurs in two stages (Figure 2.15). In the synorogenic stage, subsidence greater than the ability of the sediment source to equalize results in fluvial sedimentation over the axis of maximum subsidence close to the mountain front. Coarse-grained alluvial sediment is restricted to a narrow belt at the foot of the mountains. In the postorogenic stage, the rate of subsidence slows, the sediment source delivers alluvial sediment faster than subsidence occurs, and coarse-grained alluvial fans grow basinward and displace the axial river.

The uppermost aquifer underlying HR-1 is within the USF and is an unconsolidated to partially indurated, porous-media aquifer. The USF sediments that provide the framework for this aquifer include a heterogeneous mix of coarse- to fine-grained sands, silts, and clays that exhibit a complex sedimentary framework, characterized by variability in bedding thickness, continuity, and connectivity. The complex sedimentary framework includes the intertonguing of ancestral Rio Grande fluvial facies with alluvial fan facies extending westward from the highlands to the east. The fluvial facies includes thick, well-sorted, cross-stratified sand and pebbly gravel channel deposits and fine- to medium-grained sand overbank deposits. This fluvial facies is characterized by well-developed bedding, with channel deposits generally oriented north-south. The alluvial fan facies is characterized by poorly sorted, weakly stratified sand and conglomerate with an abundant silt and clay matrix. In this facies, the bedding is less continuous with alluvial channel deposits generally oriented east-west.

2.2.2 Hydraulic Properties

The surface of the uppermost SFG regional aquifer underlying the SNL/KAFB area is found in the ancestral Rio Grande fluvial facies to the west and alluvial fan facies to the east. Hawley and Haase (1992) estimated that hydraulic conductivities in the USF could range from less than 0.3 ft/d in an alluvial fan facies to more than 30 ft/d in the fluvial facies. Thorn et al. (1993) presented a summary of pumping test results, mainly from production wells located in the productive channel deposits, that had hydraulic conductivities ranging from about 7 to 150 ft/d. SWHC Project pumping tests yielded values of between 46 and 147 ft/d. Table 2.1 summarizes hydraulic conductivity data obtained from wells in the ancestral Rio Grande fluvial facies.

Hydraulic conductivity data for the alluvial fan facies are available from pumping tests performed on water supply wells located east of the eastern limit of the fluvial facies. These wells are screened over large intervals which may include intervals of fluvial facies that intertongue with the predominant alluvial fan facies. Table 2.2 summarizes hydraulic conductivity data obtained in wells completed in this facies.

Calculated storage coefficients are available from pumping tests in the Ridgecrest well field, a pumping test at the SNL CWL, and from the analysis of draw-down recovery data at monitoring well TA2-NM1-595, resulting from pumping of KAFB-11. Table 2.3 summarizes these values. Plate 1 shows geologic units present at the regional water table and wells with pumping tests.

2.2.3 Groundwater Flow Patterns

Groundwater flow includes both downward recharge flow in the exposed bedrock areas in the eastern part of the SNL/KAFB (not explicitly considered in the numerical model), in the arroyos and lateral (predominantly east to west) flow through the shallow alluvial and bedrock aquifers on the east, and across the north-south fault complex. There are two complicating factors for the conceptual model of groundwater flow beneath SNL/KAFB. The first factor is the impact of the north-south fault complex on the overall flow system. This fault complex bisects SNL/KAFB and has a very apparent impact on the area-wide flow system. This impact is seen in the large changes in water level as the faults are crossed from east to west.

The second important factor is the continual removal of large amounts of groundwater for the municipal water supply for the City of Albuquerque. Groundwater withdrawal by water supply wells from the City of Albuquerque and KAFB has resulted in significant changes to the groundwater flow regime in the SFG over the past 30 years as discharge exceeds recharge for this portion of the Albuquerque Basin (Thorn et al. 1993). Groundwater flow at SNL/KAFB has been altered from a principally westward flow to northwestward and northward flows along the western and northern portions of KAFB (Figure 2.16). The long trough extending to the south suggests that deposits of greater transmissivity exist in this area and the possibility that the Rio Grande fault is isolating the area from the hydraulic influence of the river.

Water level declines have been occurring within the Albuquerque Basin since the 1960's, when significant increases in groundwater withdrawal began. Basin-wide declines from steady-state conditions have been estimated to range from 20 to 60 ft (Thorn et al. 1993). The greatest declines are to the east of the eastern limit of fluvial deposits of the ancestral Rio Grande (Thorn et al. 1993).

Since the mid-1980's, water levels have been collected from monitoring wells on SNL/KAFB. Hydrographs from these data indicate groundwater levels are declining at rates of between 0.2 and 3.0 ft/yr within the upper unit of the SFG in HR-1. On KAFB, the rate of water level declines generally increases westward from the Sandia Tijeras fault zone and northward near water-supply production wells. Based on estimates of steady-state conditions by Thorn et al. (1993), groundwater has declined from 60 to 140 ft across the base, approximately 100 ft at the northern KAFB boundary to approximately 50 ft at the southern KAFB boundary (Thorn et al., 1993). Groundwater level surveillance by SNL since approximately 1990 (SNL 1995) indicates that wells completed west of the eastern extent of fluvial deposits have water level declines of 1.0 to 3.0 ft/yr, whereas wells on the east display declines of 1.0 ft or less per year (Figure 2.17). These groundwater declines represent only the upper 100 ft or less of the upper unit of the SFG aquifer, because most of the wells on SNL/KAFB are water-quality monitoring wells and have short screen lengths in comparison to the thickness of the aquifer.

Surface water flows through the SNL/KAFB area in arroyos, primarily Tijeras Arroyo and Arroyo del Coyote. These arroyos also function as local sources for groundwater recharge. Precipitation that falls on the area between arroyos either runs off into the arroyos or is evapotranspired (the combined processes of evaporation and transpiration of water by plants).

Currently it is thought that essentially no groundwater recharge occurs in the interarroyo areas west of the foothills. Arroyos outside of Tijeras and Arroyo del Coyote drainages almost never reach the Rio Grande. These arroyos widen into pseudo-playas from which the water evaporates. The western portions of these arroyos are underlain with caliche, even where well channelized, indicating that they seldom flow and are not natural recharge sources. Near the mountains, flows in the southern arroyos may be more frequent, and channel-bottom materials may be more permeable, thus allowing natural recharge.

2.3 Conceptual Model Summary

The salient points of the conceptual model are summarized as follows:

- Channel deposits of the ancestral Rio Grande extend through the west SNL/KAFB area in a north-south direction.
- Alluvial fan deposits extend from the east into the ancestral Rio Grande deposits.
- Sharp contrasts in hydraulic properties occur as a result of the abutment of lithologies deposited in distinctly different environments.
- Recharge occurs mainly from Tijeras Arroyo, Arroyo del Coyote, and the Manzano Mountains mountain front, with some component of flow from the bedrock.
- Sediments decrease in hydraulic conductivity with depth as the USF grades into the Middle Santa Fe (MSF) and Lower Santa Fe (LSF), which were deposited under different (mainly low-energy alluvial) environments.
- The top of the aquifer is in the USF.
- Large amounts of groundwater flow are from storage release (i.e. dewatering).

- Pumpage greatly exceeds recharge from all sources (precipitation, Rio Grande leakage).
- Fault systems in the SFG probably act as restrictions to groundwater flow, abutting low-flow lithologies and cementation of the fault gouge.

Table 2.1 Hydraulic Conductivity for Ancestral Rio Grande Fluvial Facies of the Santa Fe Group

Data Source	Data Type	Hydraulic Conductivity (ft/day)
Data from Other Publications		
Hawley and Haase (1992)	Estimated for the fluvial facies	>30.0
KAFB IRP Investigation (USGS 1993)	Slug Test Analysis (KAFB IRP Monitoring Wells in Fluvial Facies)	0.2 to 10.5
Water Supply Well Analysis (GMI 1988a, 1988b)	Pumping Test Analysis (Yale and Burton Well Fields)	12.0 to 121.5
Data from SNL/ER Projects		
Site Wide Hydrogeologic Characterization Project (SNL/NM 1996)	1995 Pumping Test Analysis at PL-2 and MRN-1 (Appendix D)	46.6 to 147.1
	1995 Slug Test Analysis at PL-2 and MRN-1 (Appendix D)	0.26 to 2.6

Table 2.2 Hydraulic Conductivity for Alluvial Fan Facies of the Santa Fe Group

Data Source	**Data Type**	**Hydraulic Conductivity (ft/day)**
	Data From Other Publications	
Hawley and Haase (1992)	Estimated for Alluvial Fan Facies	<0.3
KAFB IRP Investigation (USGS 1993)	Slug Test	0.08 to 13.0
Water Supply Well Analysis (GMI 1988c)	Pumping Test (Ridgecrest Well Field)	9.66 to 44.7
	Data from SNL/NM ER Projects	
Chemical Waste Landfill (IT 1985, SNL/NM 1993, 1995a)	1990 pumping test at MW-2A	0.39
	1990 laboratory analysis of samples from MW-4	0.01 to 10.8
	1985 slug tests at MW-1, MW-2, and MW-3	0.07 to 0.09
	1994 slug tests at BW-3, BW-3, and BW-4A	0.014 to 0.031
	1995 slug tests in MW-1A, MW-2A, MW-3A, MW-5 (upper), and MW-6 (upper)	0.02 to 0.33
	1995 slug test in MW-2B (lower)	6.74
	1995 pumping tests in BW-4A	0.01
	1995 pumping tests in MW-2B (lower)	6.74
	1995 pumping tests in BW-4A	0.01
	1995 pumping tests in MW-2B (lower)	2.16
	Observation wells MW-5 (lower and MW-6 (lower) during 1995 pumping test in MW-2B (lower)	25.9 to 27.4
Mixed Waste Landfill (SNL/NM MWL Project Files)	1994 pumping test in MW-4 (upper)	0.072
	1994 pumping test in MW-4 (lower)	1.48
	Recovery data from water-sampling operations (MW-1, MW-2, and MW-3, and BW-1)	0.001 to 0.055
LWDS and TA-4 (SNL/NM LWDS and TA-V Project Files	1995 slug tests at LWDS MW-01 and MW-02; TA5 MW-01 and MW-02	0.04 to 2.38
Site-Wide Hydrogeologic Characterization Project (SNL/NM 1995 and 1996)	1994 Pumping Test at SFR-3P (HR-2)	10.34
	1995 slug test at KAFB-0311	6.14
	1994 analysis of draw-down recovery data from TA2-NW1-595 (well response due to pumping at KAFB-11)	14.5

Table 2.3. Storage Coefficient Values from Aquifer Tests in the Santa Fe Group

Data Source	**Data Type**	**Storage Coefficient (dimensionless)**
	Data from Other Publications	
Water supply well analysis (GMI 1988c)	Pumping test analyses (Ridgecrest well field)	0.001
	Data from SNL/ER Projects	
Chemical Waste Landfill (SNL/NM 1995a)	1995 Pumping test at CWL (MW-5 [lower] and MW-6 [lower])	0.00017 to 0.000033
Site-Wide Hydrogeologic Characterization Project (SNL/NM 1996))	1995 analysis of draw-down recovery data from TA2-NW1-595 (well response due to pumping at KAFB-11)	0.00024

This page intentionally left blank.

3.0 GROUNDWATER FLOW MODEL CONSTRUCTION

A general protocol has been developed for model application (Anderson and Woessner, 1992; ASTM Standard Guide D5447-93, "Application of a Ground-Water Flow Model to a Site-Specific Problem"). This protocol includes code selection issues, model conceptualization and design, calibration, sensitivity analysis, prediction, and reporting. Figure 3.1 illustrates the steps in the protocol. The approach taken in this analysis follows this protocol. The verification and postaudit steps are typically not performed. Verification is the comparison of independent model prediction to data not used in calibration. It is often impossible to verify a model, because usually only one set of field data is available, which is needed for calibration (Anderson and Woessner, 1992). A post audit is the comparison of model prediction to reality some period of time (often several years) after the modeled action is implemented.

3.1 Code Selection

The most widely used computer program for groundwater flow modeling in the world (Rumbaugh and Ruskauff, 1993) is the USGS MODFLOW code (McDonald and Harbaugh, 1988). Andersen (1993) describes the code verification with several analytic and comparisons with other numerical models. MODFLOW is capable of simulating transient or steady-state groundwater flow in one, two, or three dimensions. A number of different boundary conditions are available, including specified head, areal recharge, injection or extraction wells, evapotranspiration, drains, and rivers. MODFLOW simulates groundwater flow using a block-centered, finite-difference approximation for the solution of the governing equation for flow. Aquifers can be simulated as unconfined, confined, or a combination of unconfined and confined. The finite-difference equations may be solved with a strongly implicit procedure (SIP), slice-successive over-relaxation (SSOR), or preconditioned conjugate gradient (PCG) methods. MODFLOW was selected for use on this project because of its widespread scientific and regulatory acceptance and the number of commercially available software tools to expedite data preparation and output analysis. In addition, third-party modifications allow the addition of various extra features, including solute transport and unsaturated flow. Finally, the use of the Albuquerque Basin Model (ABM) in conjunction with MODFLOW provided the following advantages:

- MODFLOW has been extensively used to analyze groundwater flow conditions in New Mexico, and thus state and municipal agencies are familiar with it.
- Data input for the ABM MODFLOW already existed and were available for use. This data could easily by modified to meet SNL/KAFB requirements.

- The SNL/KAFB model can be directly tied to the basin physical boundaries on the west and east and a reasonable representation of the effects of the other boundaries and pumping included on the northern and southern boundaries in a fashion consistent with regional trends.
- The ABM is used by the City of Albuquerque for water resources planning and will be periodically updated. SNL/KAFB can work closely with both agencies through the Albuquerque Basin Contact Group to keep the model current in the area.
- The State Engineer may also use the ABM to support water resources planning and adjudication of water rights in the Albuquerque Basin. Therefore, using MODFLOW would be consistent with the primary state and municipal agencies that use models and with whom SNL/KAFB interacts.

Groundwater capture zones and flow paths were delineated with the MODPATH (Pollock, 1989) computer program. MODPATH, developed by the USGS, works in conjunction with MODFLOW, using the simulated heads and flows to compute the velocity field. With the particle tracking technique, the movement of a parcel of water in the aquifer is computed using the simulated velocity field. Particle tracking is a simple form of contaminant transport analysis that disregards the effects of dispersion, retardation, and other chemical reactions. Particles can be moved forward with the flow field in a manner akin to a marble rolling down a plane surface to determine their final destination, or particles can be moved backwards (reverse) from a final location to an origin. Each type of analysis is useful and presents different aspects of the situation.

A primary difficulty with numerical models such as MODFLOW is quality control when preparing large datasets. These datasets are filled with numbers that must be formatted precisely for the program to execute; incorrect entries may cause the program to crash, or worse, execute improperly with no warning. To help alleviate this problem, a class of software known as *preprocessors* has been developed to aid in model input. Preprocessors help streamline data preparation and provide better quality control. The initial ABM data sets prepared by the USGS were constructed using the ARC/INFO GIS as described in Kernodle et al. (1995). The preprocessor *Groundwater Vistas*, version 1.61 by Environmental Simulations, Inc. (1996) was used to prepare data sets for the final phase of this analysis. Model output is seldom directly usable, and must be *postprocessed* into some usable format. *Groundwater Vistas* includes built-in support for contouring simulated heads, velocity vector maps, and pathline plotting from MODPATH particle tracking results. In addition, ARC/INFO, in conjunction with ArcView, was used to process input and output for display. *Groundwater Vistas* stores the model design in a model-independent format, so the model design can be translated to more complex codes if it should become necessary in the future.

3.2 Calibration Strategy and Data

Calibration targets are a set of field measured values, typically groundwater hydraulic heads, to which model predicted values are compared. The goal in selecting calibration targets is to define a set of measurements that are reliable and spatially distributed throughout the model area. Comparisons should be made between point measurements of hydraulic heads rather than maps of these heads, because the contour lines are the result of interpretation of data points and are not considered basic data in and of themselves. The groundwater flow model should be true to the essential features of the conceptual model and not to their representation (ASTM Standard Guide D5490-93).

Water levels have been declining in the Albuquerque Basin since the 1960's, as discussed in section 2.4.4. Under these conditions the time-varying nature of flow is required to analyze groundwater conditions at SNL/KAFB. A transient simulation typically begins with steady-state initial conditions and generates a set of computed heads for each time step. It is important to recognize that the initial conditions for a transient simulation must be determined by modeling since this assures that the initial heads, model boundary conditions, and aquifer parameters are consistent. If an interpretation (e.g., contour map) were used as initial conditions, the model response in early time would reflect not only the conditions under study but the adjustment of model head values to offset the lack of correspondence between model boundary conditions, aquifer properties, and the initial head field (ASTM Standard Guide D5610-94 "Defining Initial Conditions in Ground-Water Flow Modeling"). Transient simulations are more complicated than steady-state simulations for the following reasons:

1. An additional aquifer property, storage coefficients, must be specified.
2. Errors in initial conditions can propagate into the transient analysis.
3. Pumping and other effects may propagate out to model boundaries and cause the boundary conditions to become inappropriate.
4. The time dimension in addition to the space dimension must be discretized.
5. More input and output must be managed, and data management becomes complex.

Transient calibration was conducted for the period from January 1, 1980, to March 31, 1995. Data existed from about 1987 onward. The USGS made its predictions by simulating forward from 1980, and the same convention was followed here. A total of 43 wells was used for calibration targets, with 1 to 80 measurements available for each well, for a total of 1,378 observations used for the calibration. Table 3.1 summarizes this information. Initial conditions and calibration goals are discussed further in sections 3.5 and 4.0, respectively.

3.3 Model Discretization

3.3.1 Spatial Discretization

The finite-difference solution of the governing equations requires that the system (conceptual model of the aquifer) be divided into a set of discrete blocks. This discretization allows each block to be assigned a different set of properties. These blocks form the model grid with a node located at the center of each block. The process of dividing the area of the aquifer to be simulated is called discretization. Water levels computed for each node are the average over the volume of each block. Thus, adequate discretizaiton is required to resolve features of interest and yet not be computationally burdensome. An algebraic equation that describes groundwater flow is written for each block in terms of the surrounding blocks and results in a set of linear equations. The set of linear equations is iteratively solved until the change between iterations meets a preset criterion established by the analyst; a rule of thumb is to set the convergence criteria one to two orders of magnitude lower than the level of accuracy desired in the head results (Anderson and Woessner, 1992).

The empirical 50-percent rule was followed in the discretization process (Anderson and Woessner, 1992). That is, no block changed size more than 50 percent relative to the adjacent blocks. This is necessary to control numerical truncation errors and preserve fluid mass balance. The finite-difference method assumes that aquifer properties are constant within a block and that hydraulic heads vary linearly between nodes. Thus, smaller blocks were used over most of the area where the influence of pumping causes the hydraulic head surface to curve rapidly. Block dimensions were uniform in the column at 656 ft, or x direction, and from 650 ft in the north to 3,700 ft in the south of the row, or y direction. The grid was designed so that boundary conditions would correspond with physical or hydrologic boundaries where possible (e.g. Rio Grande, basin boundary to the east). See Figure 3.2.

Vertical discretization may be approached using either a quasi-three-dimensional or fully three-dimensional technique. In the first approach, the aquifer system is considered to be an alternating series of permeable and impermeable beds, with the primary resistance to vertical flow occurring in the impermeable beds separating the permeable layers. The low-permeability unit is represented mathematically as a resistance term for fluid flow between the permeable units. Alternatively, each geologic unit, regardless of its properties, is represented in the model. The fully three-dimensional approach was used in the KAFB model. Thus all the units in the SFG were each represented in the model as a layer. The top of the model was the pre-1901 water table.

Each of the upper four layers in the model are 20 ft thick at the Rio Grande and approximately 30 ft thick at the northeast boundary of the SNL/KAFB model (Figure 3.3). The thickness of layers 5 through 11 is constant across the model. Individual layer thickness ranges between 50 ft in layer 5 to 500 ft in layer 11. The purpose of the relatively thin upper layers is to account for surface water/groundwater interaction (Kernodle et al. 1995). The total modeled thickness includes the major pumping zones in Albuquerque within the SFG.

3.3.2 Temporal Discretization

Just as it is desirable to use appropriately sized grid blocks, it is also desirable to use an appropriate time-step size for transient simulations. A good order of magnitude estimate for the initial time step is obtained by assuming the aquifer is homogenous and isotropic with a regular grid. The critical time step, t_c, is defined as follows (deMarsily, 1986):

$$\Delta t_c = Sa^2 / 4T \tag{3.1}$$

where
S is storativity (-),
T is transmissivity (ft^2/d),
a is a representative grid block size.

In more general applications, t_c can be approximated by selecting a representative grid block dimension a and properties. The transient solution is sensitive to rapidly fluctuating pressures caused by introducing a hydraulic stress, making it important to use time steps on the order of t_c to capture the early response of the system even if one is interested only in the solution at later times. For instance, using a storativity of 1×10^{-4}, a 600 ft grid block spacing, and a transmissivity of 4,500 ft^2/d; t_c is 172 seconds. Clearly, this time step size is not practical to use for all time steps in the transient simulation. Although time steps can be increased as a geometric progression with a ratio of 1.2 to 1.5 (Anderson and Woessner, 1992) this will still result in prohibitive simulation run times. Alternatively, the results for the first few time steps could be ignored. If this approach is taken, the solution should proceed through five time steps, during which there are no significant changes in sources, sinks, or boundary conditions before the solution is considered accurate (deMarsily, 1986). The SNL/KAFB model uses time stepping identical to the USGS ABM. The USGS did not follow the above criteria, but their approach appears to be adequate considering the available information on pumping and water levels. Practically speaking, the effects of using the USGS temporal discretization are probably minor. Any computational errors introduced will be evident as mismatch between model and data.

The period between January 1, 1980, and March 31, 1995, was divided into 30 stress periods and 414 time steps. A stress period in MODFLOW terminology is a time span in which all boundary conditions remain constant. The first stress period was from January to August 1980 divided into eight time steps. Thereafter stress period were divided into six-month periods with seven time steps to mimic the pumping and water-use cycle in the basin, which declines abruptly in the fall through winter and peaks during summer. The time step multiplier was 1.5, which, using the formula presented by McDonald and Harbaugh (1988), gives an initial time step size of 5.7 days, with successive time steps of 8.53, 12.8, 19.2, 28.8, 43.2, and 64.8 days.

3.4 Boundary Conditions

Once the area of interest has been discretized, it is implicitly assumed that the rest of the surrounding area can be ignored. The model, however, must account for the effects of external conditions that may affect the area of interest and allow water to flow in or out. These effects are accounted for by the use of appropriate boundary conditions. Model boundaries should be chosen to correspond to natural hydrologic boundaries of the groundwater flow system where identifiable.

The specified rate, or flux, conditions allow a given quantity of water to be applied to a unit area of the model per unit time. The specified-rate condition is used to represent both flow from the ABM to the SNL/KAFB submodel, recharge, and wells in MODFLOW. In order to remove the SNL/KAFB area from the ABM, either specified head or specified flux conditions could be used to link the ABM to the submodel. The time-weighted average flow in each cell on the submodel boundary was computed using the ABM. One average value was computed for each cell during each stress period from 1980 to 1995. The well package was used to introduce these flows. A comparison of ABM and SNL/KAFB submodel simulated heads showed that the difference was within 1 ft for all layers. Irrigation and septic-return flow were simulated with the recharge package.

Private water-supply wells, KAFB water-supply wells, and City of Albuquerque wells are located within the SNL/KAFB model area. The majority of the City of Albuquerque wells are located to the north and northwest of KAFB. The KAFB well fields are located in the middle of the SNL/KAFB model. Private wells are located west of KAFB and along the south boundary of the model. Well rate data as used in the ABM by the USGS were maintained in the submodel.

Value-dependent flux boundary conditions are implemented as the drain, evapotranspiration, general head, or river conditions in MODFLOW. These boundaries are called the value-dependent flux condition because the flux entering or exiting the groundwater flow model is dependent upon the head difference between the value computed at the model boundary and a source of water maintained at a constant level outside the model. The source is visualized as being connected to the model through a conduit of aquifer material of specified length. This type of boundary is more flexible than the constant head or constant flux boundaries because both the simulated flow rate and head can vary. River, drain, and evapotranspiration boundaries were used in the SNL/KAFB model.

The Rio Grande and its drain system were represented with the river and drain packages. For the transient calibration, the Rio Grande stage was required for each stress period. The same stage was used for each stress period (wet and dry), with the number of active river cells in dry conditions about one fourth of that in wet conditions to reflect lower river flow. These boundaries were not altered since it is likely that the USGS has the best information on them.

3.5 Initial Conditions

The ABM was first calibrated to estimated steady-state conditions along the inner valley of the basin from 1901, and then those results were used as the starting point for the transient simulation from 1901 forward. Before removing the SNL/KAFB subarea from the ABM, some gross adjustments were made (e.g. areas of higher hydraulic conductivity representing the ancestral Rio Grande not in the ABM) and the model run forward from 1980 conditions. A more rigorous approach would have been to recalibrate the 1901 steady-state model with the changes and then run it forward through 1995. However, the ABM results for wells near and on SNL/KAFB show general agreement between simulated and observed heads, and it is felt that, given the project goals and the inherent uncertainty in this problem, that this approach is acceptable. Sensitivity of the model to initial conditions is investigated in section 4.4.4.

3.6 Parameter Zonation

Simulation of groundwater flow requires knowledge of the hydraulic properties of the aquifer. The areal distribution of aquifer properties (e.g. hydraulic conductivity) is required as input to MODFLOW for each grid block in the model. Clearly, no amount of site characterization will completely determine aquifer properties, and some simplification must be made. The technique of parameter zonation was used to define the spatial variation of aquifer parameters. The method requires the delineation of zones within which a constant value of a parameter is assigned. When possible, the zones are chosen based upon hydrogeologic information such as the nature and thickness of strata. The average value and the extent of each zone were determined during the calibration process.

3.7 Initial Model Parameters

Initial parameter values were obtained from the ABM as described by Kernodle et al. (1995). Plates 2 and 3 show the initial parameter value and distributions in the ABM area of the submodel. Results from this model and its fit to the SNL/KAFB data are discussed in section 4.2.1, and the reasons for the changes made during calibration are discussed in sections 4.2.2, 4.2.3. Model sensitivity to various parameters is analyzed in section 4.2.4.

Table 3.1 Summary of Data Used for Calibration

Well Name	Period of Record
CWLBW3M	Oct. 88-Dec. 95
CWLMW1A	Oct. 88-Dec. 95
CWLMW2	Jan. 86-Aug. 95
CWLMW3A	Oct. 88-Aug. 95
MWLBW1	Nov. 89-Nov.95
MWLMW1	Jan. 89 - Nov. 95
NWTA-03	Nov. 89-Nov. 95
SWTA-03	Nov. 89-Nov. 95
LWDSMW1	Nov. 93-Nov. 95
LWDSMW2	Mar. 94-Nov. 95
TAVMW1	Jun. 95
TAVMW2	Jun. 95-Nov. 95
AVN1	Mar. 95-Nov. 95
AVN2	Mar. 95-Nov. 95
KAFB-9	Jun. 89- May 92
KAFB-10	Jan 89-Jul 95
KAFB-0107	Jul 89-Aug 95
KAFB-0213	Jul 89-Aug 95
KAFB-0214	Apr 92-Dec 93
KAFB-0215	Apr 92-Dec 93

KAFB-0216	Aug 92-Dec 93
KAFB-0217	Aug 92-Dec 93
KAFB-0218	Jul 92-Dec 93
KAFB-0501	Jan 91-Dec 95
KAFB-0502	Jan 91-Dec 95
KAFB-0503	Jan 91-Dec 95
KAFB-0504	Jan 91-Dec 95
KAFB-0901	Dec 90-Nov 95
KAFB-0902	Dec 90-Nov 95
KAFB-1001	Jul 92-Jun 96
KAFB-1002	Jul 92-Jun 96
KAFB-1003	Jul 92- Dec 93
KAFB-1004	Jul 92- Dec 93
KAFB-1005	Jul 92-Jun 96
MVMWJ	Jul 89-Dec 95
MVMWK	Jul 89-Dec 95
TA2NW1595	Sep 93-Sept 95
San Jose 3	Mar 90-Sep 93
San Jose 9	Mar 90-Sep 95
KAFB-310	Mar 91-Mar 95
Chava	Mar 90- Mar 95
SBLF-1	Mar 90- Mar 95
SBLF-4	Mar 90- Mar 95
Yale 3	Mar 90- Mar 95

This page intentionally left blank.

4.0 GROUNDWATER FLOW MODEL CALIBRATION

Calibration of a groundwater flow model is the process of adjusting model parameters until the model reproduces field-measured values of head and flow rates. Successful calibration of a flow model to observed heads and flow directions enables the model to be used in the prediction of groundwater flow paths and heads.

Model calibration is judged by quantitatively analyzing the difference (called a residual hereafter) between observed and model-computed values. Several statistical and graphical methods are used to assess the model calibration. These statistics and methods are described in greater detail in ASTM (American Society for Testing Materials) standards D5490-93 "Comparing Ground-Water Flow Model Simulations to Site-Specific Information". The mean error (ME) is defined as:

$$ME = \frac{1}{n}\sum_{i=1}^{n}(h_m - h_s)_i \qquad \textbf{(4.1)}$$

where
h_m is measured hydraulic head, and
h_s is simulated hydraulic head.

A positive mean error indicates that the model has systematically underestimated heads, and a negative error indicates the reverse. It is possible to have a ME near 0 and still have considerable errors in the model (i.e., errors of +50 and -50 give the same mean residual as +1 and -1). Thus an additional measure, standard deviation (SD) of the errors, is used to quantify model goodness of fit. It is defined as follows:

$$SD = \sqrt{\frac{1}{n}\sum_{i=1}^{n}(h_m - h_s)_i^2} \qquad \textbf{(4.2)}$$

A large SD means that there is wide scattering of errors around the mean error.

Finally, the sum of the residuals squared is used as the objective function in parameter estimation and is defined as:

$$SS = \sum_{i=1}^{n}(h_m - h_s)_i^2 \qquad \textbf{(4.3)}$$

In addition to summary statistics, calibration is also assessed using a variety of graphical methods. Two commonly used graphical methods to assess model calibration are a plot of observed versus simulated water levels and a histogram of the errors. If the observed and simulated water levels matched exactly (i.e. perfect calibration), the data would fall on a straight line with a slope of 1. In a real-world calibration, however, there will be some scatter of residuals about the line of perfect match. Bias is revealed by clustering of data above (overprediction, or too wet) or below (underprediction, or too dry) the perfect-fit line. A histogram is useful for diagnosing the variability of model errors.

The time periods for calibration and the available targets were discussed in section 3.2. These measurements have an inherent error component due to instrument and sampling scale limitations. It is important to define the level of plausible uncertainty in order to know when the model calibration is as good as warranted by the data and to set goals in the context of the above statistical measures.

There are several types of errors associated with water-level measurements and their calculation by a model. These errors require realistic assessment so that achievable accuracy can be quantified. Errors associated with field measurements are typically about 0.04 ft, and elevation surveys commonly accumulate errors that average about 0.1ft (Anderson and Woessner, 1992). Another type of error is that related to the scale of measurement of an observation well. Averaging of water levels occurs over the portion of a well open to the aquifer. A well completed in only part of an aquifer may give a different value than a fully screened well at the same location. For instance, CWL MW-6U and CWL MW-6L are located about 20 ft apart at ground surface, with screens separated by 55 ft vertically, and have groundwater levels about 3 ft different. Error from small-scale heterogeneity that cannot be modeled may also occur. This is because the grid blocks in a model represent average properties within the block, but field measurements may be influenced by small-scale variations. Gelhar (1986) presents a technique for estimating what this error is for a three-dimensional flow system. The error from unaccounted-for, small-scale heterogeneity is estimated at about 0.6 ft. Finally, if the calibration target location does not coincide with the center of the grid block, there will be an interpolation error. A maximum interpolation error of between 0.65 and 4 ft is estimated from block size of 650 and 3000 ft, respectively. The sum of all the above errors is 4.74 ft. Alternatively, a general rule of thumb is that no target should have an error greater than 10 to 15% of the total measured change in head across the model domain. The total measured change for the calibration period is 94 ft giving an allowable error of 9.4 ft.

Based upon the calibration goal, the following calibration criteria were established:

- The ME be less than 10 percent of the total measured head change, or 9.4 ft.
- The ratio of the SD to total head change be less than 10 percent, for a SD of 9.4 ft.
- The SS be about the calibration level squared times the number of observations in the SNL/KAFB model, or 110,000 ft^2.

Table 4.1 summarizes these goals and what was achieved during calibration.

4.1 Parameter Estimation Technique

Two approaches are typically used to calibrate models: trial-and-error and automated inverse procedures. The trial-and-error approach is tedious and subject to the analyst bias (Anderson and Woessner, 1992). The automated inverse procedure is similar to the trial-and-error approach in that a large number of simulations are run to determine model sensitivity to selected parameters. However, the inverse procedure checks the computed heads and adjusts the model parameters in a systematic fashion to minimize the deviation between observed and computed heads. The advantage to using an automated calibration technique is that it provides a structured, systematic approach to the calibration process, and it allows the analyst to focus more on conceptual model development (Anderson and Woessner, 1992; Olsthoorn and Kamps, 1996). In addition, inferences can be drawn from the results of the appropriateness of the model conceptualization in describing the physical system when an automated inverse method is used (Poeter and Hill, 1996). For instance, extremely large confidence intervals around the estimated value can reveal that the problem is not well constrained by the data.

Most of the calibration was done by trial and error by identifying facies distribution and then assigning representative values for model parameters derived from site-specific and regional data. A limited automated inverse analysis was conducted to aid in refining parameter values and to test the conceptual model and the resulting distribution of associated parameters.

The PEST (parameter estimation) code by Watermark Computing, Inc. version 1.08 was used in conjunction with MODFLOW to perform parameter estimation. PEST uses a nonlinear regression procedure known as the Guass-Marquardt-Levenberg technique (Watermark 1994; Hill 1992) to minimize the deviations between a set of observations and model-computed results. PEST works by taking control of MODFLOW and modifying its data sets as it runs. For more details see the PEST User's Guide (Watermark 1994).

4.2 Calibration Results

4.2.1 Initial U.S. Geological Survey Model Results

The initial model based upon USGS regional data did not match well. In particular, the impact of pumping was too subdued, and the draw-down trough was poorly developed. Water-levels were systematically overpredicted, although the gross flow field flow direction was correct. A plot of observed versus model computed water levels is shown in Figure 4.1. Figure 4.2 shows a histogram of the residuals. About 45% of the observations are within the error bound established; however, there is a strong bias toward overprediction as can be seen by the large amounts of data on the left of the plot. The summary calibration statistics were ME of -7.6 ft, SD of 9.65 ft, RSS of 230,000 ft^2, and a ratio of SD to total head change of 10.2% (see Table 4.1). Figure 4.3 shows the simulated and mapped flow field in model layer 4, which is reasonably representative of the regional system and has the most data. Plates 2 and 3 show the distribution of model parameters.

4.2.2 Changes to the Model

Based upon the conceptual model developed by the SWHC Project, the following major changes were made to the numerical model:

- An extensive north-south oriented region over most of SNL/KAFB was treated as axial channel deposits.
- Low hydraulic conductivity sediments representative of alluvial fan deposits (measurements taken at CWL) were added along the eastern margin of the model.
- Recharge along Tijeras Arroyo was reduced by over an order of magnitude to the value of 2.2×10^6 ft^3/yr estimated by the SWHC Project.

The impact of recharge along Tijeras Arroyo was further investigated by using the SWHC conceptual geologic model with both the USGS and SWHC estimates of recharge.

4.2.3 Transient Calibration (January 1, 1980 to March 31, 1995 Data)- USGS Tijeras Arroyo Recharge

Figure 4.2 shows a histogram of the residuals. Of the 1,378 calibration targets, about 43 percent were within the error bound established, with some bias towards overprediction (too much water in the model). The distribution of errors shows less bias than the base USGS model with less spread in the overall errors.

A plot of the observed versus model computed water levels for January 1980 to March 1995 is shown in Figure 4.4. In general, the data are scattered symmetrically around the line of perfect match, although overall there is an overpredictive (too wet) bias. The group of points at the upper right hand of the plot is the data from KAFB-9. The model match to this point could be improved by increasing hydraulic conductivity in the area.

The simulated and mapped water levels in layer 4 are shown in Figure 4.5. In general the observed and simulated water levels match reasonably. The quantitative calibration criteria established in section 3.3 are all met or exceeded, with the mean residual of -2.91 ft, SD of 6.31 ft, SS of 74,400 ft^2, and ratio of SD to total observed head change of 6.7 percent (see Table 4.1); therefore the model is considered calibrated to existing conditions. The distribution of hydraulic conductivity and leakance for this model is shown in Plates 4 and 5.

4.2.4 Transient Calibration (January 1, 1980 to March 31, 1995 Data)- SWHC Project Tijeras Arroyo Recharge

A plot of the observed versus model computed water levels for January 1980 to March 1995 is shown in Figure 4.6. Simulated and observed hydrographs are shown in Appendix A. In general, the data are scattered symmetrically around the line of perfect match, although overall there is an underpredictive (too dry) bias. The group of points at the upper right hand of the plot is the data from KAFB-9. Figure 4.2 shows a histogram of the residuals. About 45% of the errors are within the established bounds, with some underpredictive (too little water in the model) bias present.

The simulated and mapped water levels in layer 4 are shown in Figure 4.11. The quantitative calibration criteria established in section 3.3 are all met or exceeded, with the mean residual of 4.25 ft, SD of 6.36 ft, SS of 90,100 ft^2, and ratio of SD to total observed head change of 6.7% (see Table 4.1); therefore, the model is considered calibrated to existing conditions. The distribution of hydraulic conductivity and leakance for this model is shown in Plates 6 and 7.

4.2.5 Final Sensitivities

The calibrated model has over 100 different inputs that describe the hydrogeologic regime and could be adjusted to improve calibration. Obviously, some assessment of which parameters are important is required to understand the important aspects of the numerical implementation of the conceptualization. This was done by perturbing the parameter and noting the resulting change in the SS. From this a sensitivity coefficient was computed as follows (Freeze and Reeves, 1996):

$$S_i = \frac{|\Delta SS|}{\Delta \text{parameter}_i} (\text{initial parameter}_i \text{ value})$$

Note that this is the ratio of the absolute value of the incremental change in SS divided by the fractional change in the parameter value. This removes the difference that occurs when comparing results from parameters that have many orders of magnitude differences and different units (e.g. recharge with a value of 0.001 and transmissivity with a value of 1,000's). Other forms of sensitivity analysis are described in ASTM Standard Guide D5611-94 "Conducting a Sensitivity Analysis for a Ground-Water Flow Model Application". It is important to note that the sensitivity of a parameter may change as its value does. A parameter that initially is too high may not show any sensitivity over the initial range investigated, but as its value is lowered it may become sensitive.

Table 4.2 shows the results of this sensitivity analysis for 26 of the numerical model parameters. The most sensitive parameters are initial head, specific yield, leakance zone 2660 (corresponds to a value of 2.663×10^{-4} 1/d) hydraulic conductivity zone 4 (alluvial fan near TA-V in the northeast quadrant of the model), and specific storage in layers 6 to 11. The deposits of the Rio Grande to the west of the axial channel deposits are also sensitive, probably because they control the influence of the Rio Grande on the shape of potentiometric surface. Since the model is somewhat sensitive to the representation of these deposits, it would seem reasonable that the Rio Grande fault system in the same general area should also be a sensitivity parameter. That this is not observed suggests that the representation of the fault may be inadequate.

Historical initial steady-state heads are not known outside of the inner Rio Grande valley; any uncertainty from this source is not reducible. The sensitivity of specific yield and specific storativity confirms the conceptual model that has large amounts of flow from storage (i.e. dewatering the basin) as the primary source of water pumped from the SFG. Specific yield and specific storativity were assumed by the USGS. Comparison of SWHC Project pumping tests with the assumed value of specific storage suggests that it is reasonable. However, the model is more sensitive to specific yield than specific storage (which is reasonable since more water is released from storage per unit decline of the potentiometric surface under water table than confined conditions), which is not well characterized on SNL/KAFB or in the basin in general. Thus it is likely that compensating errors between storativity, transmissivity, and water budget exist.

To some extent the sensitivity of parameters is controlled by the distribution of the data. For instance, where Tijeras Arroyo runs near TA-2 (see Figure 1.1) hydraulic gradients are steep, and observation wells tend to be clustered. This combination means that slight parameter changes can produce large changes in the potentiometric surface shape, greatly affecting a relatively large amount of the calibration data.

4.3 Flowpath Analysis

Particle tracking analysis with the calibrated flow field was conducted to assess groundwater pathways and containment. The trajectories of these particle tracks generally describe the migration of dissolved constituents in groundwater. It is possible that local preferential flow paths can cause the true paths to be different than those estimated by the model. However, the general flow paths should be similar to those suggested by the model results.

The MODPATH program (Pollock, 1989), a companion program to MODFLOW, was used for the particle tracking analysis. MODPATH uses the computed water levels and flow rates between cells to calculate an average interstitial velocity. In general, the velocity can be computed as follows:

$$V = K\, I / n$$

where

V is the average velocity of a particle of water (ft/d),

K is the hydraulic conductivity (ft/d),

I is the hydraulic gradient (ft/ft),

n is the effective, or connected, porosity through which water flows (dimensionless).

Table 4.3 shows the starting locations, discharge points, and travel times for groundwater from various locations on SNL/KAFB. A uniform, effective porosity of 0.2 was assumed for all layers. Note that if the porosity were higher, the travel time would be longer. Figure 4.8 shows the particle trajectories. The ultimate discharge points are the KAFB and Ridgecrest well fields, at the northern area of the model. These supply wells have a dramatic regional-scale impact on the potentiometric surface.

Travel times for all particles are in excess of 50 years. The location furthest from the model's northern edge and the supply wells had the lowest travel time (the Chemical Waste Landfill). The location closest to the northern edge had the longest travel time (Technical Area 2). This occurred because the groundwater particle released at the CWL flowed only a short distance in low permeability deposits before entering the ancestral Rio Grande axial channel deposits in which groundwater flows much faster. The groundwater particle from TA-2 flowed entirely through low permeability deposits associated with the Tijeras Arroyo alluvial fan. These results illustrate some main points of the SWHC conceptual model.

4.4 Sources of Error and Model Limitations

A model is an approximation of a real-world system. Simplifications are inherent in the construction of a model and may result in application limitations.

The use of specified-flow boundaries representing connection to the north and south of the ABM is another potential source of error. Since the ABM steady-state model was not recalibrated with the revised aquifer properties at SNL/KAFB and the simulation rerun in its entirety, the possibility exists for some inconsistency between flows and aquifer properties. However, the model was able to be calibrated while reasonably honoring site-specific geologic and hydraulic test data, which implies that any inconsistency is minor. Insufficient water-level data exists to make a more detailed assessment of this potential problem. Since the model matches the data reasonably well, any error associated with these boundaries would result in misspecification of model parameters rather than a change in results and conclusions.

ASTM Standard Guide D5611-94 "Conducting a Sensitivity Analysis for a Ground-Water Flow Model Application" describes several types of sensitivity, and in their terminology, the sensitivity of the specified-flow boundaries would be termed a Type I or Type II sensitivity. In a Type I sensitivity, variation of an input causes insignificant changes in model calibration and conclusions drawn from the model. The sensitivity analysis described in section 4.2.4 shows that the model is sensitive to these boundary flows. Thus a Type II sensitivity, when variation of an input parameter causes significant changes in model calibration but insignificant changes in conclusions drawn from the model, is attached to the specified-flow boundaries. If, for instance, flow through the northern boundary was really 50 percent higher, it is probable that the model would not be calibrated, voiding any conclusions until its recalibration, which, if it met the established calibration goals, would show the same features observed in this calibration. Thus the conclusions would remain unchanged. If the model showed little sensitivity to such flow, the conclusions would also remain unchanged.

Another assumption was the assignment of water pumped from the production wells to discrete model layers. Production wells in the Albuquerque Basin may be screened over long portions of the aquifer, with no attempt to isolate productive intervals. Thus, flow into the wells would come from many poorly defined intervals. A common method of allocating pumpage among multiple layers is to apportion the flow based upon transmissivity of each layer. Thorn et al. (1993) allocated flow to each model layer based upon the proportion of the screen in a layer to the total screen length. The effects of incorrect production well extraction of water from a layer would be to affect estimated hydraulic conductivity and leakance. If, for instance, too large a flow was allocated to a layer, a compensating error in the form of increased hydraulic conductivity would be the result. Over the scale of the basin and the level of detail of the model, any error introduced by pumping misspecification is probably minor, and, in any event, insufficient data exists to quantify this error. A Type I sensitivity is probably associated with this aspect of the model.

Some subtle aspects of the conceptual model cannot be tested, except in an exclusionary sense. For instance, mappings of the USF suggest axial channel deposits are present in the southwest part of the CWL. There is a strong contrast in hydraulic gradient across the area, which also suggests a strong contrast in hydraulic properties. The uppermost water-bearing unit in alluvial facies south of Tijeras Arroyo consists of up to 50 ft of silty clay. Below this interval is an interval of approximately 85 ft that includes several sand layers, each about 10 to 15 ft thick. In the TA-III/V area there are monitoring wells completed in one of the underlying sand units. This hydraulic conductivity of these units is 100 to 1,000 times higher, and the hydraulic head is lower than the head in the overlying fine-grained unit. At the CWL, monitoring wells completed in a deeper sand interval and separated by a horizontal distance of up to 300 ft responded together during a pumping test. This indicates that the sand intervals are relatively continuous at the scale of the CWL and may be connected to the fluvial deposits to the west, which would allow preferentially more flow through these units. Introduction of a higher hydraulic conductivity material in the southwestern and south central area of the CWL, which before this change were over 30 ft too high, was able to bring simulated heads into reasonable agreement. Thus, it appears that some kind of higher hydraulic conductivity sediments are an important feature in this area, but it is not possible to say whether they are fluvial or alluvial.

One issue is whether the faults on SNL/KAFB are low- or high-permeability features. Available data do not strongly support either interpretation. Haneberg (1995) reported on modeling results that he suggested were indicative that these faults are low-permeability features. However, the generic aquifer system Haneberg considered was for confined aquifers with head differences across faults being piezometric, rather than elevational (free surface) heads. While the SNL/KAFB-area aquifers do behave as though they are confined, most often free water is present in the aquifer materials at the height of the peizometric surface, suggesting that the aquifers are only partially confined. Sensitivity analysis showed that, at least with the current representation, the conceptual model is not sensitive to the faults. Part of the difficulty is that the faults are represented by 1 to 3 blocks of lower hydraulic conductivity material embedded in an area where hydraulic conductivity is an order of magnitude or more greater. Because of averaging of properties between blocks (see McDonald and Harbaugh 1988) to compute effective interblock parameters, a single low permeability block does not have the full effect. It might be more appropriate to use the horizontal flow barrier package (Hsieh and Freckleton 1993) to represent the faults as line features.

Since the model boundary flows are derived from the ABM, their use for any long term forecasts must be considered carefully, since the boundary flows will largely control the draw down and flow pattern within the SNL/KAFB. The primary purpose of the SNL/KAFB model was to explore and test various conceptualizations of the area and not act as a long-term predictive tool. It would be better for long term predictions to rely on the ABM after it has been updated and recalibrated to include the new information collected in the SNL/KAFB area.

4.5 Monte Carlo Analysis

In trial-and-error and automated solutions of the inverse problem, discrete sensitivity analysis is used to analyze uncertainty in the solution due to incomplete data. The framework of stochastic analysis was developed to address the role of natural variability and its influence on subsurface processes. In this approach, the heterogeneity is represented in terms of random hydraulic parameters characterized by a limited number of statistical parameters. These random parameters are then input to the classical equations that describe groundwater flow. The resulting predictions are then represented by probability distributions or in terms of statistical moments (i.e. mean and variance). Analytical stochastic solutions exist for simple system configurations, but the complex heterogeneity often encountered in reality requires numerical methods.

There are several methods that can be used to perform such an analysis, including the Monte Carlo, first order uncertainty analysis, and response surface analysis (Peck et al. 1988). Peck et al. (1988) indicate that the Monte Carlo method is possibly the most powerful method available for uncertainty analysis because it requires fewer assumptions than other methods. The modification of MODFLOW by Ruskauff (1994) for Monte Carlo analysis was used. The model input parameters are varied according to preselected probability distributions (or geostatistically simulated spatial distributions) and use the numerical model (MODFLOW) to propagate this variability or heterogeneity into variation in the results using the groundwater flow model as the transfer function. Each new sampling of the input variables is called a realization, and is a single simulation performed with a deterministic model using a particular set of input values. The essentially infinite set of possible variations is called the ensemble. The variability of the results can be analyzed to assess the likelihood of the event of interest occurring.

Zimmerman et al. (1991) proposed a slightly altered form of Monte Carlo simulation in which certain runs were selectively excluded from the analysis. The simulations in which model-predicted head compared poorly with observed head were excluded. The term post-conditioning has been coined to describe this process. The rationale for this exclusion was that the poor match resulted from unrealistic transmissivity realizations inconsistent with the conceptual model. The basis for comparison was a simple hand-calibrated model. Deutsch and Journel (1993) also describe a similar procedure. They state that selecting realizations based on some data not initially input to the model (e.g. a known range in travel time between two points) amount to further conditioning by additional unused information. The realizations selected in this manner are better conditioned to actual data and are better models of the phenomenon being analyzed.

The approach used here embodies the notion, as described above, that a given realization must have some reasonable agreement with reality. Unlike the above approaches, all realizations were kept, but the reasons for poor agreement (or improved calibration) were examined to gain insight into uncertainty in the conceptual model.

A difficulty with the Monte Carlo procedure is determining how many realizations to generate, which is not a trivial consideration for transient simulations as large as the SWHC model. Clifton and Neuman (1982) found that about 300 realizations were sufficient to establish a reasonable level of uncertainty. Jacobson et al. (1985) found that 100 realizations were insufficient to characterize variability. Nichols and Freshley (1993) generated 50 to 70 realizations of a one-dimensional unsaturated flow and transport model to investigate the contribution to travel-time uncertainty from several variables. A total of 50 realizations were generated of the SWHC model. Following the approach of Nichols and Freshley (1993), the purpose of this analysis was more reconnaissance than rigorous determination of statistical fluctuation, and in any case even 50 realizations produced large amounts (>900 MB) of output to be analyzed.

The realizations were generated by drawing samples from the parameters shown in Table 4.4. The parameters to be uncertain were selected based on the sensitivity analysis (see Table 4.2) and availability of data. Ancestral Rio Grande deposits, for instance, in the layers 6 and lower were sensitive, but no data exist as to their properties, thus they were not included. Initial heads were very sensitive but were not included because they are not part of the conceptual model. The sampled value of the parameter was applied to all locations in the model that corresponded to the property of interest (see Ruskauff [1994] for a discussion on sampling strategies). For instance, in sampling ancestral Rio Grande axial channel deposits, a value is drawn from the distribution and then inserted into the model in all places where those deposits occur. The choice of distribution type, range, and variability should ideally be made from statistical analysis from data in the area of interest. However, even the characterization performed by the SWHC Project does not provide sufficient data to perform such an analysis. Typically it is assumed (often with little justification) that hydraulic conductivity is lognormally distributed, with a characteristic tail of high values and with zero an inadmissible value. Young et al. (1991) evaluated the univariate distribution of hydraulic conductivity at a site and concluded that the hypothesis of lognormality could not be theoretically justified. They also concluded that from a practical standpoint, assuming lognormality was reasonable, but the standard assumption of lognormality for hydraulic conductivity should be evaluated on a site-specific basis and with regard to the project objectives.

The objectives of the Monte Carlo analysis were to examine model uncertainty and the interactions between parameters. In this sense, simple distributions are easier to justify. Also, normal distributions will tend to produce values clustered around the mean, which, if the distribution were actually known, would be reasonable, with the occasional extreme value providing unusual results. Ruskauff (1996) performed a univariate statistical and geostatistical analysis on the basin pumping test data summarized by Thorn et al. (1993) and found that multiple, nonlognormal distributions existed. If anything, the individual distributions may be characterized as normal. Woodbury et al. (1995) investigated the effects of assuming the distribution in stochastic analysis. They used an expression based on the uniform distribution and Gaussian distribution to analyze outcomes of draw down from a pumping well. The results of sampling from a uniform distribution had considerably more spread than the results from a Gaussian distribution, because the Gaussian distribution will draw more values near the mean than from the extremes. They point out that it is possible to obtain bounding estimates of parameters that are used directly in a uniform distribution, but it may be difficult to obtain enough data to assign a site-specific distribution. For these reasons, simple, uniform distributions were used for all variables. The bounds for Rio Grande axial channel and Rio Grande flood plain deposits were established from the 95 percent confidence interval from inverse parameter estimation. The others were set within ranges deemed to be reasonable from SWHC Project data.

The basis for examining realizations was the SS, normalized by the calibrated model value. Figure 4.9 shows the normalized SS as a function of realization. An interesting feature of this plot is the apparent plateau of normalized SS below 1.0, which suggests some limiting value of a sensitive parameter has been reached. Figures 4.10 to 4.14 show normalized SS plotted against sampled parameter value. Most of the plots suggest little relationship between normalized SS and the sampled parameter value, which indicates relative insensitivity. In Figure 4.10, for instance, both low and high values of normalized SS occur over the entire range sampled. Specific yield (Figure 4.13) shows a distinct correlation between normalized SS and sampled value. Values lower than the calibrated 0.15 cause a deterioration in fit; values greater improve it to a certain extent. Beyond values much above 0.16, model fit is not improved with increasing specific yield. Values decreasing from 0.15 steadily degrade model fit. The number of points for which normalized SS is greater than 1 (specific yield less than 0.15) in Figure 4.13 is the same as in the other figures, confirming what the sensitivity analysis suggested, that specific yield is a very sensitive parameter in the model. The scattering of results for alluvial fan hydraulic conductivity and leakance is somewhat greater than for the other parameters, thus they are influencing the results to some extent (as suggested by the sensitivity analysis).

The improvement of model fit with increasing specific yield is consistent with the fact that the model has a bias towards underprediction (too dry). Increasing specific yield allows more flow from storage to buffer the decline in heads. If a similar analysis were performed on the SWHC conceptual model with USGS recharge, the reverse would be true since that model has an overpredictive (too wet) bias. It is significant that only about a 7 percent change in specific yield has such a large impact on model results since specific yield is not known with this level of accuracy. Indeed, no specific yield data is available for the basin, and a generally plausible range of values is 0.1 to 0.25 (Johnson, 1967) for sediments such as the SFG.

Table 4.1. Calibration Criteria and Achieved Values

Criteria	Goal	Baseline USGS Model	SWHC CM, USGS Tijeras Arroyo Flow	SWHC CM, SWCH Tijeras Arroyo Flow
Mean error, ME (ft)	9.4	-7.6	-2.91	4.23
Error standard deviation, SD (ft)	9.4	9.65	6.31	6.35
Ratio of SD to total observed head change	10%	10.2 %	6.7 %	6.7 %
Sum of errors squared, SS (ft^2)	110,000	230,000	74,400	89,800

Table 4.2. Calibrated Model Sensitivity Coefficients				
Parameter	Base Value	Perturbed Value	SS (ft^2)	Sensitivity(-)
Tijeras Arroyo Recharge	$2.2x10^6$ ft^3/yr	22 x 10^6 ft^3/yr	78300	1311
K252[a], Rio Grande Axial Deposits Layers 1-5	210 ft/d	150 ft/d	90700	2100
K4, Alluvial Fan, Layers 1-5	5 ft/d	10 ft/d	77600	12500
K2, Alluvial Fan, Layers 1-2	0.01 ft/d	0.1 ft/d	89700	44
K130, Transitional, Layers 1-5	40 ft/d	15 ft/d	94000	6240
T711[b], Layer 11	2000 ft^2/d	3000 ft^2/d	98	1600
T1255, Layer 10	12000 ft^2/d	10000 ft^2/d	91100	3000
T1291, Layer 9	37500 ft^2/d	50000 ft^2/d	89600	1500
T1290, Layer 8	30000 ft^2/d	40000 ft^2/d	89300	2400
T1289, Layer 7	22500 ft^2/d	30000 ft^2/d	89400	2100
T1268, Layer 6	15000 ft^2/d	20000 ft^2/d	89700	1200
T32, Fault in layers 1-5	3.0 ft/d	0.3 ft/d	89800	333
Initial Head	Median = 4918.7	+10 ft	72800	8.5 x 10^6
K239, Layer 3-4 Rio Grande alluvium	40	60	86200	7800
L2660[c], Layers 2-4	$2.663x10^{-4}$	$8x10^{-5}$	127000	52745
L3781, Layers 2-3	0.01	0.005	89800	600
L4386, Layers 2-3	$5.8x10^{-3}$	0.001	88900	1450
L57, Layer 10	4.4445 x 10^{-5}	1 x 10^{-4}	89400	560
L1270, Layer 9	4.6154 x 10^{-4}	1 x 10^{-3}	91200	943
L2088, Layer 8	6.6667 x 10^{-4}	1 x 10^{-3}	90300	400
L2252, Layer 7	8.5715 x 10^{-4}	3 x 10^{-3}	92000	760
L2455, Layer 6	1.2 x 10^{-3}	0.05	93100	78
L2847, Layer 5	1.8265 x 10^{-3}	0.05	89800	11
Specific Storage (S_s), Layers 1-5	2 x 10-6 ft^{-1}	3 x 10-6 ft^{-1}	89500	1200
Specific Storage (S_s), Layers 6-11	2 x 10-6 ft^{-1}	3 x 10-6 ft^{-1}	84500	11200
Specific Yield (S_y)	0.15	0.25	167000	115350

[a] K denotes hydraulic conductivity zone
[b] T denotes transmissivity zone
[c] L denotes leakance zone

Table 4.3 Groundwater Travel Times and Discharge Locations for Various Locations on SNL/KAFB

Starting Location	Final Location	Travel Time (years)
Technical Area 2	KAFB-5	73
Chemical Waste Landfill	Ridgecrest 5	54
Mixed Waste Landfill	Ridgecrest 3	64
LWDS	Ridgecrest 3	70

Table 4.4 Monte-Carlo Analysis Input Parameters

Parameter	Distribution Type	Limits
K4 Alluvial Fan	Uniform	1-10 ft/d
K130 Rio Grande floodplain	Uniform	5-75 ft/d*
K252 Rio Grande axial channel deposits	Uniform	138-280 ft/d*
L2660 Alluvial Fan Leakance	Uniform	8×10^{-4} - 8×10^{-5} d^{-1}
S_y Specific Yield layers 1-5	Uniform	0.1 - 0.2

* 95 percent confidence limits from parameter estimation

5.0 DISCUSSION AND CONCLUSIONS

The conceptual model of the hydrogeology of SNL/KAFB developed by SWHC was the basis for the numerical model. The major points of the conceptual model are summarized as follows:

- Channel deposits of the ancestral Rio Grande extend through the west SNL/KAFB area in a north-south direction.
- Alluvial fan deposits extend from the east into the ancestral Rio Grande deposits.
- Sharp contrasts in hydraulic properties occur as a result of the abutment of lithologies deposited in distinctly different environments.
- Recharge occurs mainly from Tijeras Arroyo, Arroyo del Coyote, and the Manzano Mountains mountain front, with some component of flow from the bedrock.
- Sediments decrease in hydraulic conductivity with depth as the USF grades into the MSF and LSF, which were deposited under different (mainly low-energy alluvial) environments.
- The top of the aquifer is in the USF.
- Large amounts of groundwater flow are from storage release (i.e. dewatering).
- Pumpage greatly exceeds recharge from all sources (precipitation, Rio Grande leakage).
- Fault systems in the SFG probably act as restrictions to groundwater flow, abutting low-flow lithologies and cementation of the fault gouge.

The numerical model of the area near the KAFB was constructed using the USGS MODFLOW model and the ABM as a starting point. Goals for transient calibration were established using standard and accepted techniques. These goals were met during the model calibration process, which allows the model to be used to draw conclusions about the conceptual model at SNL/KAFB.

The modifications made to the USGS ABM included addition of a long, north-south strip of axial channel deposits, extending much further than in the ABM. In addition, SWHC Project estimates of hydraulic conductivity of alluvial fan material along the mountains were much lower than in the ABM, as was recharge from infiltration along Tijeras Arroyo. The ABM recharge along Tijeras Arroyo is over an order of magnitude higher than that estimated by the SWHC Project. Two models were calibrated to bracket the conceptual uncertainty caused by this difference. In the first, the recharge rate specified by the USGS was maintained and the model modified to reflect the SNL/KAFB conceptual model. For the second model, recharge along Tijeras Arroyo was reduced to the value estimated by the SWHC Project. The high recharge case required high hydraulic conductivities in the alluvial fan material where Tijeras Arroyo enters SNL/KAFB. The values were not unreasonable when compared with SWHC data from

Technical Area 2, but the model still exhibited a pronounced overprediction (too much water) in the area, which suggested that the Tijeras Arroyo flow rate in the ABM may be too high. In the low recharge case, hydraulic conductivities in the area where Tijeras Arroyo enters SNL/KAFB were very low.

The SWHC Project model differs from the ABM in several ways, and to some extent these differences reflect both additional data and a different approach taken between the USGS and SNL/NM. The USGS did not attempt to calibrate the ABM, rather the best conceptual representation was independently determined and then areas where significant deviation occurred were identified. The identified area did not include SNL/KAFB. One of the benefits of calibration (particularly automated methods) is that hypotheses can be tested. Thus for the SNL/KAFB model areas of significant model deviation were not left for future resolution. Resolution was attempted, and then the required adjustments examined to see how (if at all) they related to the conceptual model. One example of the difference in approach is in the area near the southwest corner of the CWL, where thin sheets of high hydraulic conductivity sand embedded in otherwise low hydraulic conductivity deposits and connected to axial channel deposits were thought to be "thief" zones. The model was unable to replicate the observed flow conditions until hydraulic conductivity in the area was raised to include the effects of these sands.

Travel times for all particles are in excess of 50 years. The location furthest from the model's northern edge and the supply wells had the lowest travel time (the Chemical Waste Landfill). The location closest to the northern edge had the longest travel time (Technical Area 2). This occurred because the groundwater particle released at the CWL flowed only a short distance in low permeability deposits before entering the ancestral Rio Grande axial channel deposits in which groundwater flows much faster. The groundwater from TA-2 flowed entirely through low permeability deposits associated with the Tijeras Arroyo alluvial fan. These results illustrate some main points of the SWHC conceptual model.

Deterministic and Monte Carlo sensitivity analyses were performed to examine the importance of various aspects of the conceptual model. Specific yield and specific storativity were sensitive parameters, which confirms the conceptual model that has large amounts of flow from storage (i.e. dewatering the basin) as a source of water pumped from the SFG. Initial conditions were extremely sensitive (which is correct since this a transient problem). Comparison of SWHC Project pumping tests with the assumed value of specific storage suggests that it is reasonable. However, the model is more sensitive to specific yield than specific storage (which is reasonable since more water is released from storage per unit decline of the potentiometric surface under water table than confined conditions), which is not well characterized on SNL/KAFB or in the basin in general. This situation has the potential to create large compensating errors, since both hydraulic conductivity and specific yield can be balanced for a given model boundary flux to yield the same rate of decline. It is unlikely, given these uncertainties, that much predictive power can be associated with any model of the basin. However, for the purpose of this analysis, a comparative use of the model is still reasonable.

This page intentionally left blank.

6.0 REFERENCES

Anderholm, S.K., and T.F. Bullard, 1987, Description of piezometer nests and water levels in the Rio Grande valley near Albuquerque, Bernalillo County, New Mexico: U.S. Geological Survey Open-File Report 87-122, 51 p.

Andersen, P., 1993, *A Manual of Instructional Problems for the U.S.G.S. MODFLOW Model*, EPA/600/R-93/010, RSKERL, Ada, OK.

Anderson, M.P. and W.W. Woessner, 1992, *Applied Groundwater Modeling: Simulation of Flow and Advective Transport*, Academic Press, Inc., New York.

Bjorklund, L.J., and B.W. Maxwell, 1961, Availability of ground water in the Albuquerque area, Bernalillo and Sandoval Counties, New Mexico: New Mexico State Engineer Technical Report 21, 117 p.

deMarsily, G., 1986, *Quantitative Hydrogeology*, Academic Press, San Diego, CA.

Deutsch, C. and A. Journel, 1993, *GSLIB Geostatistical Software Library and User's Guide*, Oxford University Press, New York, 340 p.

Environmental Simulations, Inc., 1996, *Guide to Using Groundwater Vistas*.

Freeze, G.A. and M. Reeves, 1996, "A deterministic sensitivity analysis method to aid conceptual model development," *Calibration and Reliability in Groundwater Modeling,* K. Kovar and P. van der Heijde, eds., IAHS Publication No. 237.

Gelhar, L., 1986, "Stochastic subsurface hydrology from theory to applications," *Water Resources Research*, (Supplement), v. 22, no. 9, pp. 135S-145S.

GMI (Groundwater Management Incorporated), 1988a, Pumping Test Data Analysis: Burton Well Field, City of Albuquerque, New Mexico, unpublished report prepared for Black & Veatch Entineers, Aurora, CO, February 2, 1988.

GMI (Groundwater Management Incorporated), 1988b, Pumping Test Data Analysis: Miles Road Well Field, City of Albuquerque, New Mexico, unpublished report prepared for Black & Veatch Engineers, Aurora, CO, February 2, 1988.

GMI (Groundwater Management Incorporated), 1988c, Pumping Test Data Analysis: Ridgecrest Well Field, City of Albuquerque, New Mexico, unpublished report prepared for Black & Veatch Engineers, Aurora, CO, February 2, 1988.

Haneberg, W.C., 1995, "Steady state groundwater flow across idealized faults," *Water Resources Research*, Vol. 31, No. 7, pp. 1815-1820, July 1995.

Hawley, J.W., and C.S. Hasse, eds., 1992, Hydrogeologic framework of the Northern Albuquerque Basin, New Mexico Bureau of Mines and Mineral Resources Open-File Report 387.

Hawley, J.W. and T.M. Whitworth, 1996, Hydrogeology of potential recharge areas for the basin- and valley-fill aquifer systems, and hydrogeochemical modeling of proposed artificial recharge of the Upper Santa Fe Aquifer, Northern Albuquerque Basin, New Mexico, New Mexico Bureau of Mines and Mineral Resources Open-File Report 402-D.

Haywood, C.E., 1992, Isostatic residual gravity anomalies of New Mexico, U.S. Geological Survey Water-Resources Investigations Report 91-4065, 27 p.

Hill, M.C., 1992, A computer program (MODFLOWP) for estimating parameters of a transient, three-dimensional groundwater flow model using nonlinear regression, U.S. Geological Survey Open-File Report 91-484.

Hsieh, P.A. and J.R. Freckleton, Documentation of a computer program to simulate horizontal-flow barriers using the U.S. Geological Survey's modular three-dimensional finite-difference ground-water flow model, U.S. Geological Survey Open-File Report 92-477, Sacramento, California.

Hudson, J.D., 1982, Water-level map of the San Jose well field and vicinity, Albuquerque, New Mexico, Spring 1981, U.S. Geological Survey Open-File Report 82-375, 2 p.

Jacobsen, E., M. Freshley, and H. Dove, 1985, *Investigations of Sensitivity and Uncertainty in Some Hydrologic Models of Yucca Mountain and Vicinity*, SAND84-7212, Sandia National Laboratories, Albuquerque, New Mexico.

Johnson, A.I., 1967. Specific yield-compilation of specific yields for various materials; U.S. Geological Survey Water-Supply Paper 1662-D.

Kaehler, C.A., 1990, Lithology of basin-fill deposits in the Albuquerque-Belen Basin, New Mexico, U.S. Geological Survey Water-Resources Investigations Report 89-4162,14 p.

Kelly, T.E., 1982, "History of water use in the greater Albuquerque area," Guidebook to Albuquerque Country II: New Mexico Geological Society, 33d Field Conference, J.A. Grambling and S.G. Wells, eds., p. 351-356.

Kelley, V.C., 1977, Geology of Albuquerque Basin, New Mexico: Socorro, New Mexico Bureau of Mines and Mineral Resources Memoir 33, 60 p.

Kernodle, J.M. and W.B. Scott, W.B., 1986, Three-dimensional model simulation of steady-state ground-water flow in the Albuquerque-Belen Basin, New Mexico, U.S. Geological Survey water-Resources Investigations Report 84-4353, 58 p.

Kernodle, J.M., R.S. Miller, and W.B. Scott, 1987, Three-dimensional model simulation of transient ground-water flow in the Albuquerque-Belen Basin, New Mexico, U.S. Geological Survey Water-Resources Investigations Report 86-4194, 86 p.

Kernodle, J.M., D.P. McAda, and C.R. Thorn, 1995, Simulation of ground-water flow in the Albuquerque Basin, Central New Mexico, 1901-1994, with projections to 2020, U.S. Geological Survey, Water-Resources Investigations Report 94-4251.

Kues, G.E., 1986, Ground-water levels and direction of ground-water flow in the central part of Bernalillo County, New Mexico, Summer 1983, U.S. Geological Survey Water-Resources Investigations Report, 24 p.

Kues, G.E., 1987, Ground-water level data for the Albuquerque-Belen Basin, New Mexico, through water year 1985, U.S. Geological Survey Open-File Report 87-116, 51 p.

Lambert, P.W., 1968, Quaternary stratigraphy of the Albuquerque area, New Mexico: Albuquerque, University of New Mexico Ph.D. dissertation, 329 p.

Lozinsky, R.P., 1988, Stratigraphy, sedimentology, and sand petrology of the Santa Fe Group and pre-Santa Fe Tertiary deposits in the Albuquerque Basin, central New Mexico: Socorro, New Mexico Institute of Mining and Technology, Ph.D. dissertation.

Mack, G.H. and W.R. Seager, 1990, Tectonic control on facies distribution of the Camp Rice and Palomas Formations (Pliocene-Pleistocene) in the southern Rio Grande rift, Geological Society of America Bulletin, v. 102, p. 45-53.

McDonald, M. and A. Harbaugh, 1988, A modular three-dimensional finite-difference ground water flow model, Techniques of Water-Resources Investigations 06-A1, U.S. Geological Survey, Reston, VA.

National Research Council, 1990, *Ground-Water Models, Scientific and Regulatory Applications*, National Academy Press, Washington, D.C.

Nichols, W. and M. Freshley, 1993, "Uncertainty Analyses of Unsaturated Zone Travel Time at Yucca Mountain," *Groundwater*, v. 31, no. 2, pp. 293-302.

Olsthoorn, T.N. and P.T.W.J. Kamps, 1996, "Groundwater model calibration for the Amsterdam Water Supply dune area," *Calibration and Reliability in Groundwater Modeling,* K. Kovar and P. van der Heijde, eds., IAHS Publication No. 237.

Peck, A., S. Gorelick, G. deMarsily, S. Foster, and V. Kovalevsky, 1988, *Consequences of Spatial Variability in Aquifer Properties and Data Limitations for Groundwater Modeling Practice*, IAHS Publication No. 175, Washington, D.C.

Poeter, E.P. and M.C. Hill, 1996, "Unrealistic parameter estimates in inverse modeling: a problem or benefit for model calibration," *Calibration and Reliability in Groundwater Modeling*, K. Kovar and P. van der Heide, eds., ModelCARE '96, IAHS Pub. No. 237.

Pollock, D., 1989, Documentation of computer programs to compute and display pathlines using results from the U.S. Geological Survey modular three-dimensional finite-difference ground-water flow model, U.S. Geological Survey Open File Report 89-381, Reston, VA.

Reeder, H.O., L.J. Bjorkland, and G.A. Dinwiddie, 1967, Quantitative analysis of water resources in the Albuquerque area, New Mexico–Computed effects on the Rio Grande of pumpage of ground water, 1960-2000, New Mexico State Engineer Technical Report 33.

Rumbaugh, J.O. and L.L. Ruskauff, 1993, Geraghty & Miller Modeling Survey, Analysis of May 1992 Survey Results, Geraghty & Miller Modeling Group, Reston, Virginia.

Ruskauff, G.J., 1994, "A Methodology for Performing Monte Carlo Analysis with MODFLOW and MODPATH," Proceedings of the 1994 Groundwater Modeling Conference, J.W. Warner and P. van der Heijde, eds., Fort Collins, CO, August 10-12.

Ruskauff, G.J., 1996, "Geostatistical Analysis of the Hydraulic Conductivity of the Upper Santa Fe Group, Albuquerque Basin, New Mexico, Subsurface Fluid-Flow (Ground-Water and Vadose Zone) Modeling," ASTM STP 1288, Joseph D. Ritchey and James O. Rumbaugh, III, eds., American Society of Testing and Materials.

Summers, W.K., 1992, Effects of Albuquerque's pumpage on the Rio Grande and the rate at which Albuquerque will have to release San Juan-Chama water to offset them, City of Albuquerque internal memorandum, variously paged.

SNL/NM, 1993, *Site-Wide Hydrogeologic Characterization Project Calendar Year 1992 Annual Report,* SAND93-0681, Environmental Restoration Program, Sandia National Laboratories, Albuquerque, New Mexico.

SNL/NM, 1994, *Site Wide Hydrogeologic Characterization Project Calendar Year 1993 Annual Report,* Environmental Restoration Program, Sandia National Laboratories, Albuquerque, New Mexico.

SNL/NM, 1995, *Site-Wide Hydrogeologic Characterization Project Calendar Year 1994 Annual Report,* Environmental Restoration Program, Sandia National Laboratories, Albuquerque, New Mexico.

SNL/NM, 1995a, *Chemical Waste Landfill Groundwater Assessment Report*, Environmental Restoration Project, Sandia National Laboratories, Albuquerque, New Mexico.

SNL/NM, 1996, *Site-Wide Hydrogeologic Characterization Project Calendar Year 1995 Annual Report,* Environmental Restoration Program, Sandia National Laboratories, Albuquerque, New Mexico.

Theis, C.V., 1938, "Ground-water in the middle Rio Grande valley," National Resources Committee, Regional Planning part VI-The Rio Grande joint investigation in the upper Rio Grande Basin in Colorado, New Mexico, and Texas, 1936-37: U.S. Government Printing Office, v.1, p. 268-291.

Theis, C.V., and G.C. Taylor, 1939, "Ground-water conditions in the middle Rio Grande valley, New Mexico," New Mexico State Engineer 12th-13th Biennial Reports, 1934-38, p. 263-271.

Thorn, C.R., D.P. McAda, and J.M. Kernodle, 1993, Geohydrologic framework and hydrologic conditions in the Albuquerque Basin, Central New Mexico, U.S. Geological Survey Water-Resources Investigations Report 93-4149, 106 p.

U.S. Army Corps of Engineers, 1979, Albuquerque greater urban area water supply study, U.S. Army Corps of Engineers, Albuquerque District, Hydrologic Engineering Center, 8 sec., 225 p.

U.S. Geologic Survey, 1993, *Installation Restoration Program, Stage 2A*, RI/FS Technical Report for Kirtland Air Force Base, USGS Water Resources Division, Albuquerque, NM.

Watermark Computing, Inc., 1994, *PEST User's Guide*, version 1.08.

Woodbury, A., F. Render, and T. Ulrych, 1995, "Practical Probabilistic Ground-Water Modeling," *Groundwater*, v. 33, no. 4, p. 532.

Young, S.C., J.C. Herweijer, and D.J. Benton, 1991, "Geostatistical evaluation of a three-dimensional hydraulic conductivity field in an alluvial aquifer," Proceedings of the 5th annual Canadian American Conference on Hydrogeology, Calgary, September 18-20, 1990, NWWA, Dublin, Ohio.

Zimmerman, D., Hanson, and P. Davis, 1991, *Parameter Estimation Techniques and Uncertainty in Ground Water Flow Model Prediction*, Sandia National Laboratories, Albuquerque, New Mexico, DOE Publication DE91 000405.

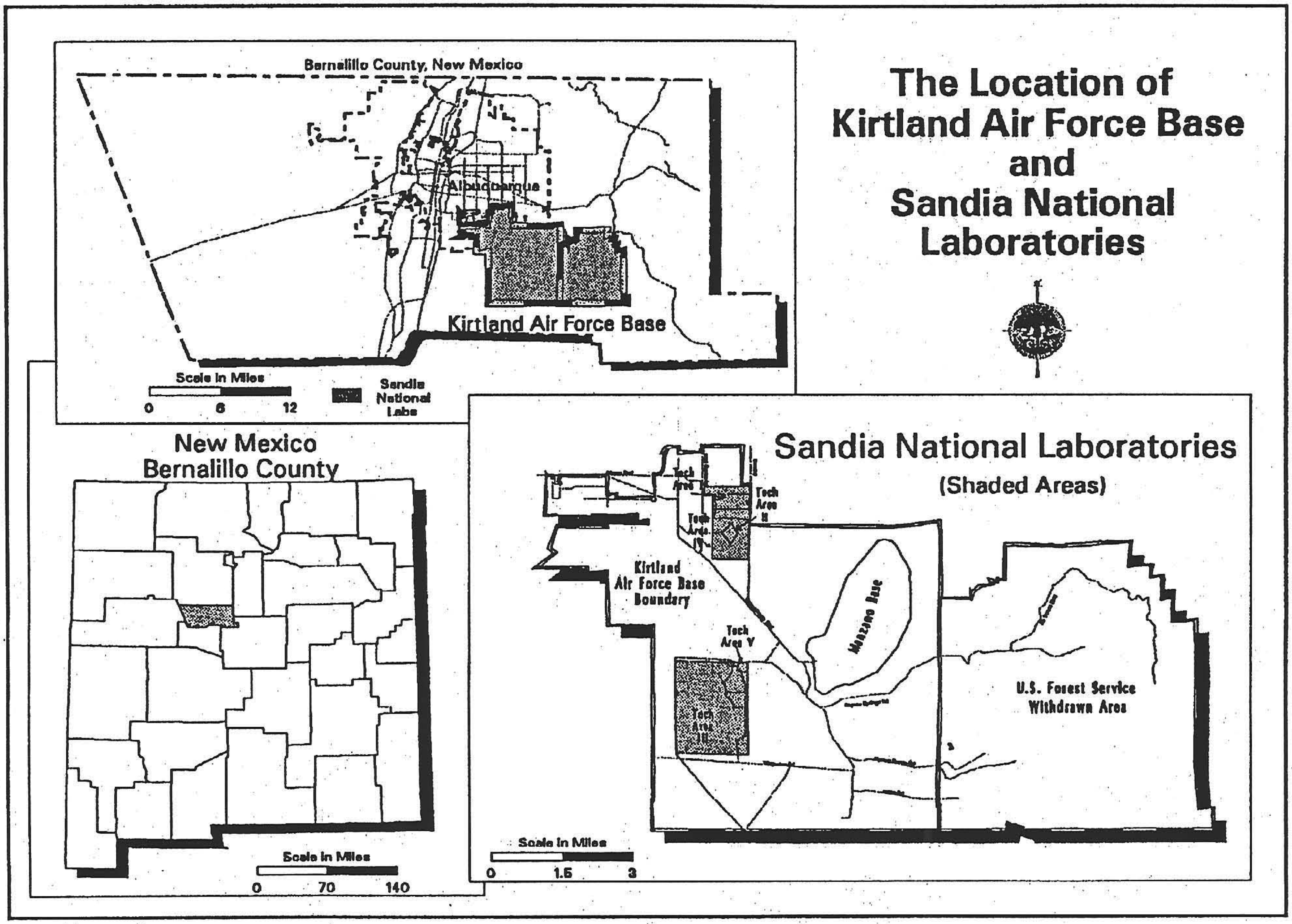

Figure 1.1. Location of Kirtland Air Force Base and Sandia National Laboratories.

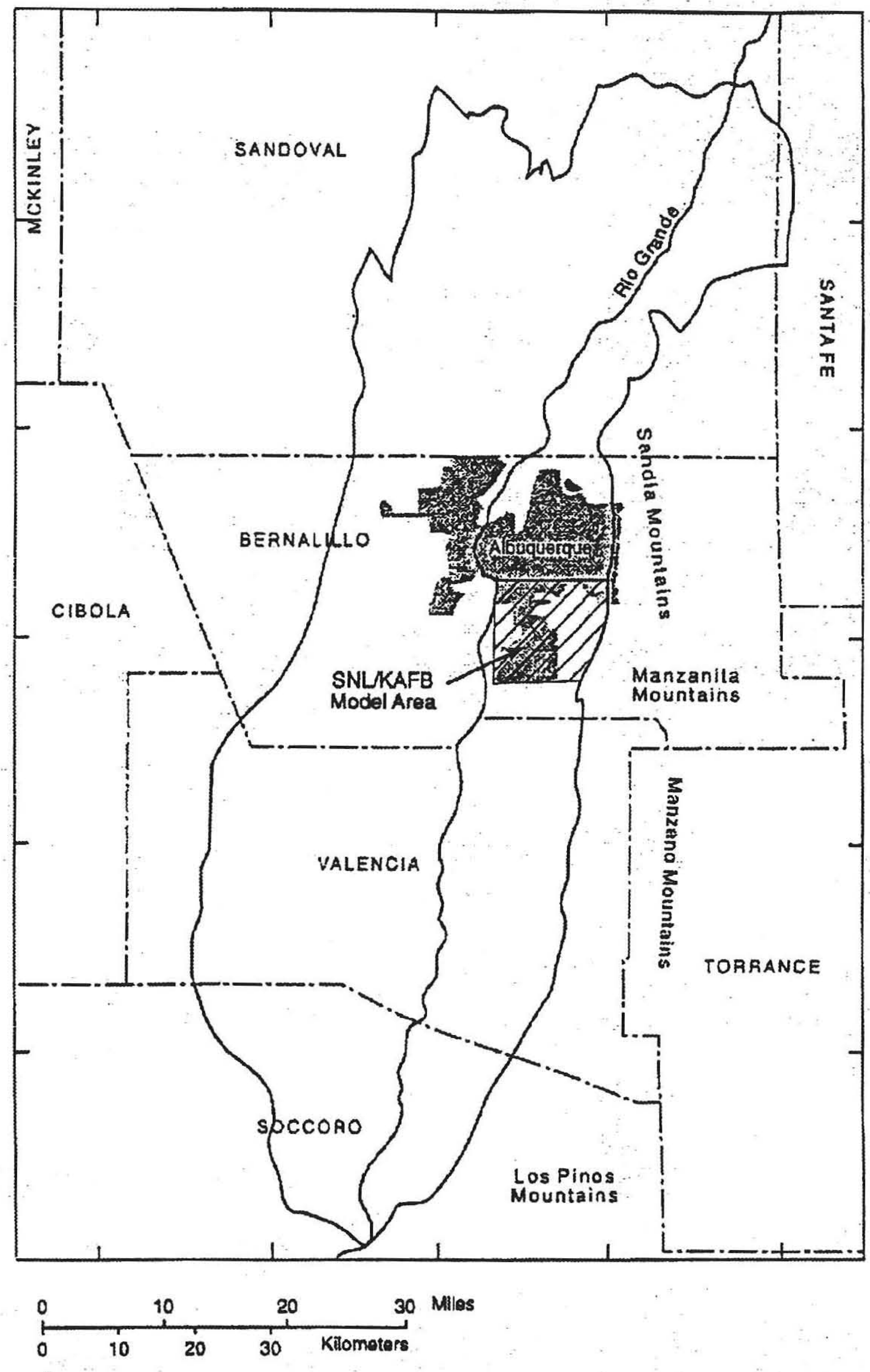

Figure 2.1. Location of the Sandia National Laboratories/Kirtland Air Force Base Model Area in the Albuquerque Basin.

ERA/SYSTEM/SERIES			UNIT/FORMATION		STRAT. COLUMN	DESCRIPTION
CENOZOIC	NEOGENE	Holocene to Middle Pleistocene	Surficial Units			Cross-bedded, fine- to medium-grained eolian sand Poorly-sorted silty sandy cobble to boulder gravel Poorly-sorted silty sandy cobble to boulder gravel with relict and buried soils *Unconformity*
CENOZOIC	NEOGENE	Early Pleistocene to Early Miocene	Santa Fe Group	Upper Santa Fe Unit		<u>Basinal</u>: coarse- to fine-grained sandstone; common buried soils <u>Marginal</u>: pebbles, cobbles in fine-grained matrix
CENOZOIC	NEOGENE	Early Pleistocene to Early Miocene	Santa Fe Group	Middle Santa Fe Unit		<u>Basinal</u>: medium- to fine-grained sandstone and mudstone; common buried soils <u>Marginal</u>; conglomeratic sandstone to pebbles and cobbles; common buried soils
CENOZOIC	NEOGENE	Early Pleistocene to Early Miocene	Santa Fe Group	Lower Santa Fe Unit		<u>Basinal</u>: medium- to fine-grained sandstone, sandy mudstones <u>Marginal</u>: conglomeratic sandstone and mudstone *Unconformity*
CENOZOIC	PALEOGENE	Oligocene	Unit of Isleta #2 Well			Fine- to coarse-grained sandstone; claystone, silt beds; volcanic detritus and ash-flow tuffs
CENOZOIC	PALEOGENE	Eocene to Paleocene	Baca/ Galisteo Formations			Sandstone, variegated mudstone, and conglomerate *Unconformity*
MESOZOIC		Upper Triassic	Santa Rosa Sandstone			Buff brown sandstone, petrified wood
PALEOZOIC		Upper Permian	San Andres Formation			Gray limestone, separated by red shale *Unconformity*
PALEOZOIC		Upper Permian	Glorieta Sandstone			Medium- to coarse-grained yellowish gray sandstone
PALEOZOIC		Lower Permian	Yeso Formation			<u>Upper</u>: gypsiferous sandstone, siltstone, and limestone <u>Lower</u>: fine-grained sandstone and siltstone
PALEOZOIC		Lower Permian	Abo Formation			Fine- to coarse-grained sandstone and conglomerate with interbedded siltstone
PALEOZOIC		Lower Permian	Madera Group	Bursum Fm.		Finely laminated silty mudstone
PALEOZOIC		Upper to Middle Pennsylvanian	Madera Group	Wild Cow Formation		Rhythmically bedded sequence: conglomerate, sandstone, siltstone, shale, and limestone
PALEOZOIC		Upper to Middle Pennsylvanian	Madera Group	Los Moyos Formation		Gray calcarenite with chert
PALEOZOIC		Middle Pennsylvanian	Sandia Formation			Fining-upwards clastic sequence: conglomerate to calcareous siltstone *Unconformity*
PRECAMBRIAN			Isleta Metasediments Tijeras Greenstone Complex Coyote Canyon Sequence Sandia Granite			Phyllite; meta-arkose; metaquartzite; greenstone; metarhyolite; quartzite; microcline and biotite granite

Figure 2.2. Generalized Stratigraphic Column of the Sandia National Laboratories/Kirtland Air Force Base Area.

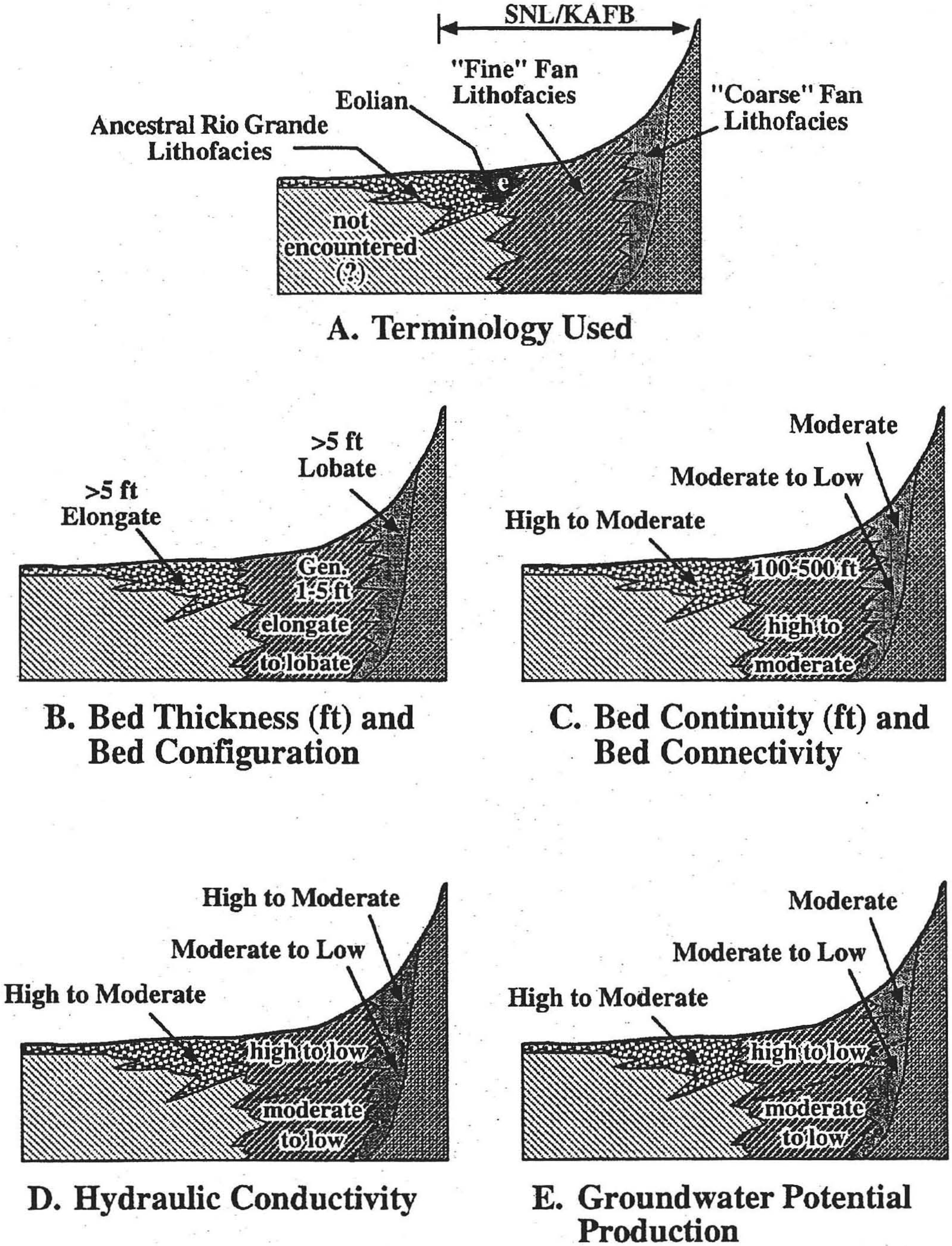

Figure 2.3. Relationship of Santa Fe Group Lithofacies to Hydrogeologic Parameters.

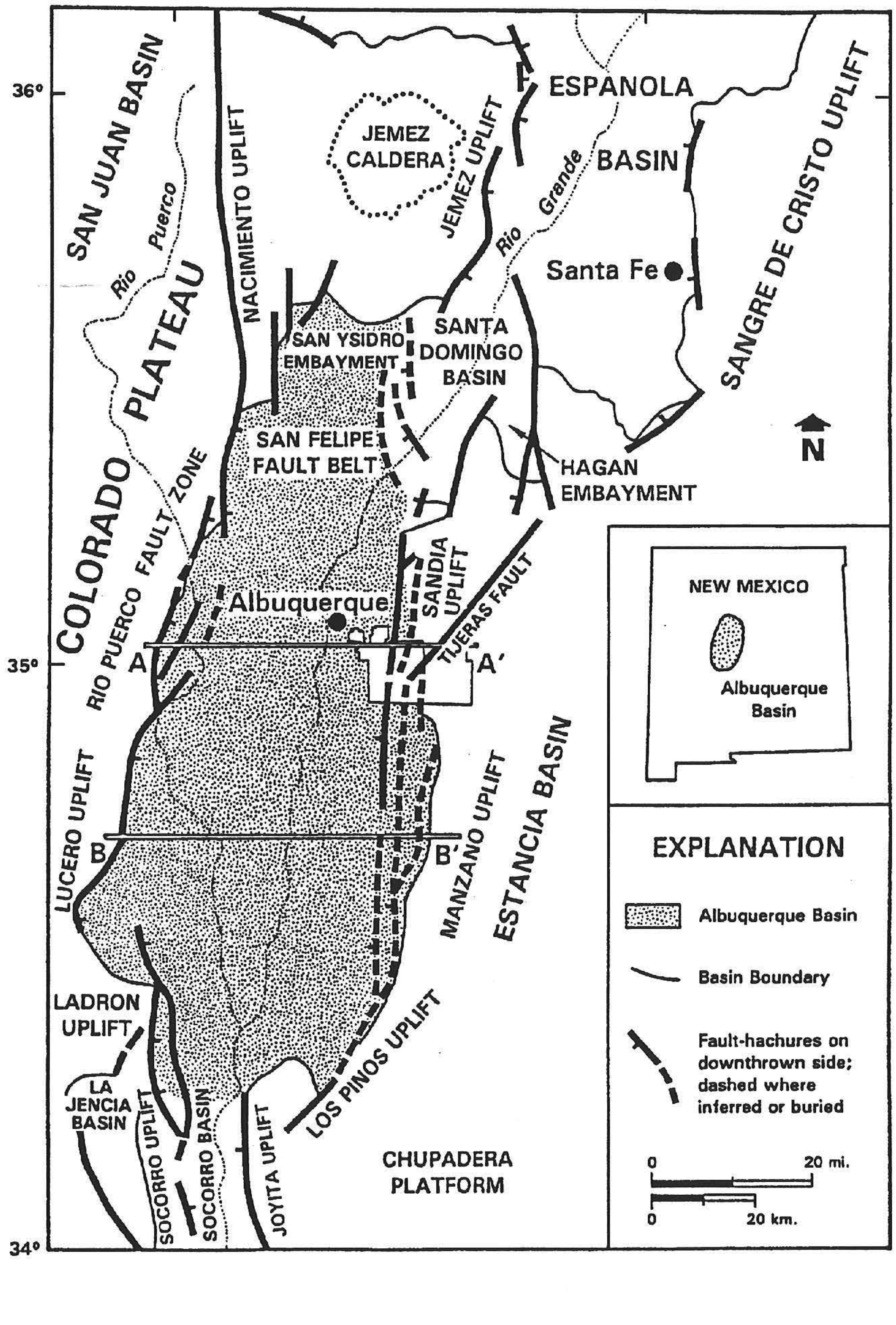

Figure 2.4. Generalized Regional Tectonic Map of the Albuquerque Basin.

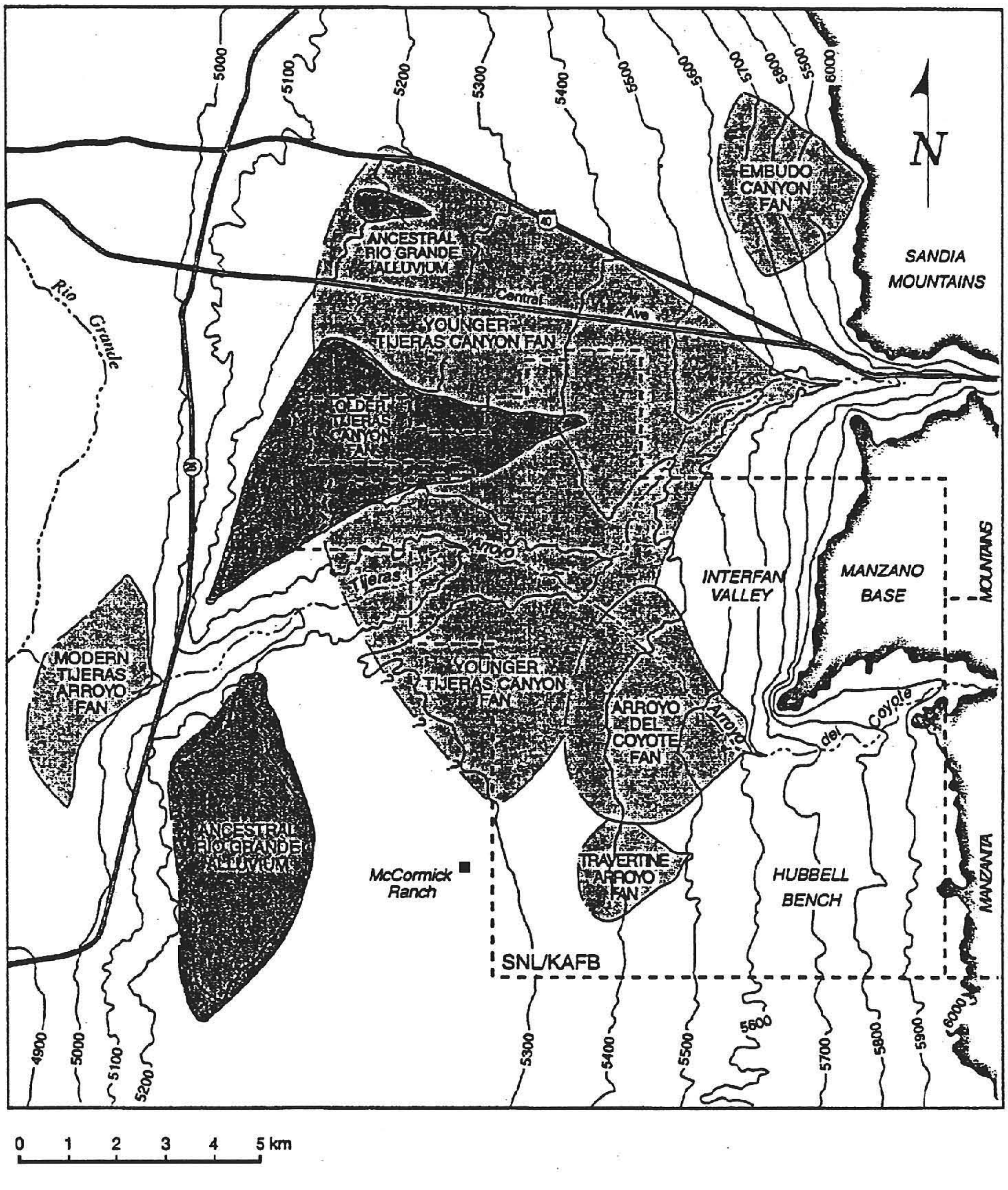

Figure 2.5. Generalized Topographic Map of the Sandia National Laboratories/Kirtland Air Force Base Area West of the Sandia and Manzanita Mountains.

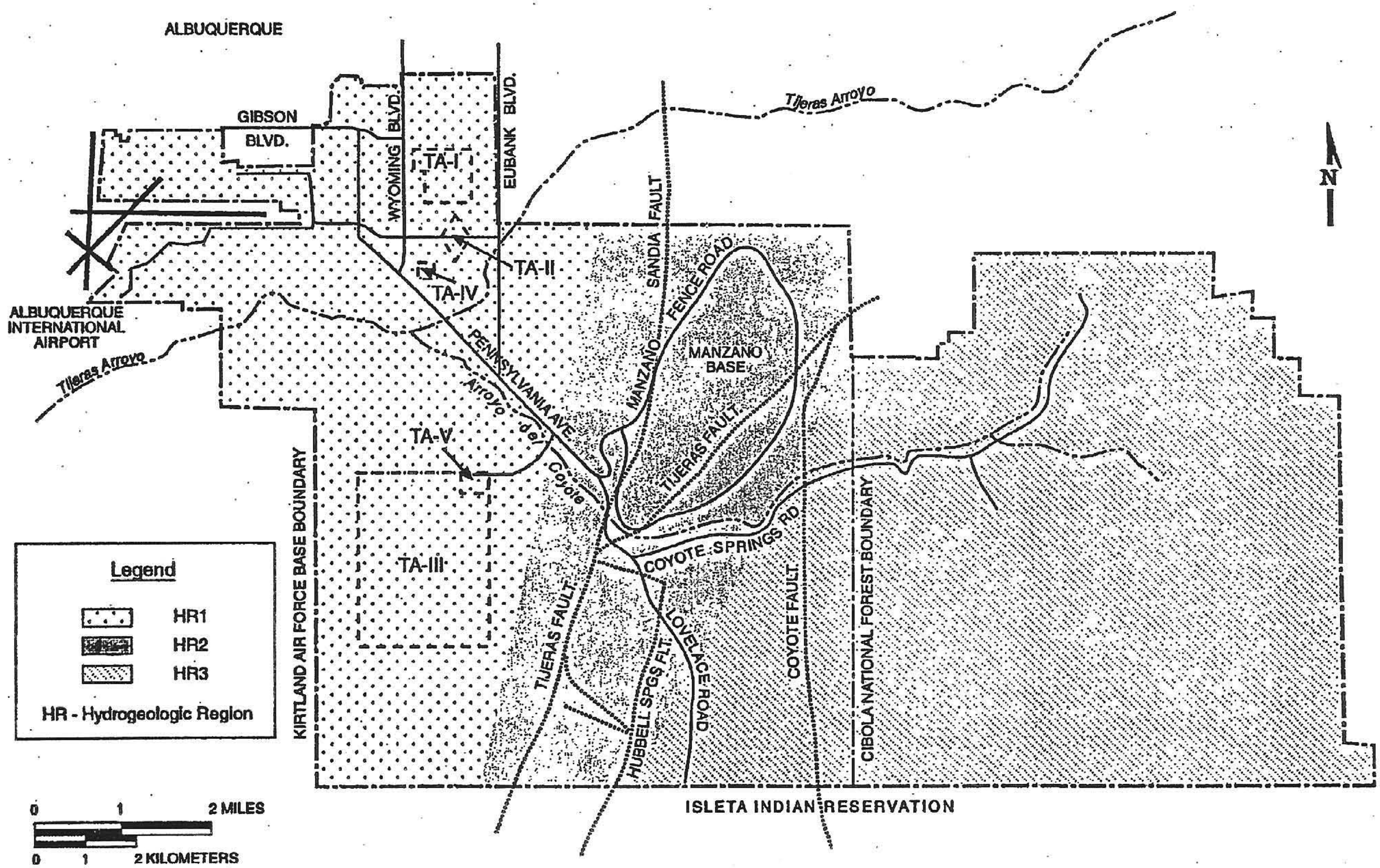

Figure 2.6. Hydrogeologic Regions Identified by Sandia National Laboratories/New Mexico.

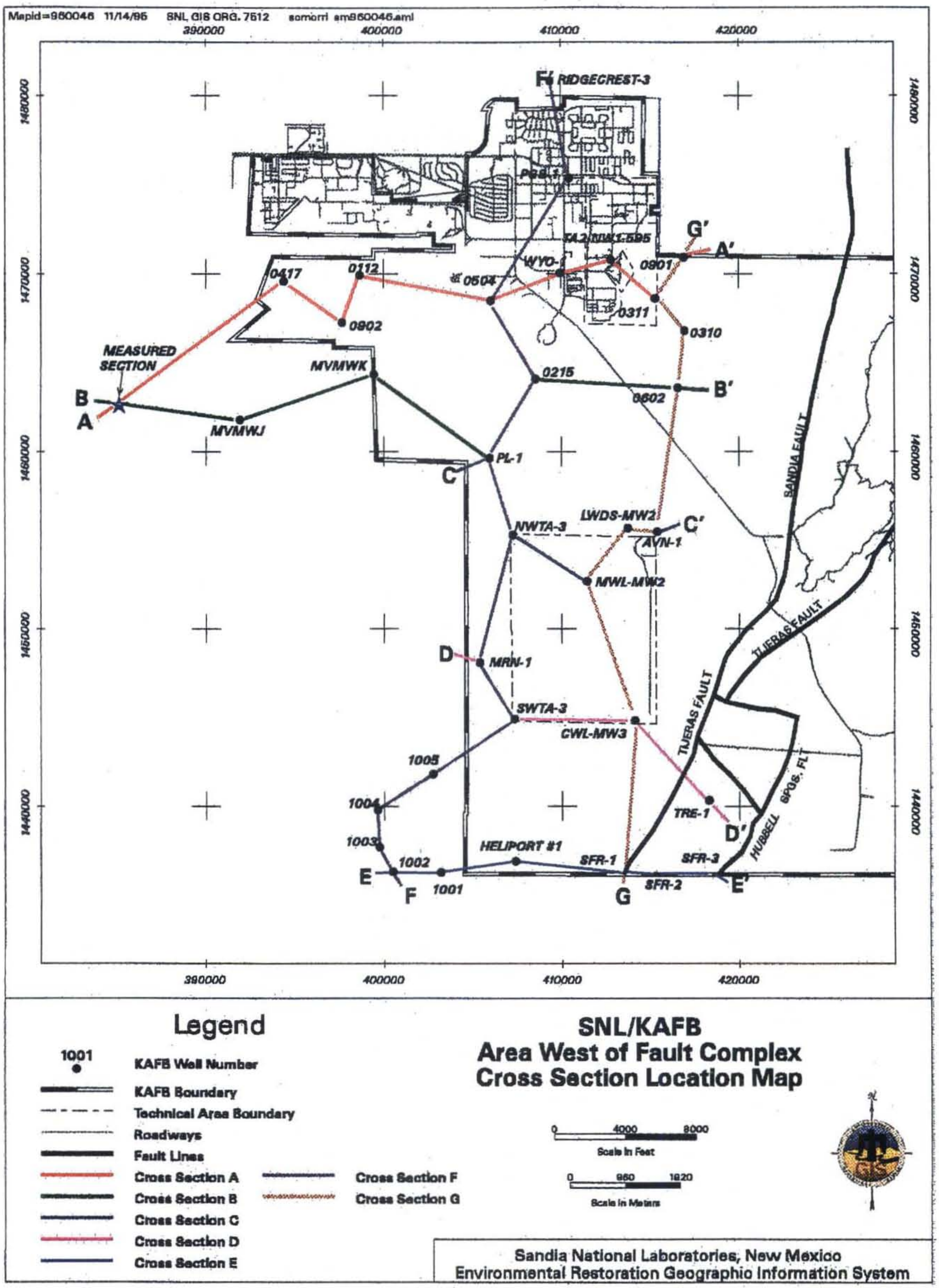

Figure 2.7 Cross Section Location Map.

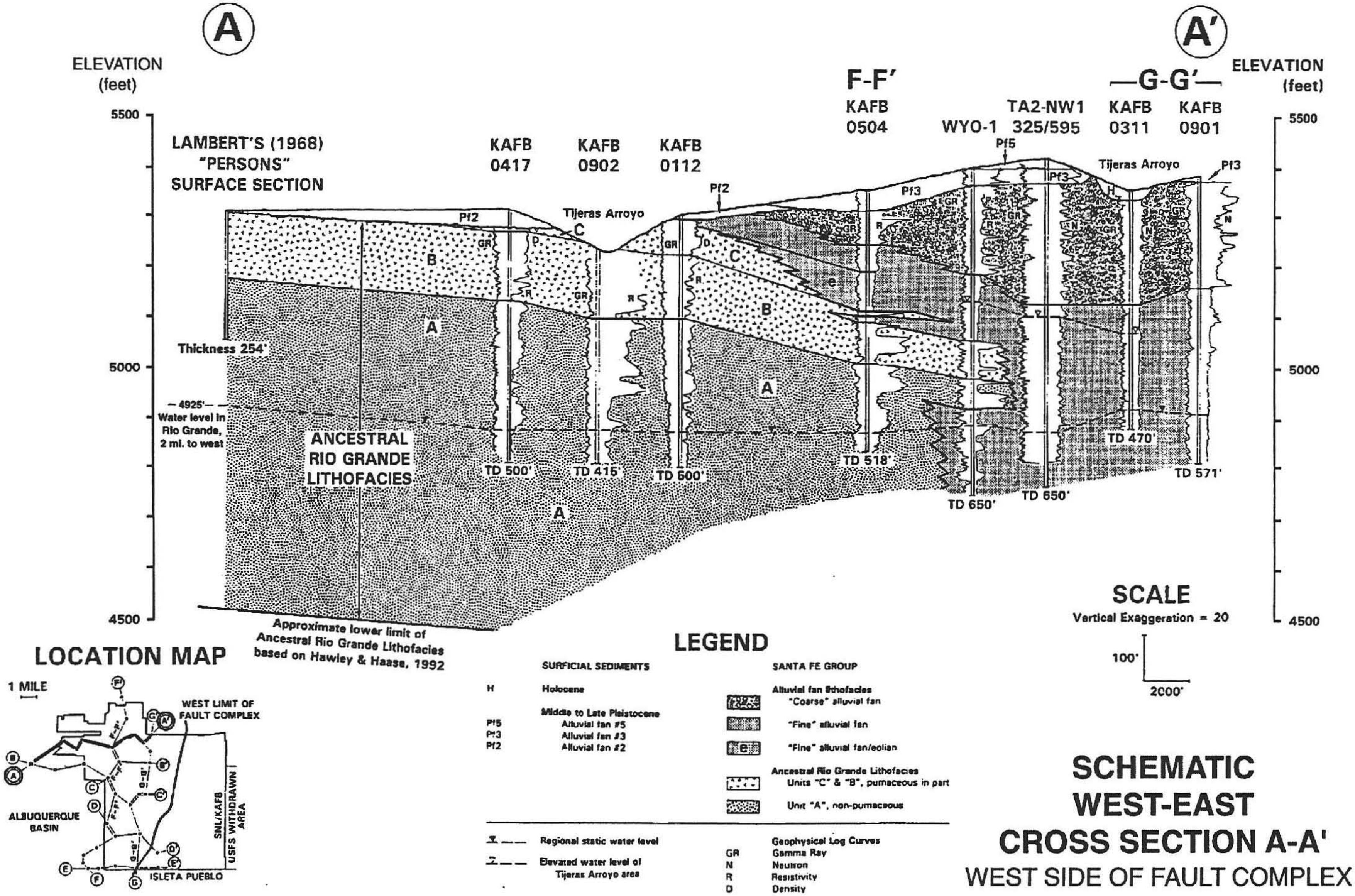

Figure 2.8. Schematic West-East Cross Section A-A' Across SNL/KAFB.

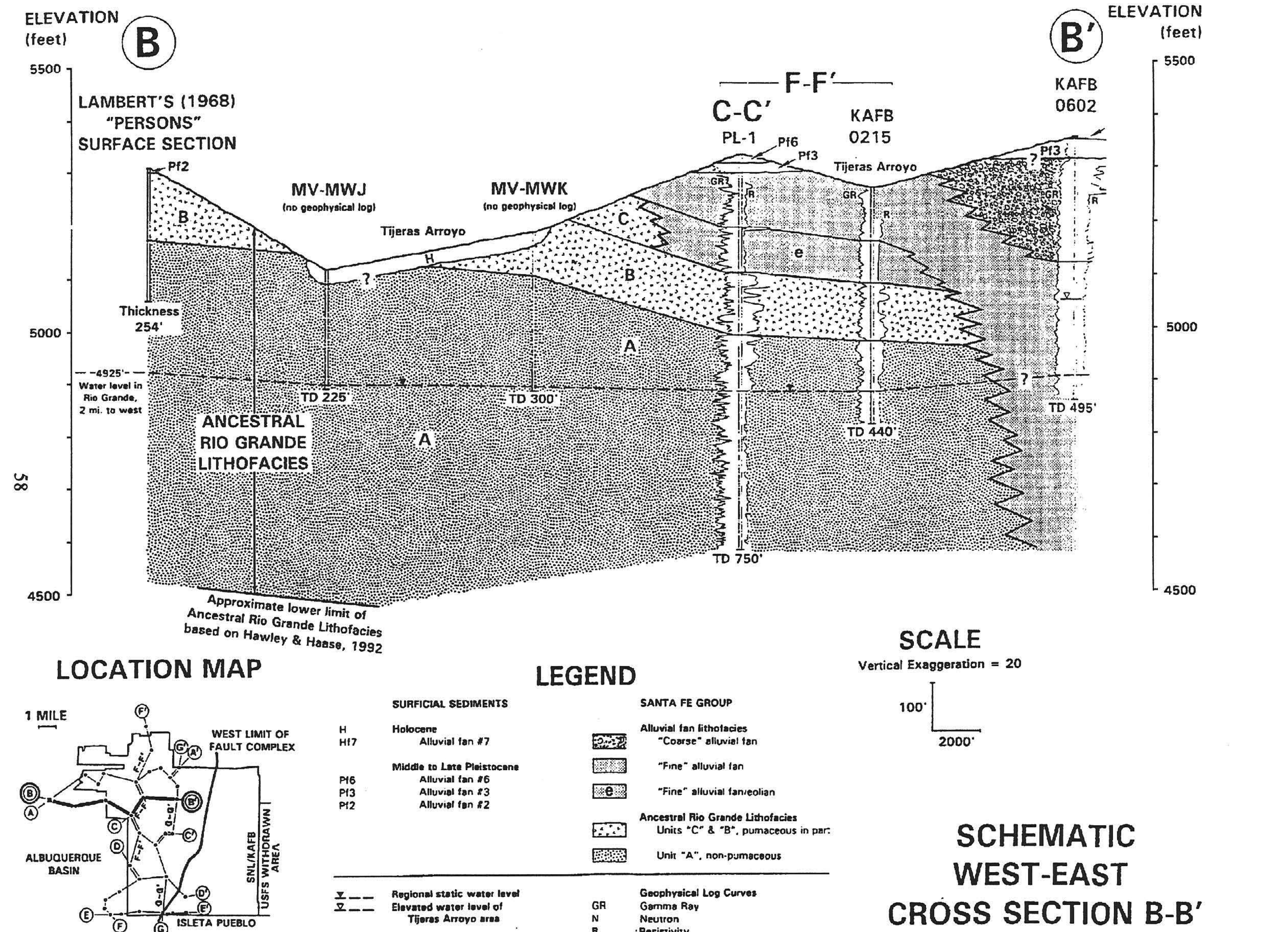

Figure 2.9. Schematic West-East Cross Section B-B' Across SNL/KAFB.

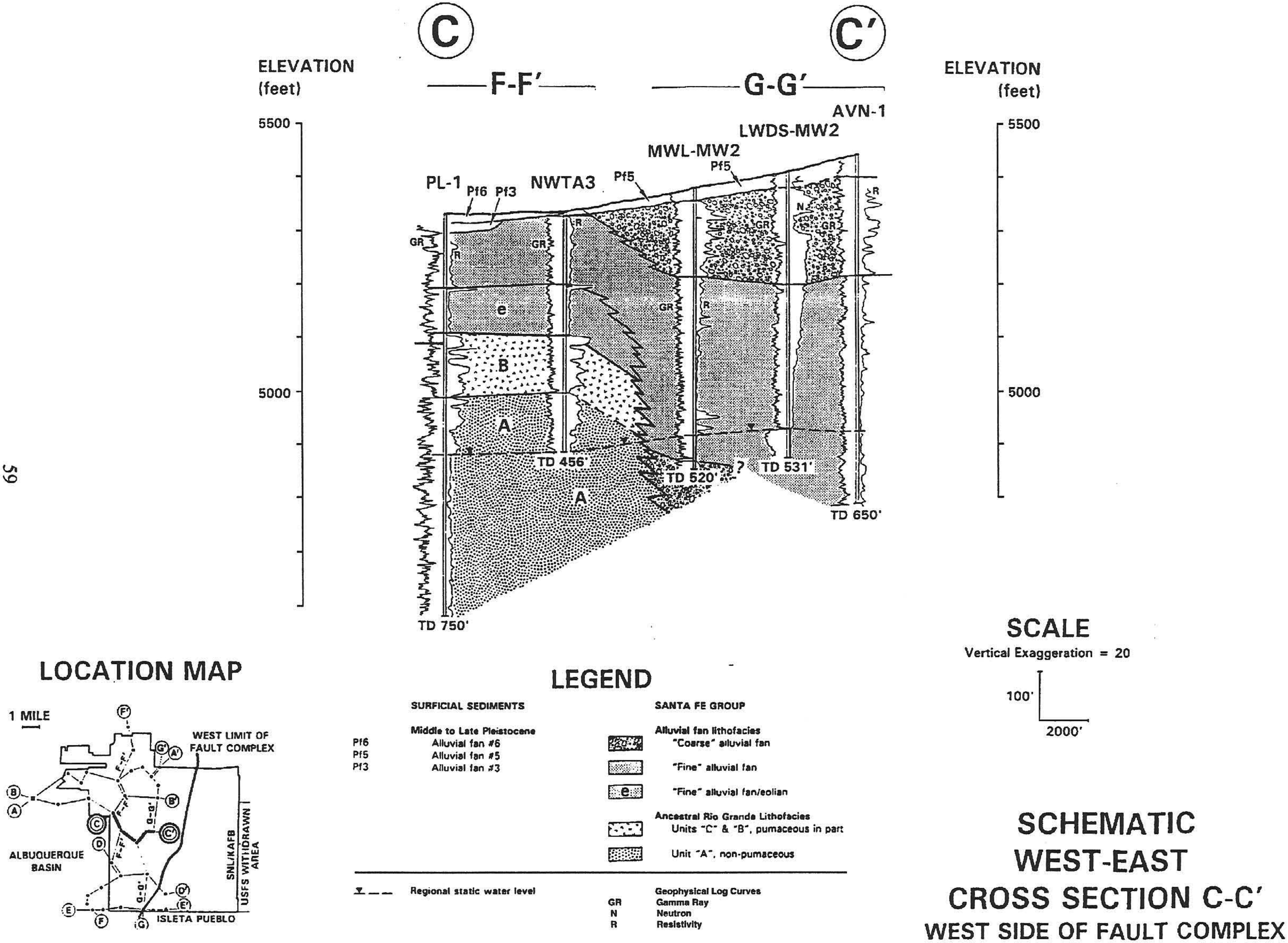

Figure 2.10. Schematic West-East Cross Section C-C' Across SNL/KAFB.

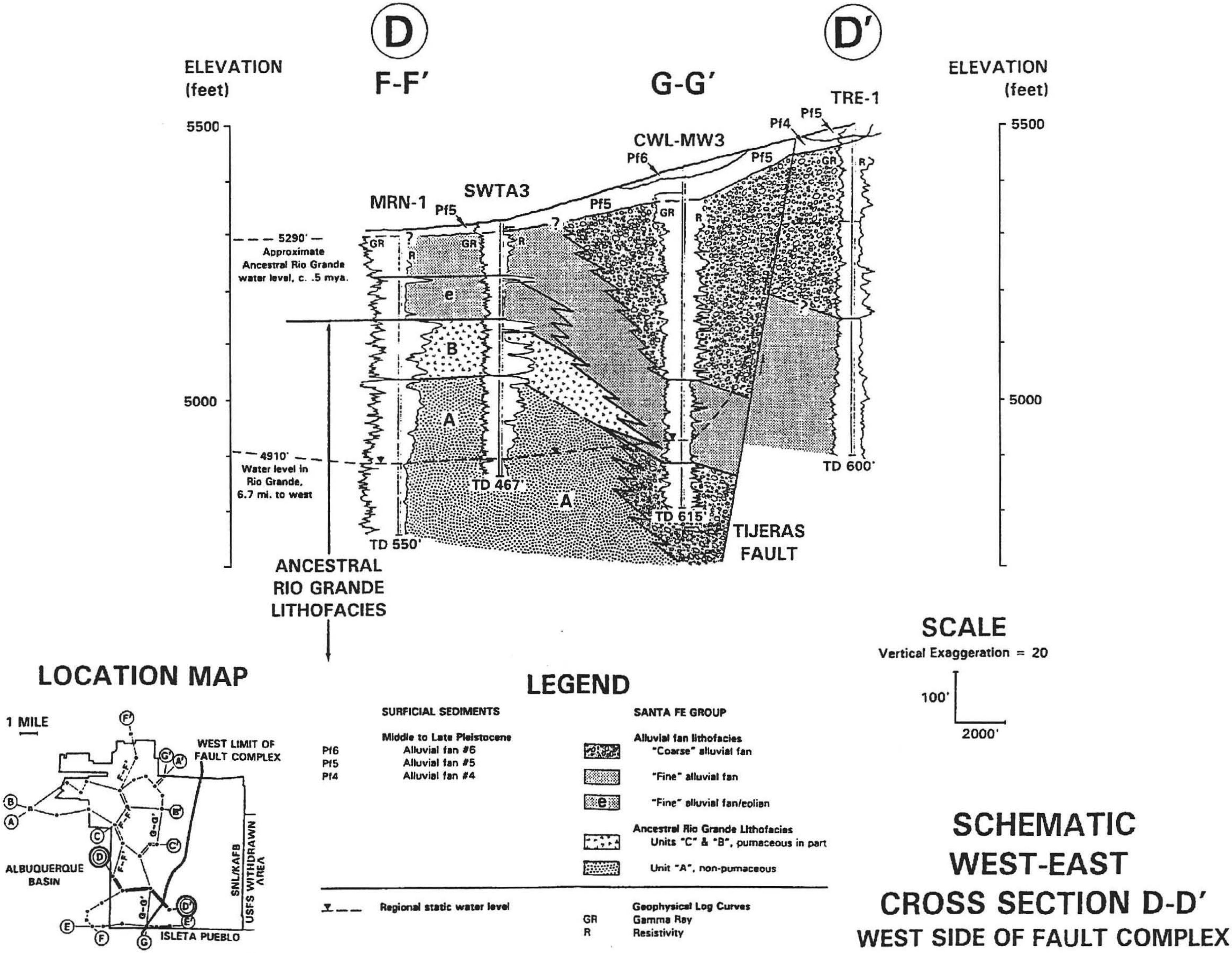

Figure 2-11. Schematic West-East Cross Section D-D' Across SNL/KAFB.

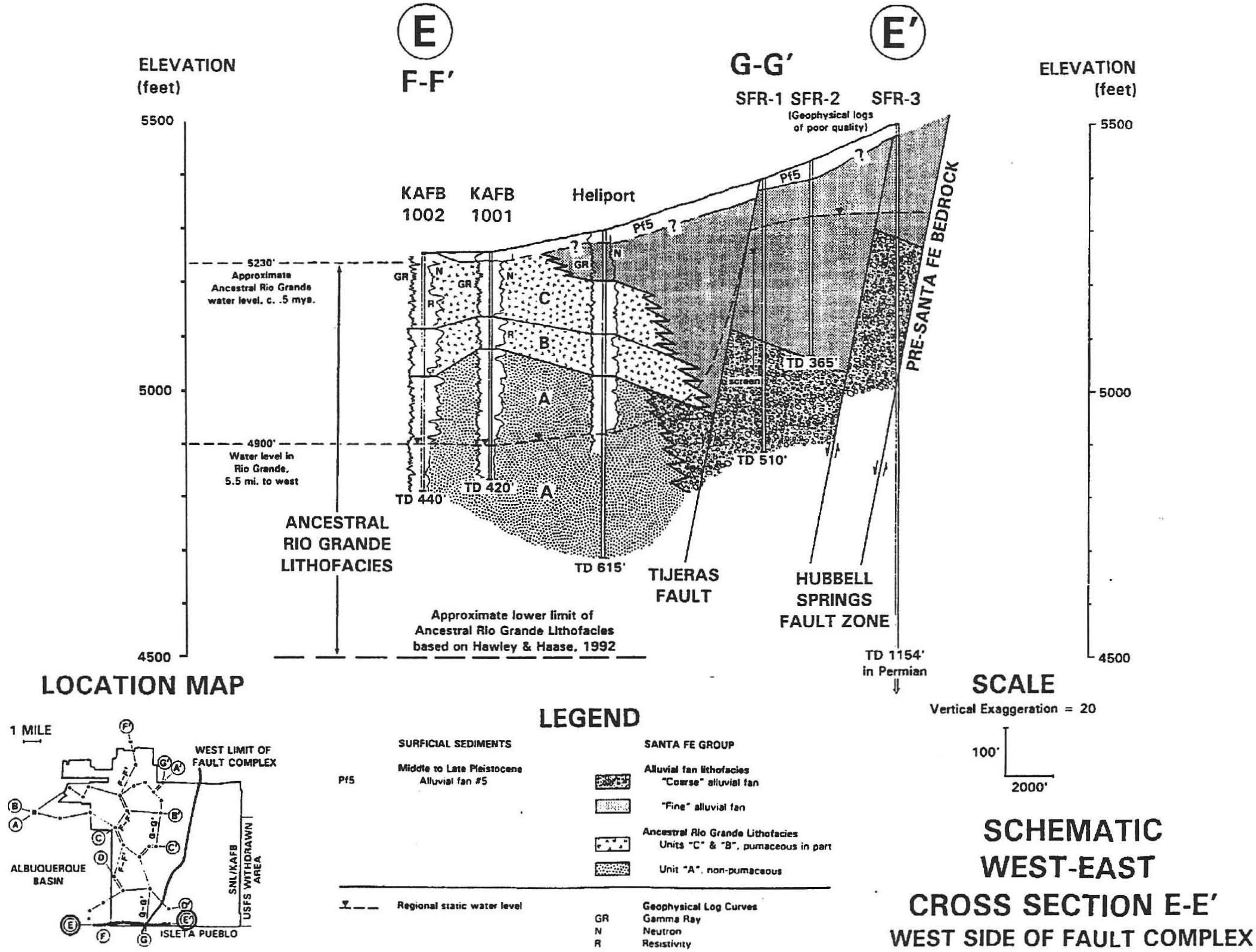

Figure 2.12. Schematic West-East Cross Section E-E' Across SNL/KAFB.

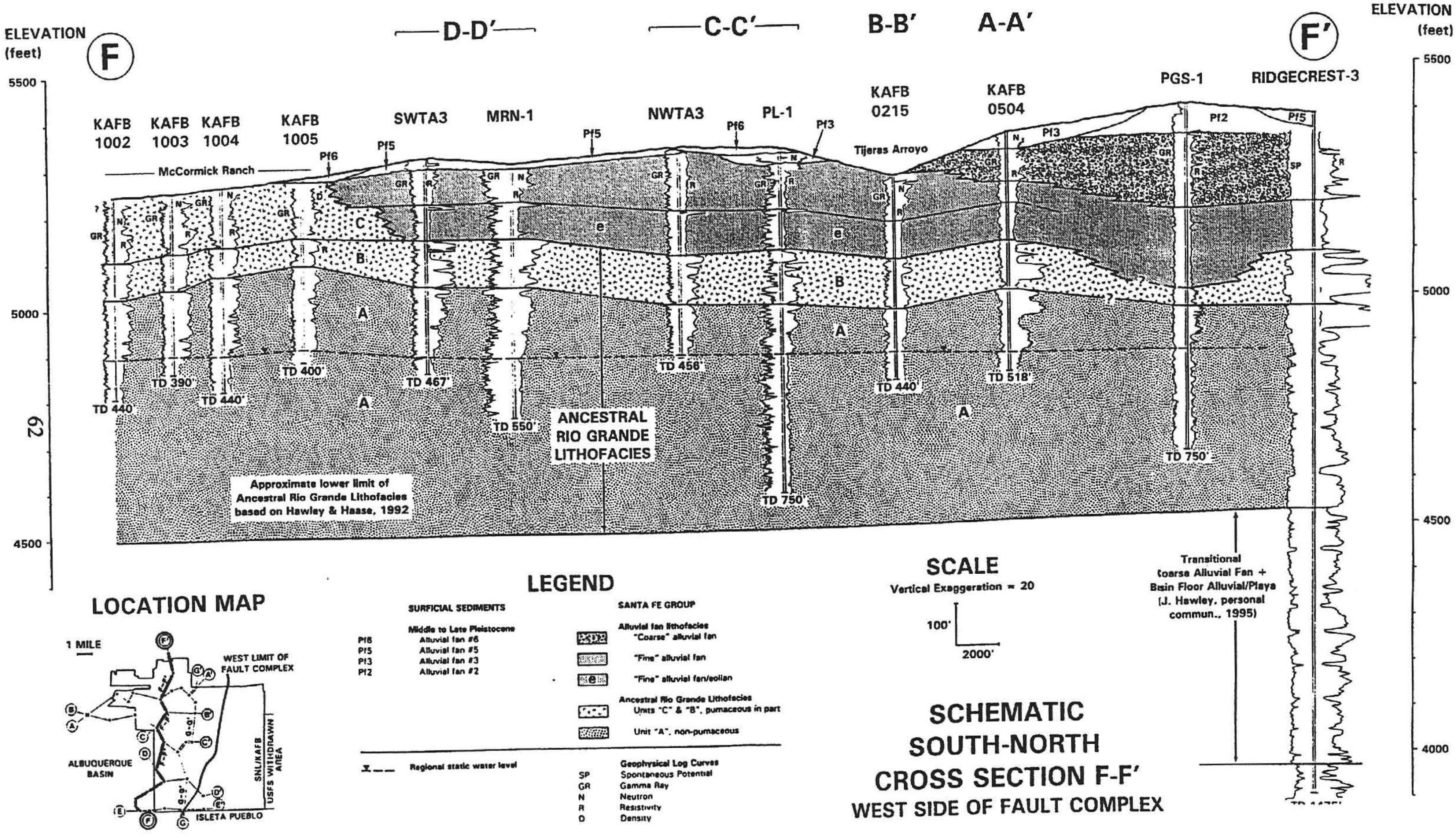

Figure 2.1.3. Schematic South-North Cross Section F-F' Across SNL/KAFB.

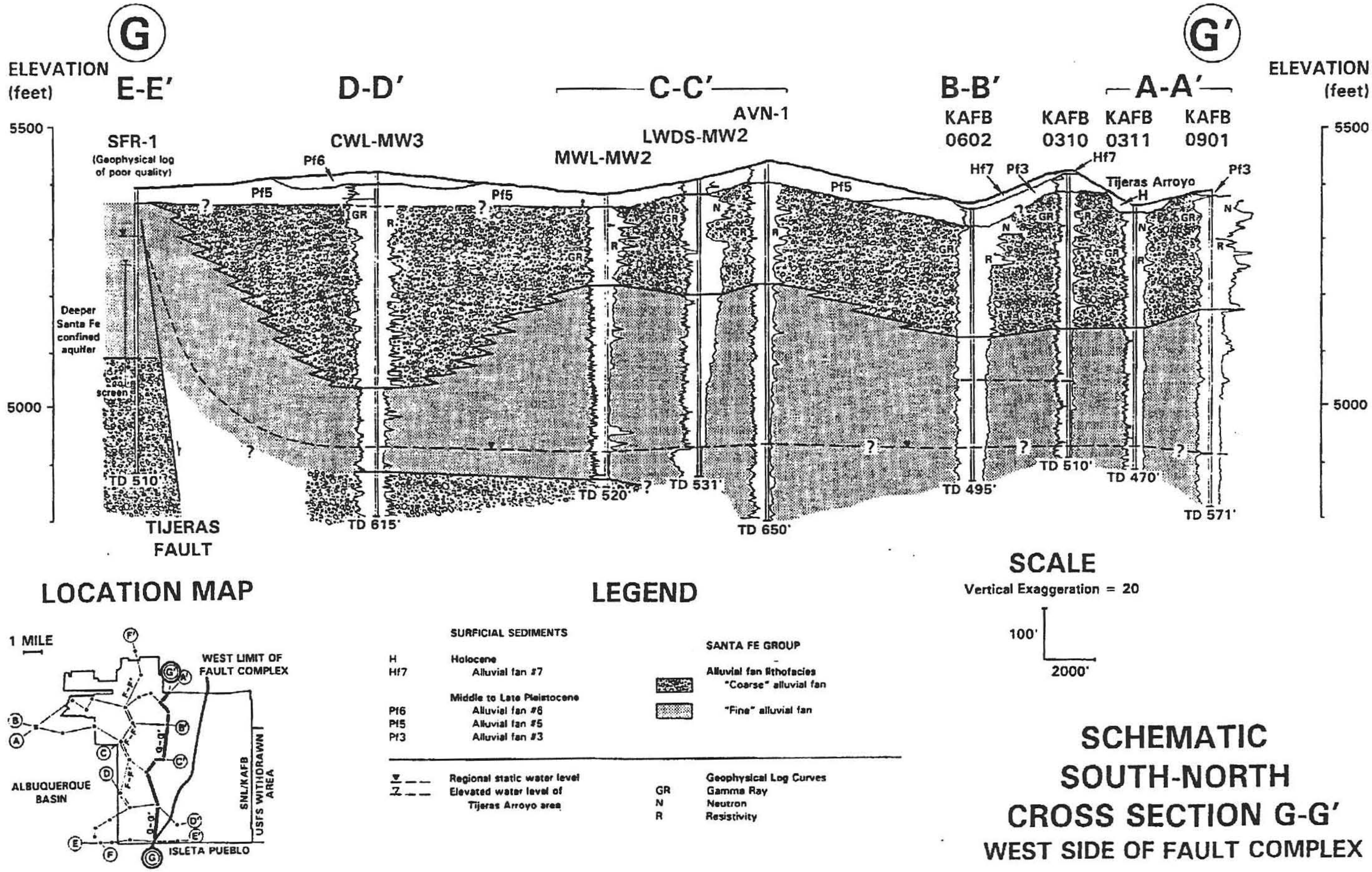

Figure 2.14. Schematic South-North Cross Section G-G' Across SNL/KAFB.

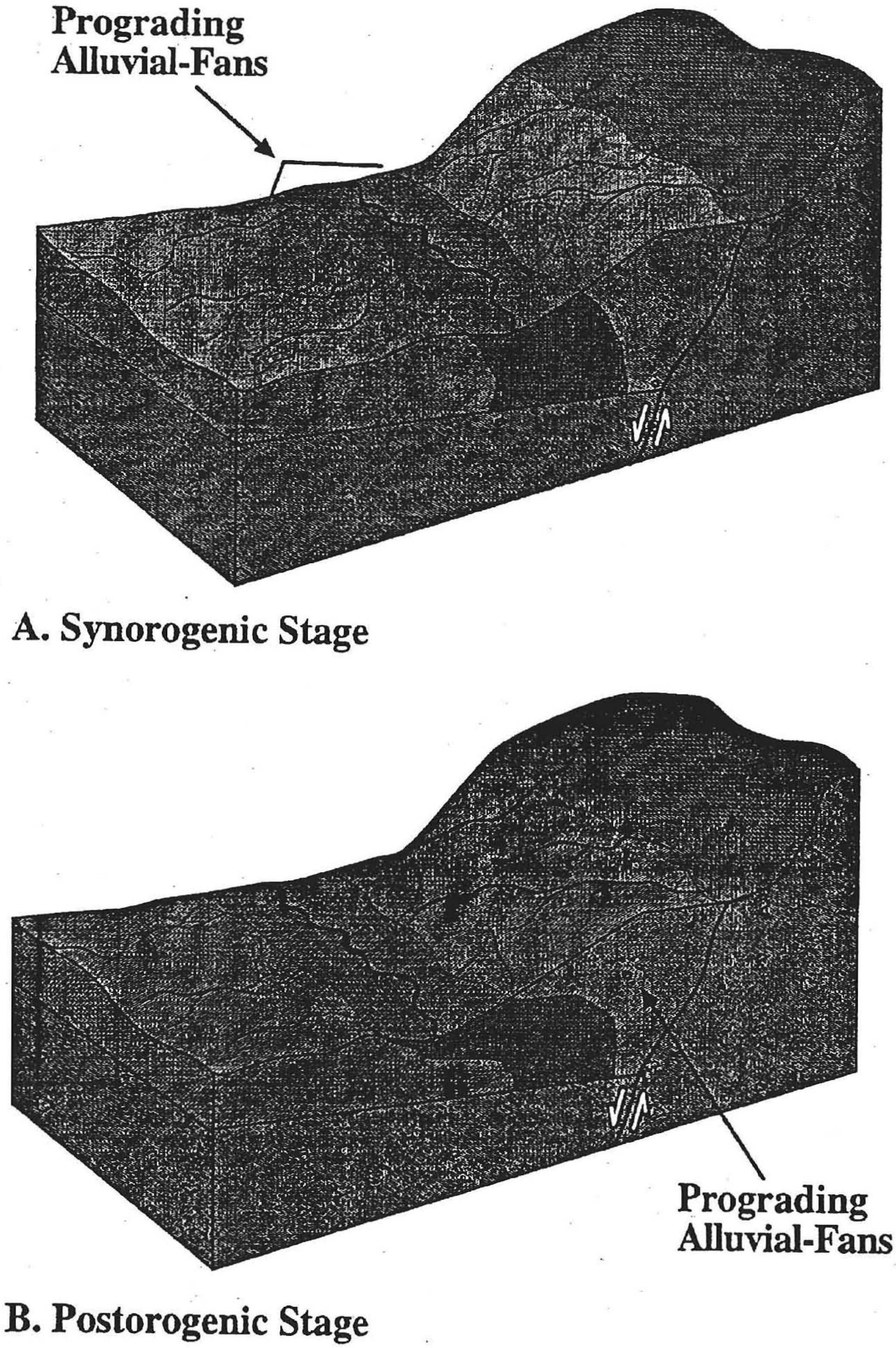

Figure 2.15. Two-Stage Depositional Model of Alluvial Fan and Axial River Sedimentation.

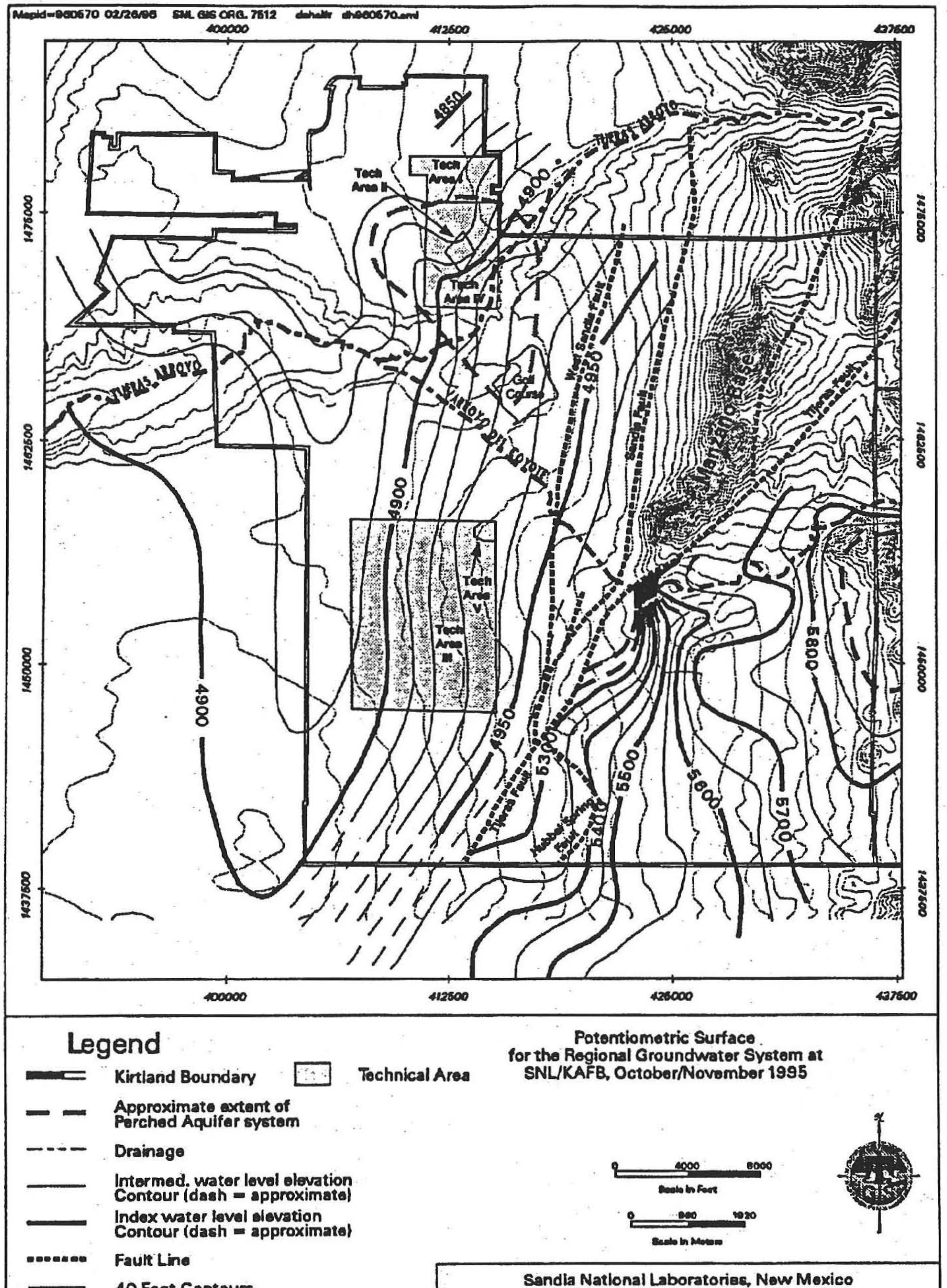

Figure 2.16. Potentiometric Surface for the Regional Groundwater System at Sandia National Laboratories/Kirtland Air Force Base, October 1995.

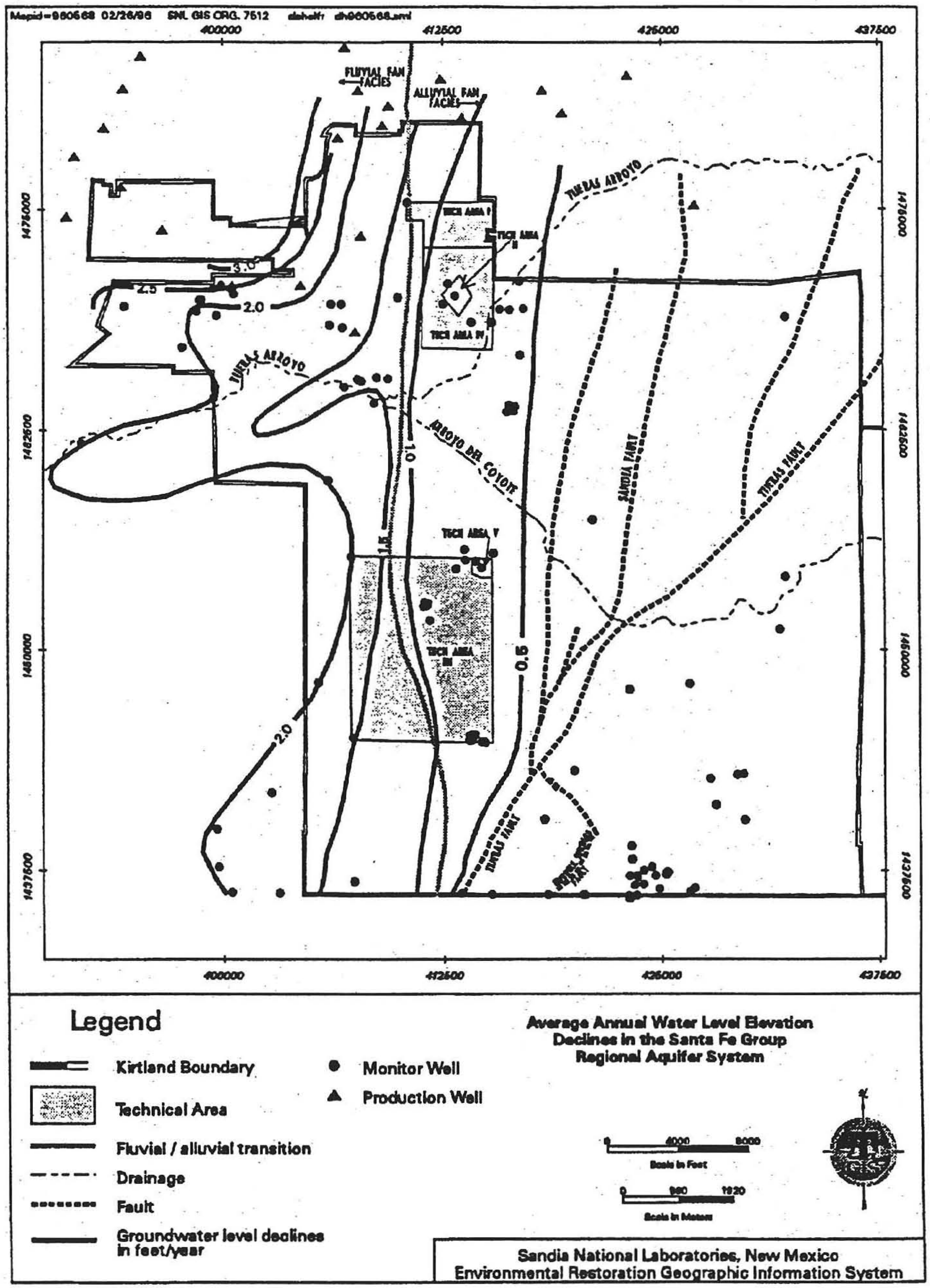

Figure 2.17. Average Annual Water Level Elevation Declines in the Santa Fe Group Regional Aquifer System.

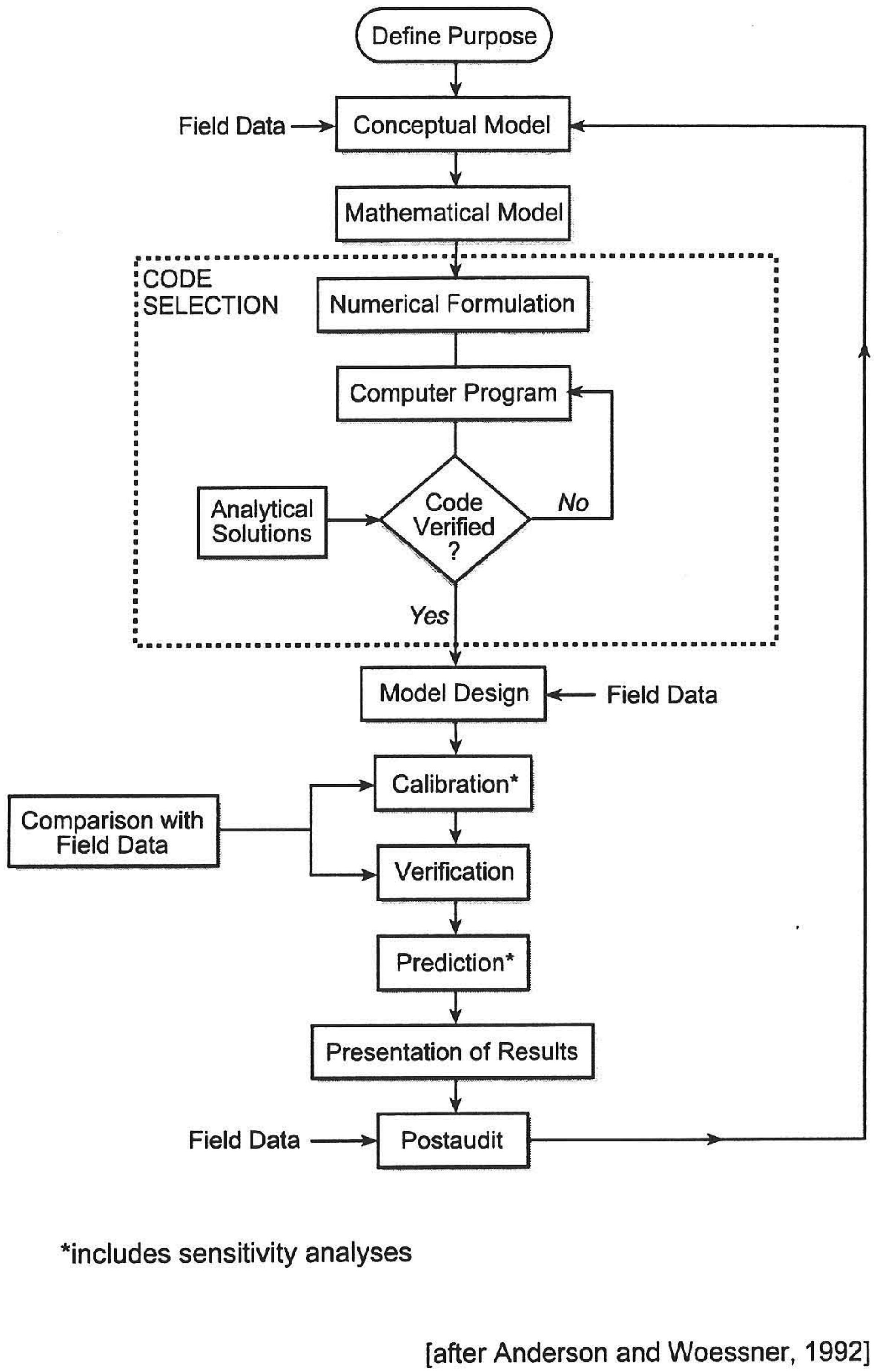

Figure 3.1. Steps in a Protocol for Model Application.

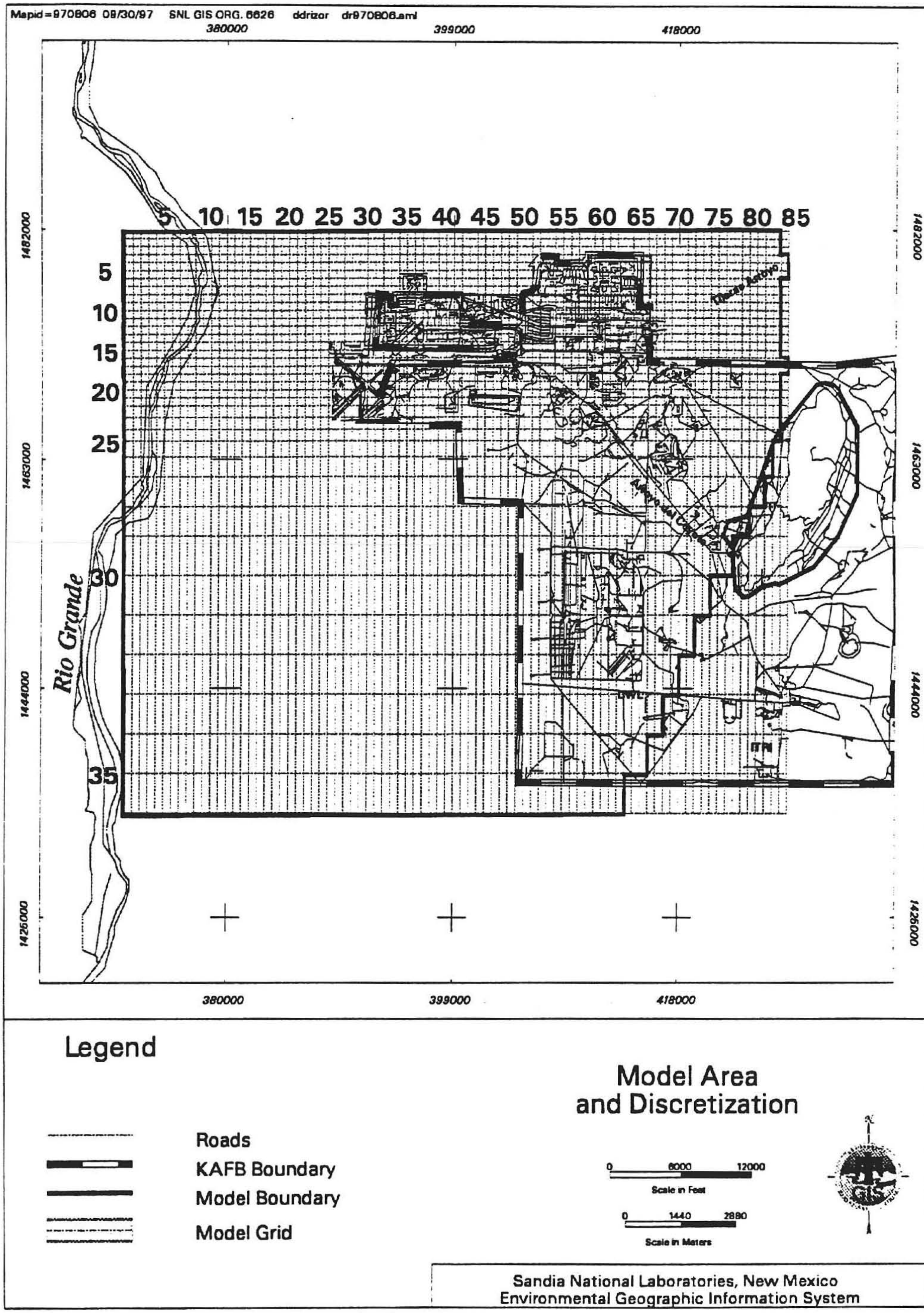

Figure 3.2. Model Area and Discretization.

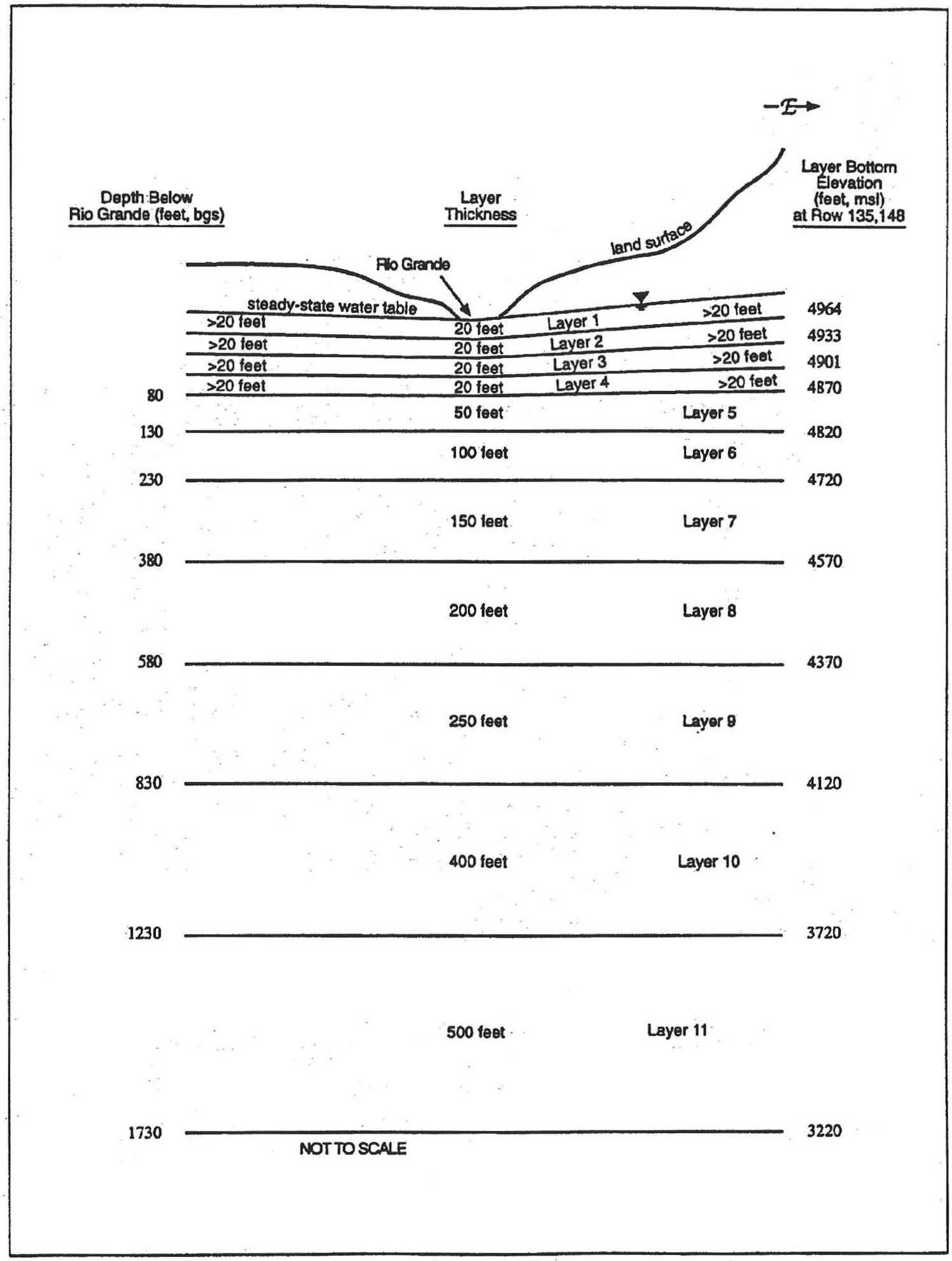

Figure 3.3. Configuration of Model Layers in the Albuquerque Basin Model.

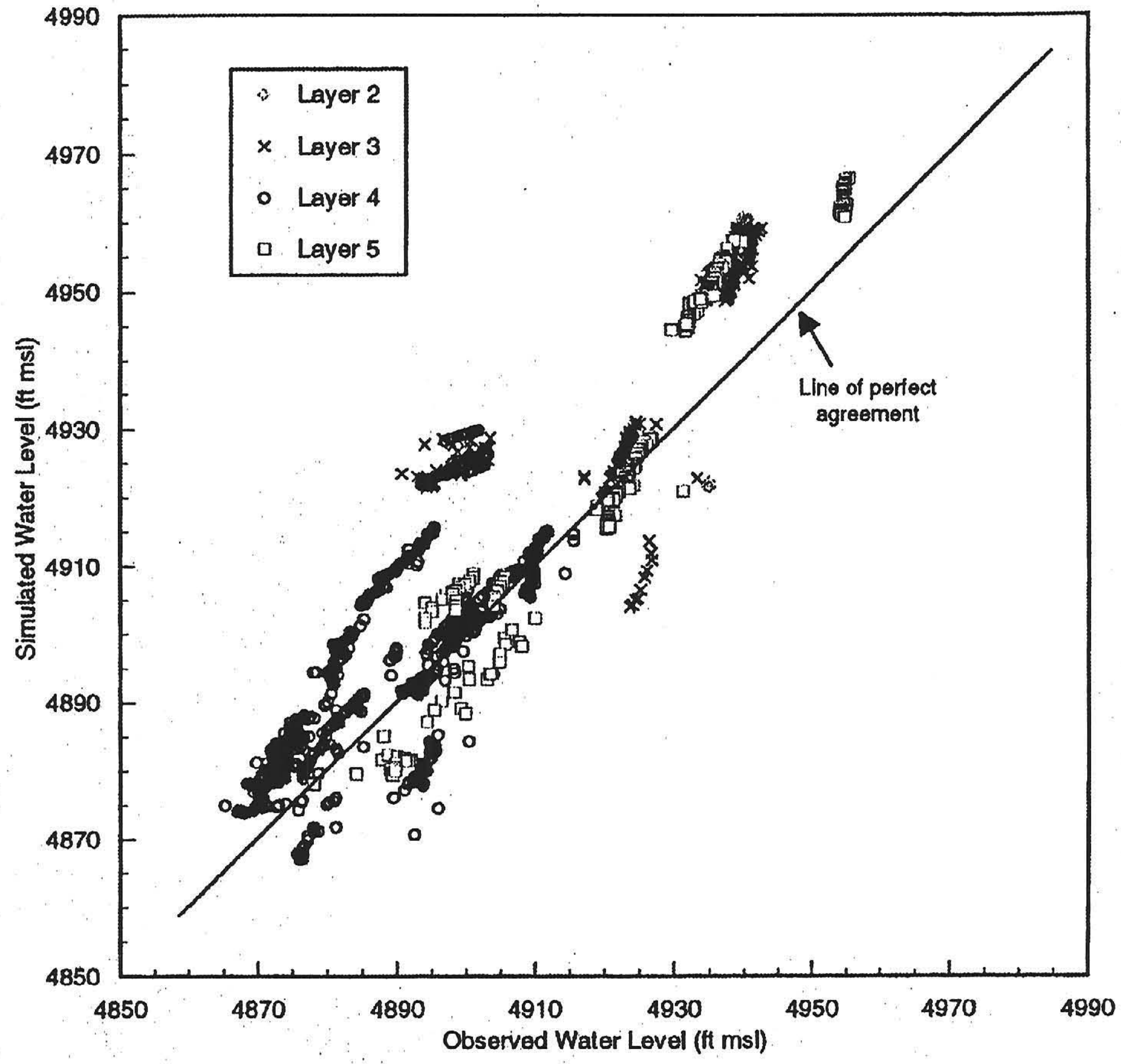

Figure 4.1. Observed versus Calibrated Water Levels, USGS Model.

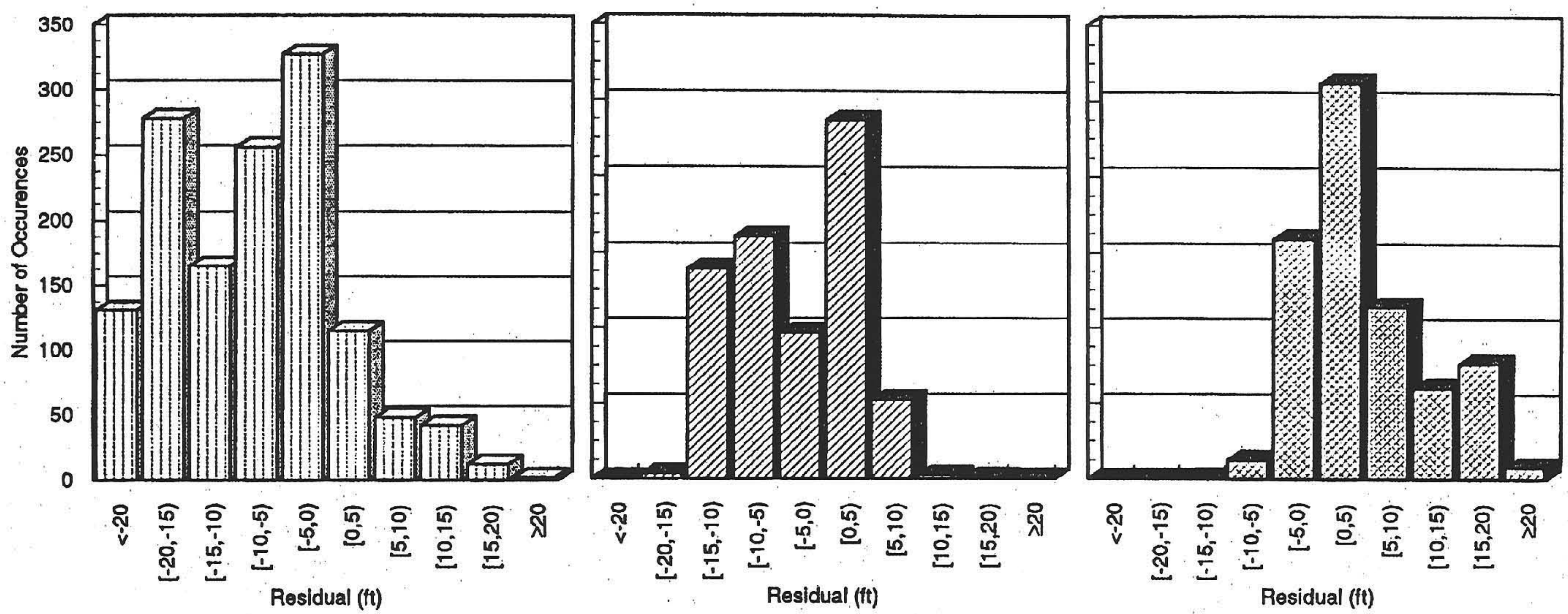

a) USGS Model

b) SWHC CM, USGS Recharge*

c) SWHC CM, SWHC Recharge

*Tijeras Arroyo recharge only

Figure 4.2. Histogram of Residuals, USGS Model; SWHC CM, USGS Recharge; SWHC CM, SWHC Recharge.

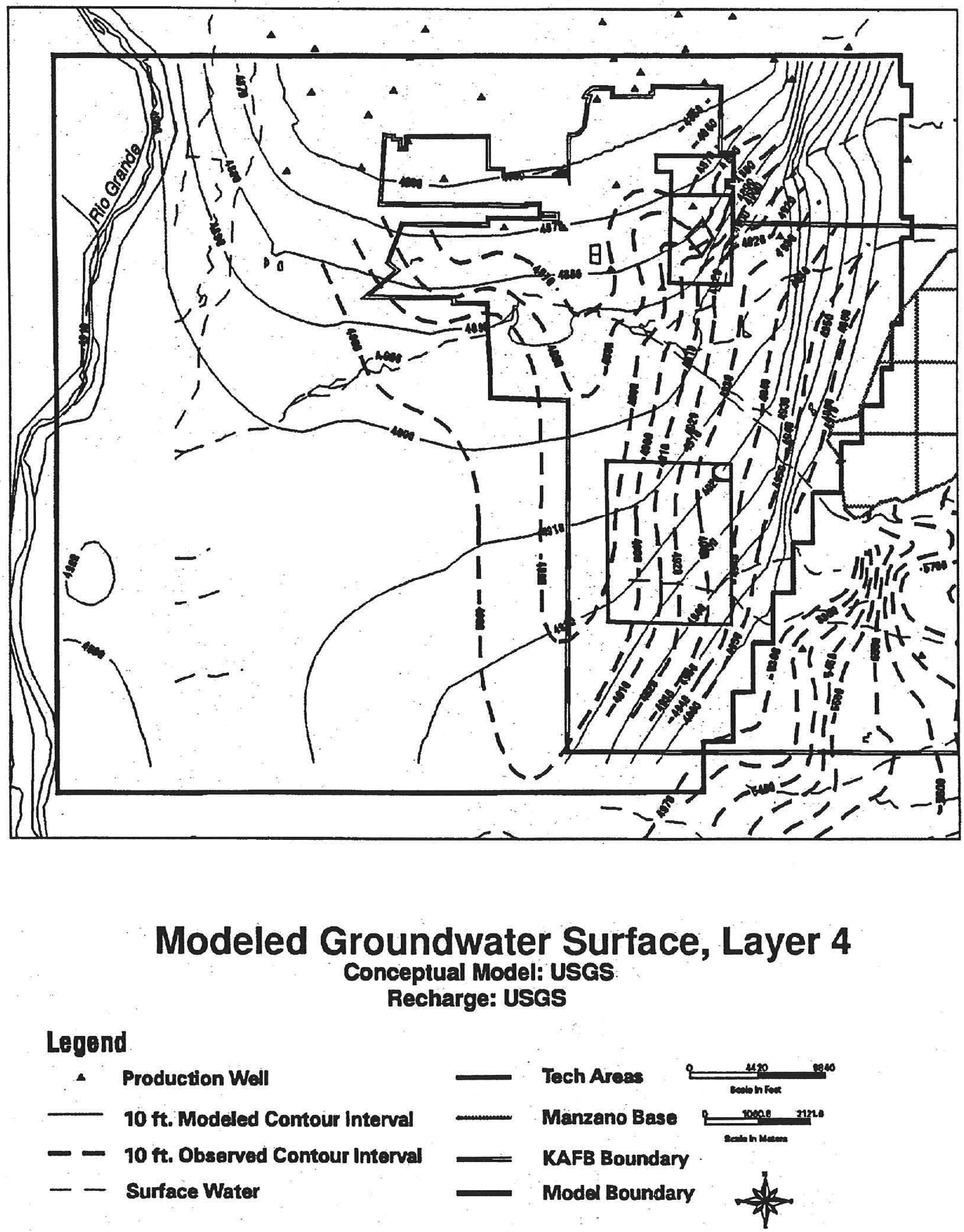

Figure 4.3. Simulated Water Levels, March 1995, Layer 4, USGS Model.

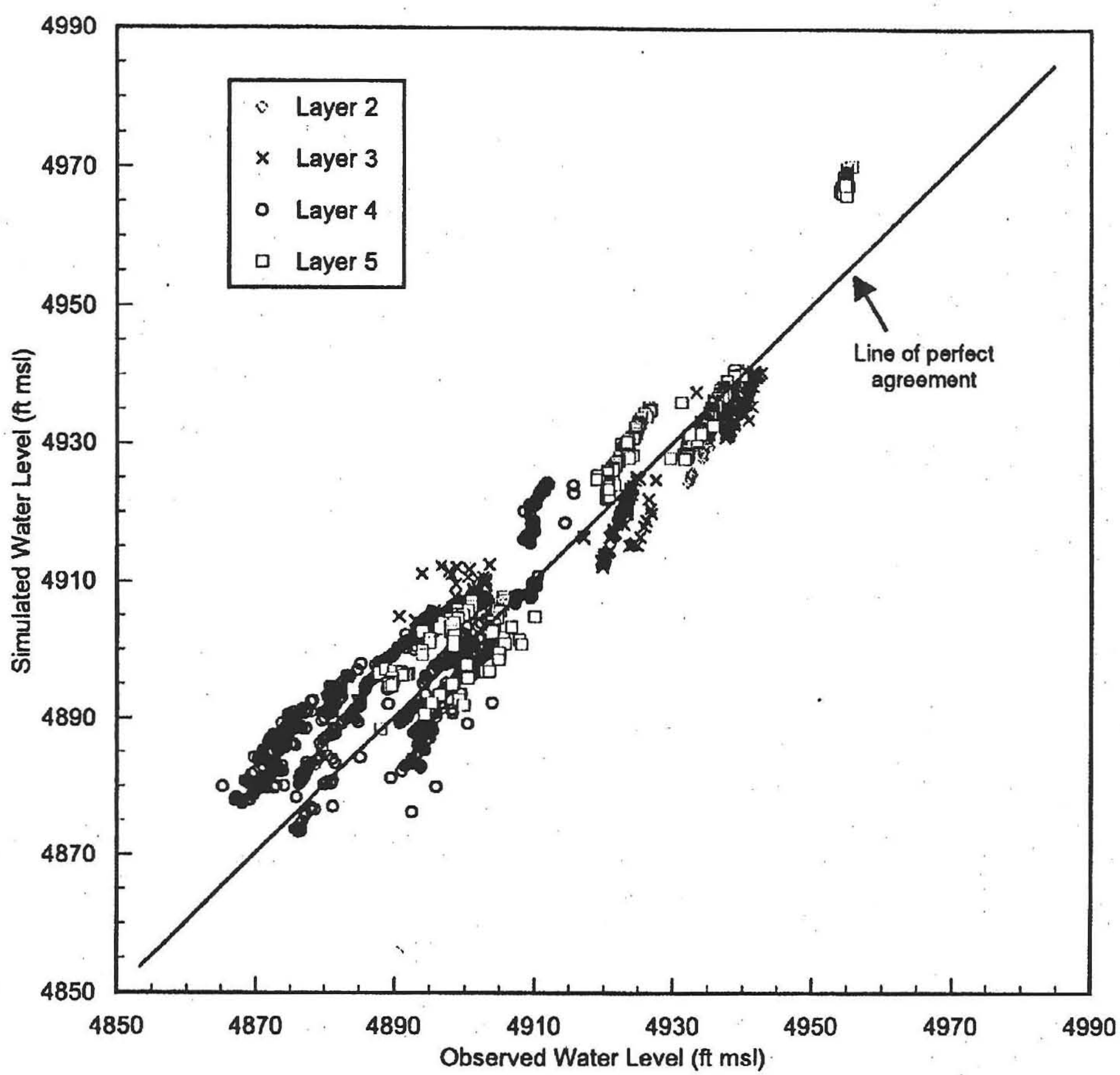

Figure 4.4. Observed versus Calibrated Water Levels, SWHC CM, USGS Recharge.

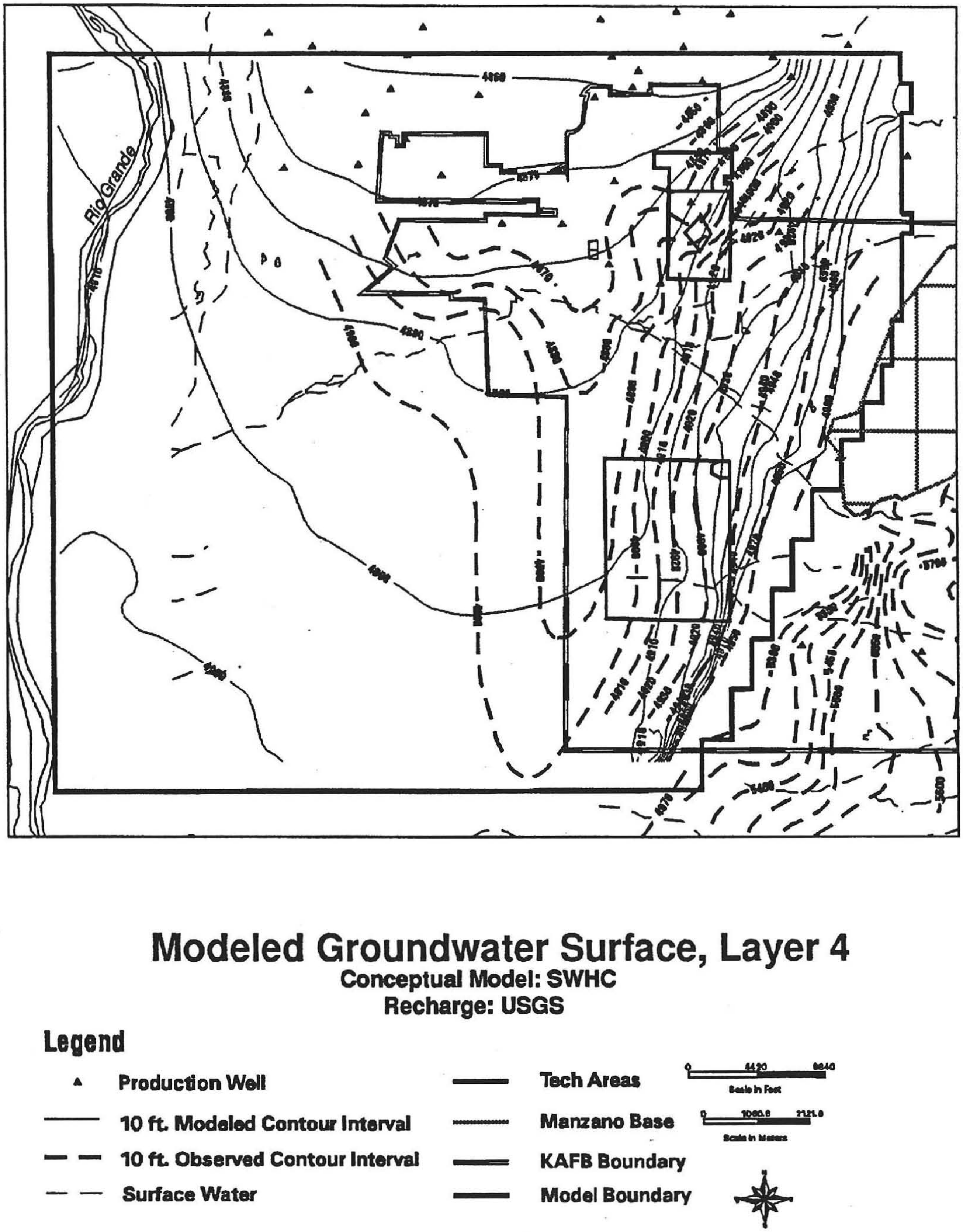

Figure 4.5 Simulated Water Levels, March 1995, Layer 4, SWHC CM, USGS Recharge

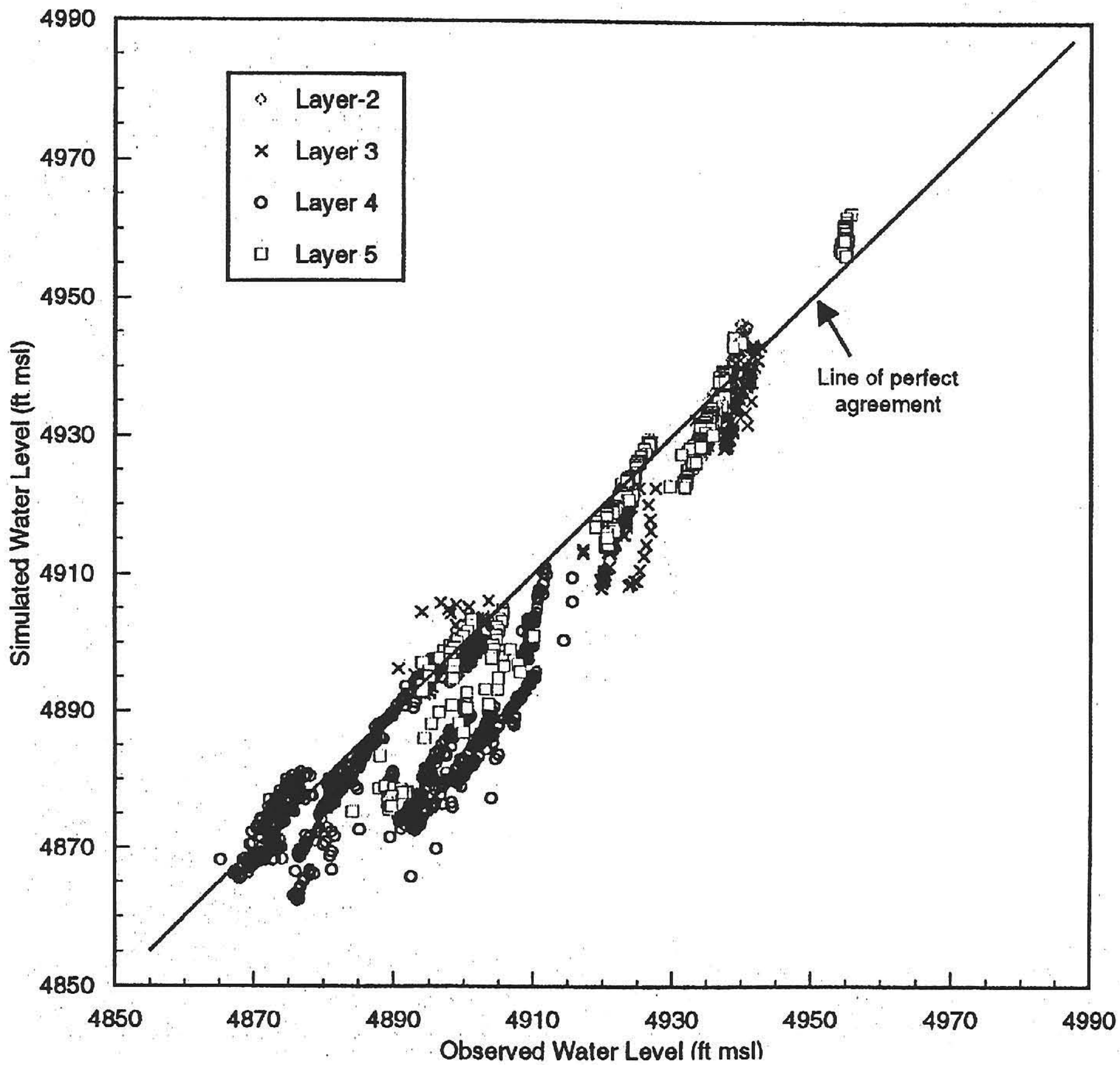

Figure 4.6. Observed versus Calibrated Water Levels, SWHC CM, SWHC Recharge.

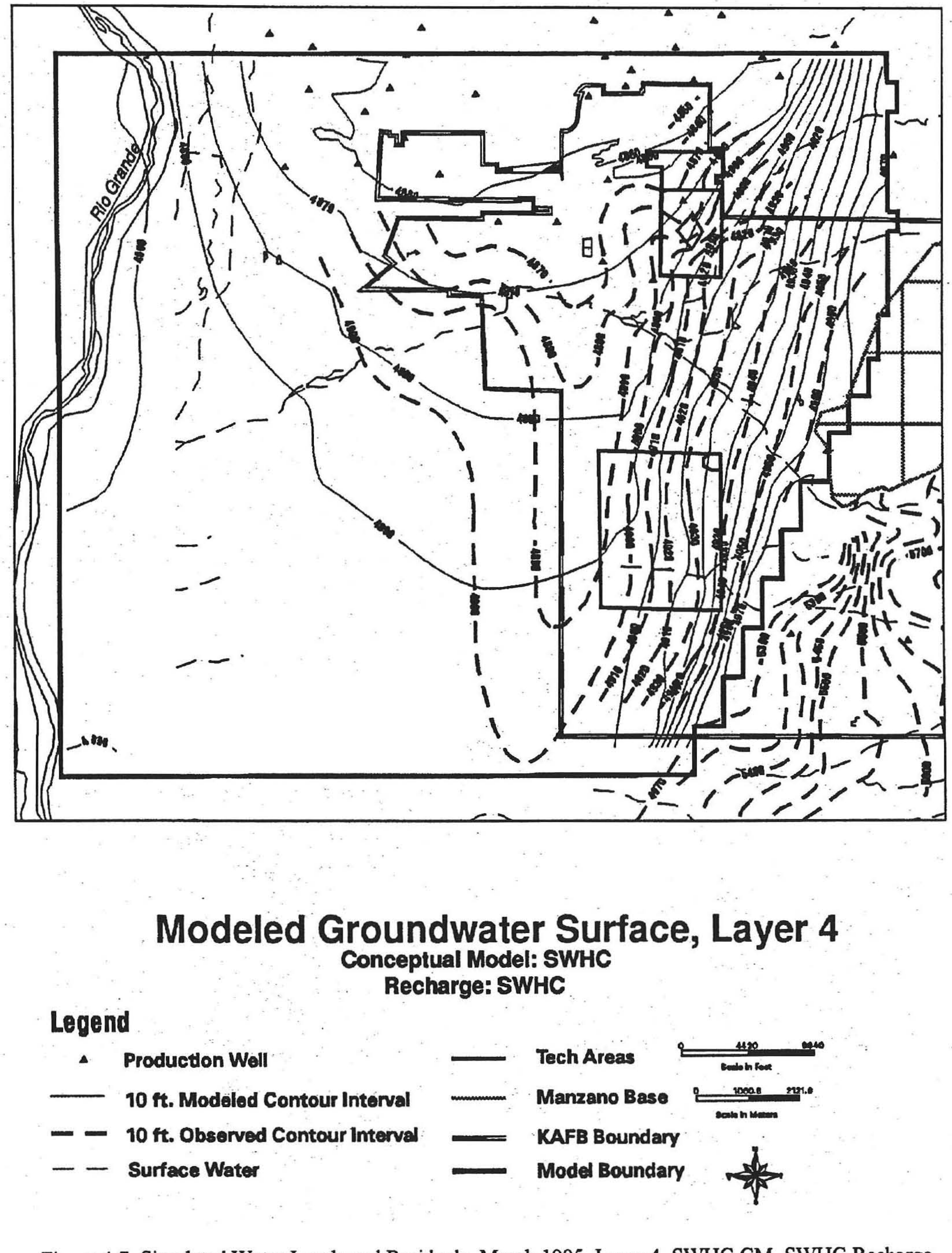

Figure 4.7 Simulated Water Levels and Residuals, March 1995, Layer 4, SWHC CM, SWHC Recharge.

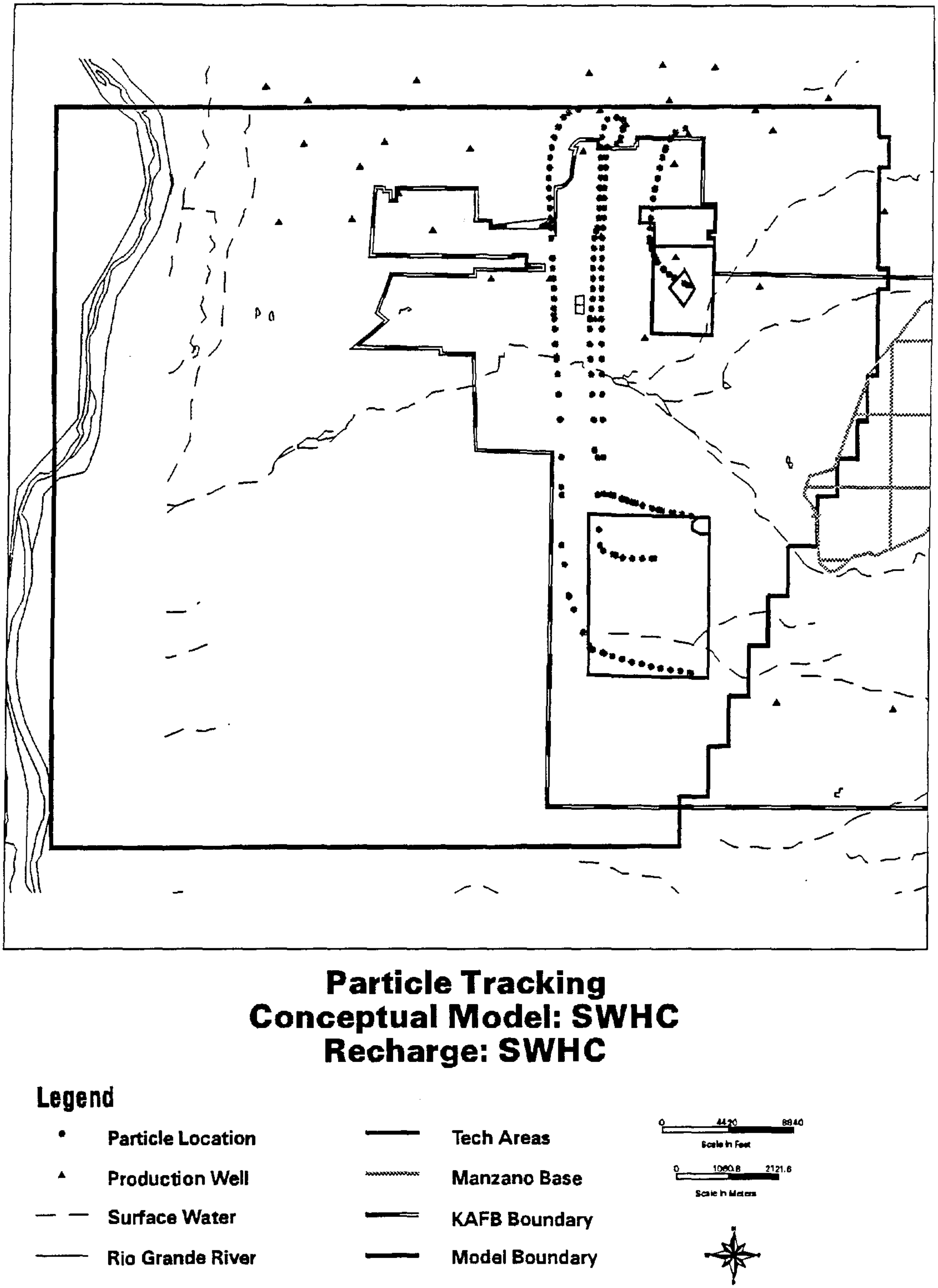

Figure 4.8 Forward Particle Tracking Results for Calibrated Flow Field.

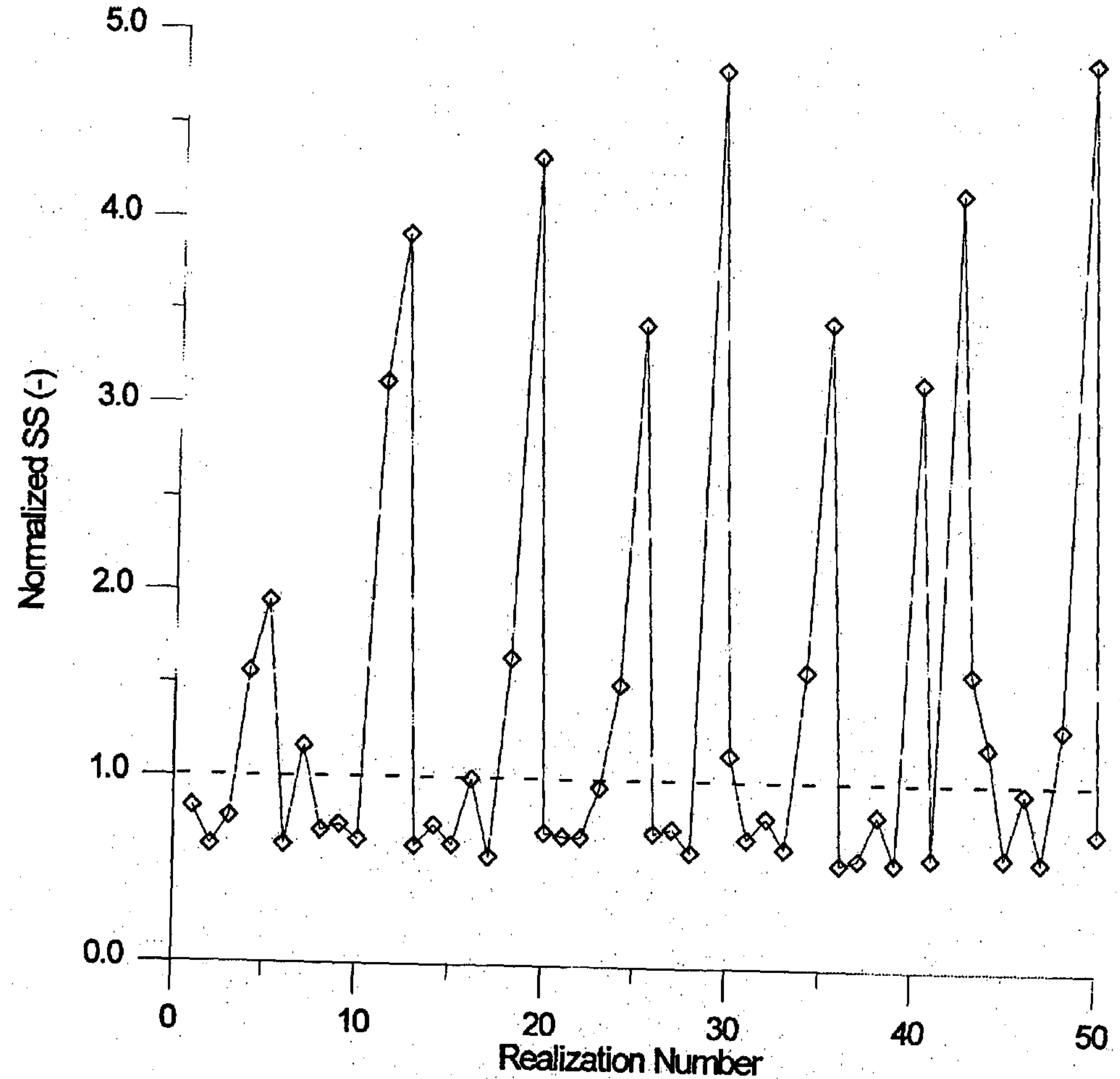

Figure 4.9 Normalized Residual Sum of Squares for 50 Monte Carlo Realizations

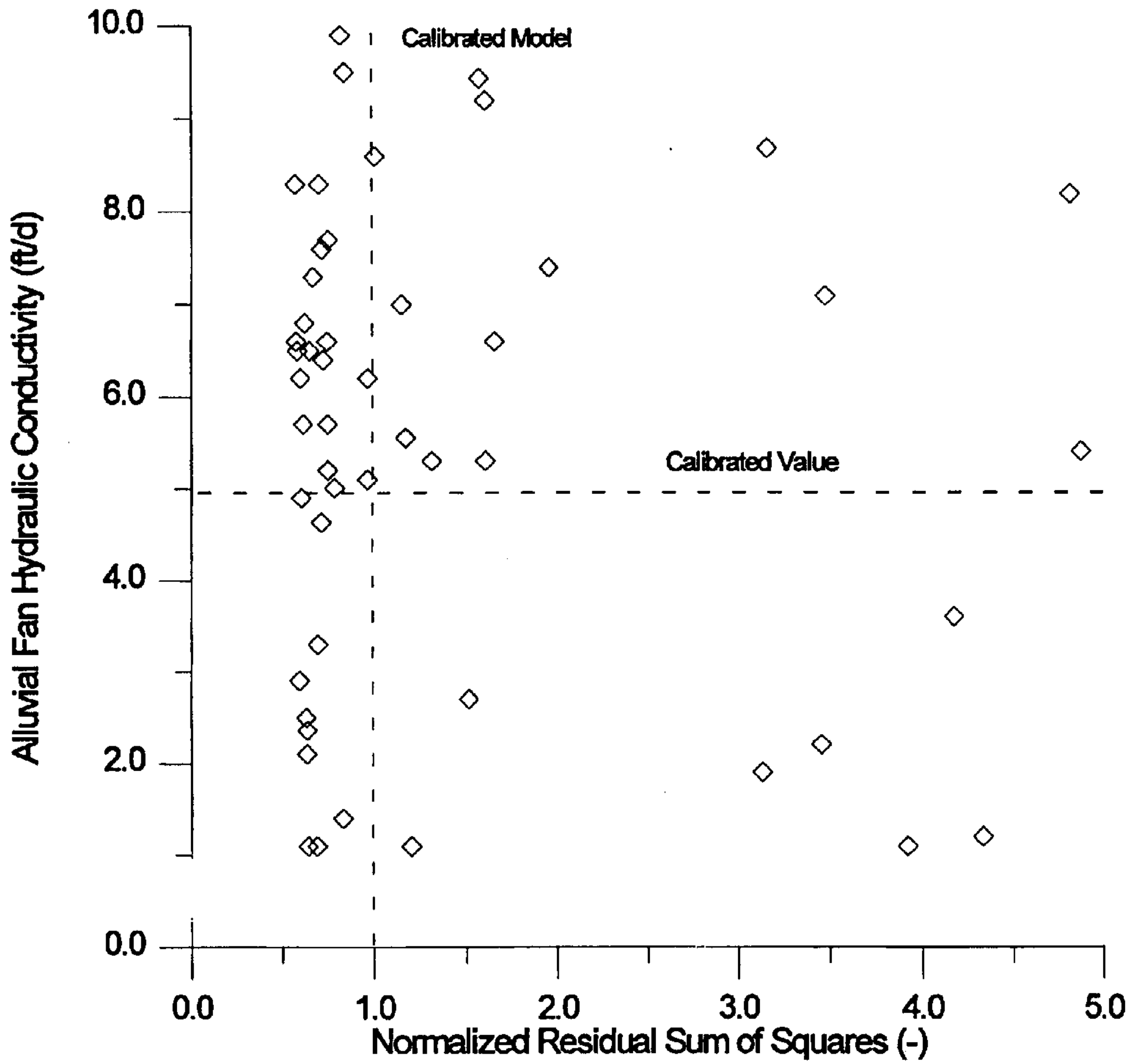

Figure 4.10 Normalized Residual Sum of Squares versus Alluvial Fan Hydraulic Conductivity

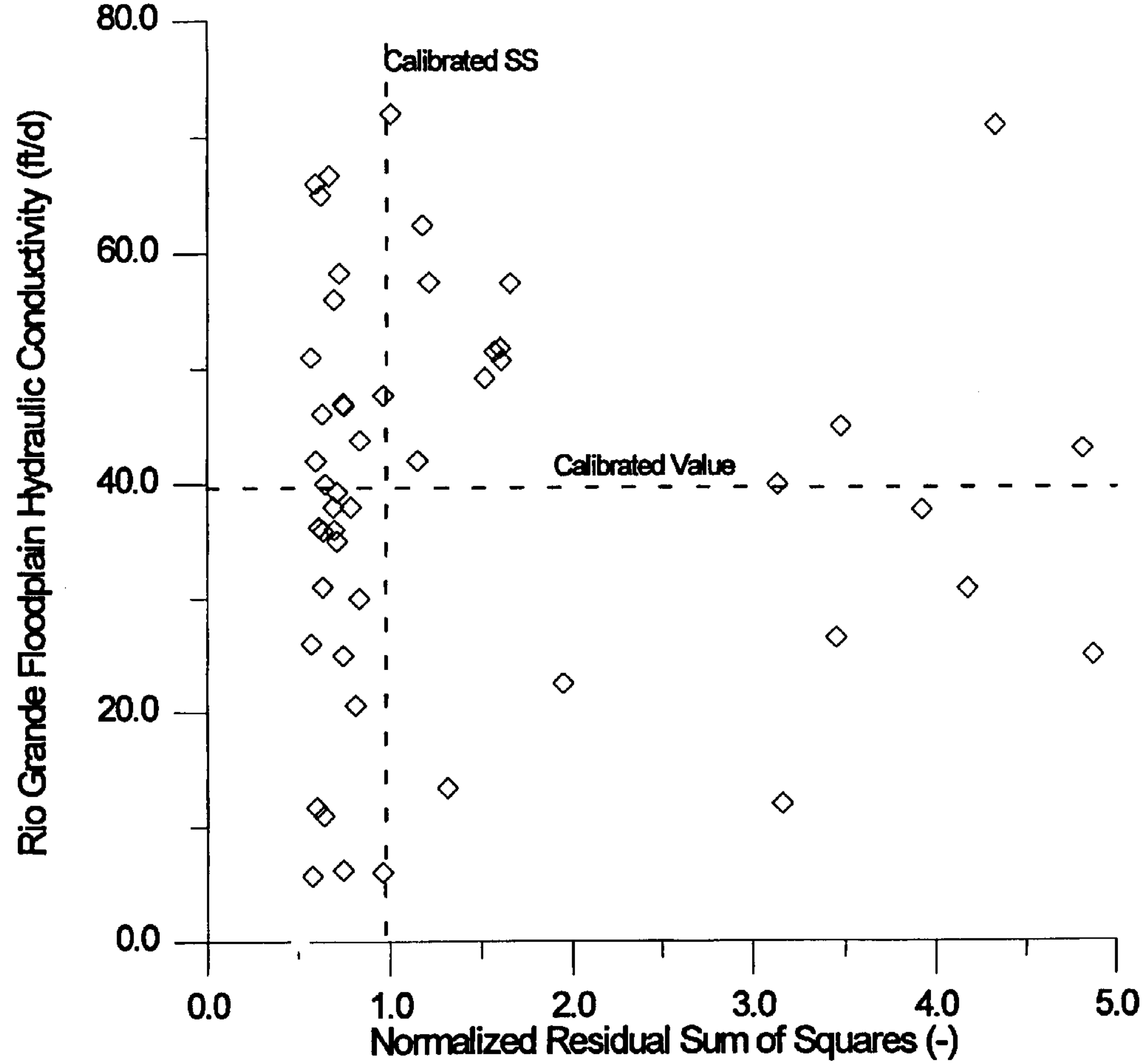

Figure 4.11 Normalized Residual Sum of Squares versus Rio Grande Floodplain Hydraulic Conductivity

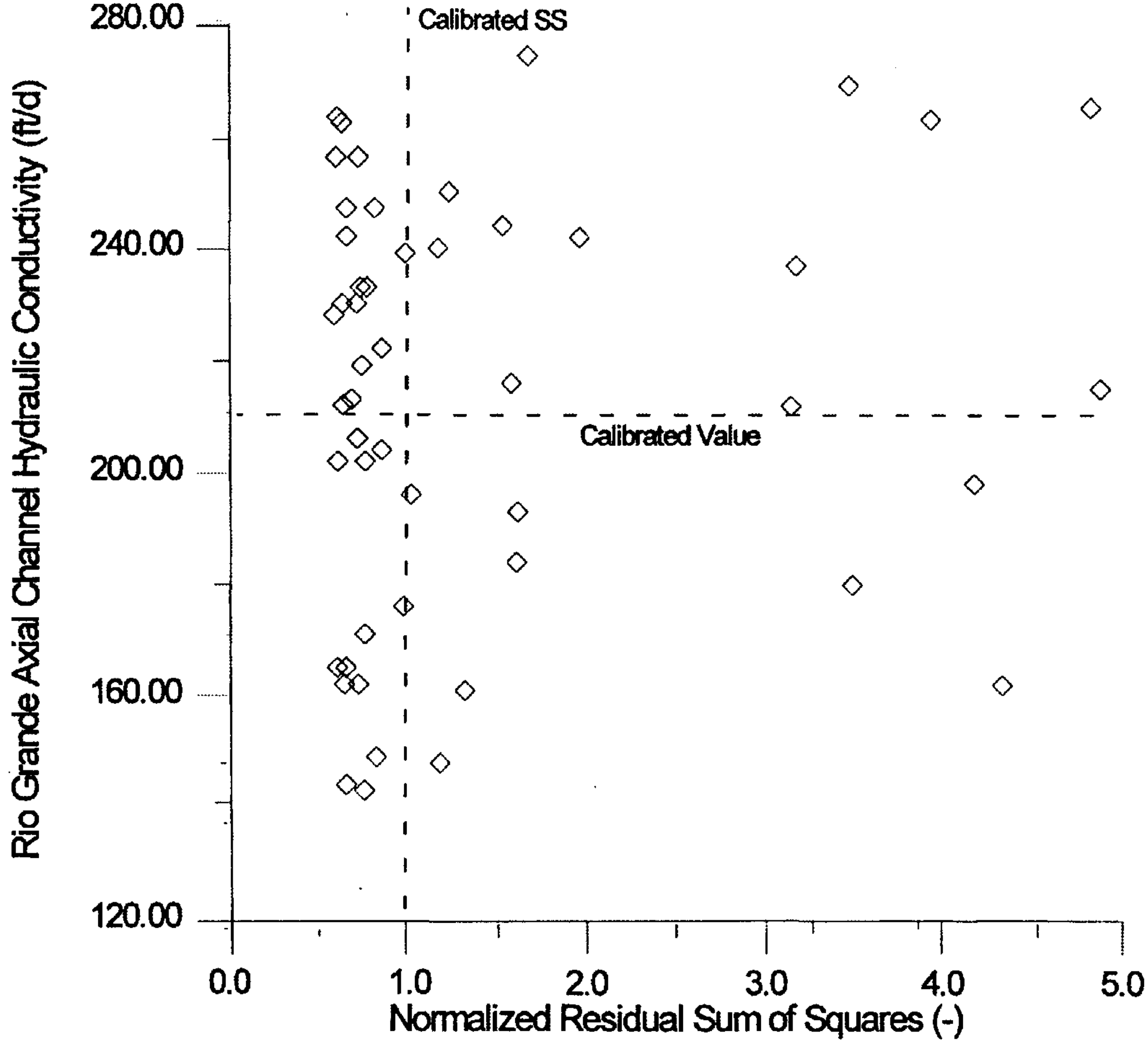

Figure 4.12 Normalized Residual Sum of Squares versus Rio Grande Axial Channel Hydraulic Conductivity

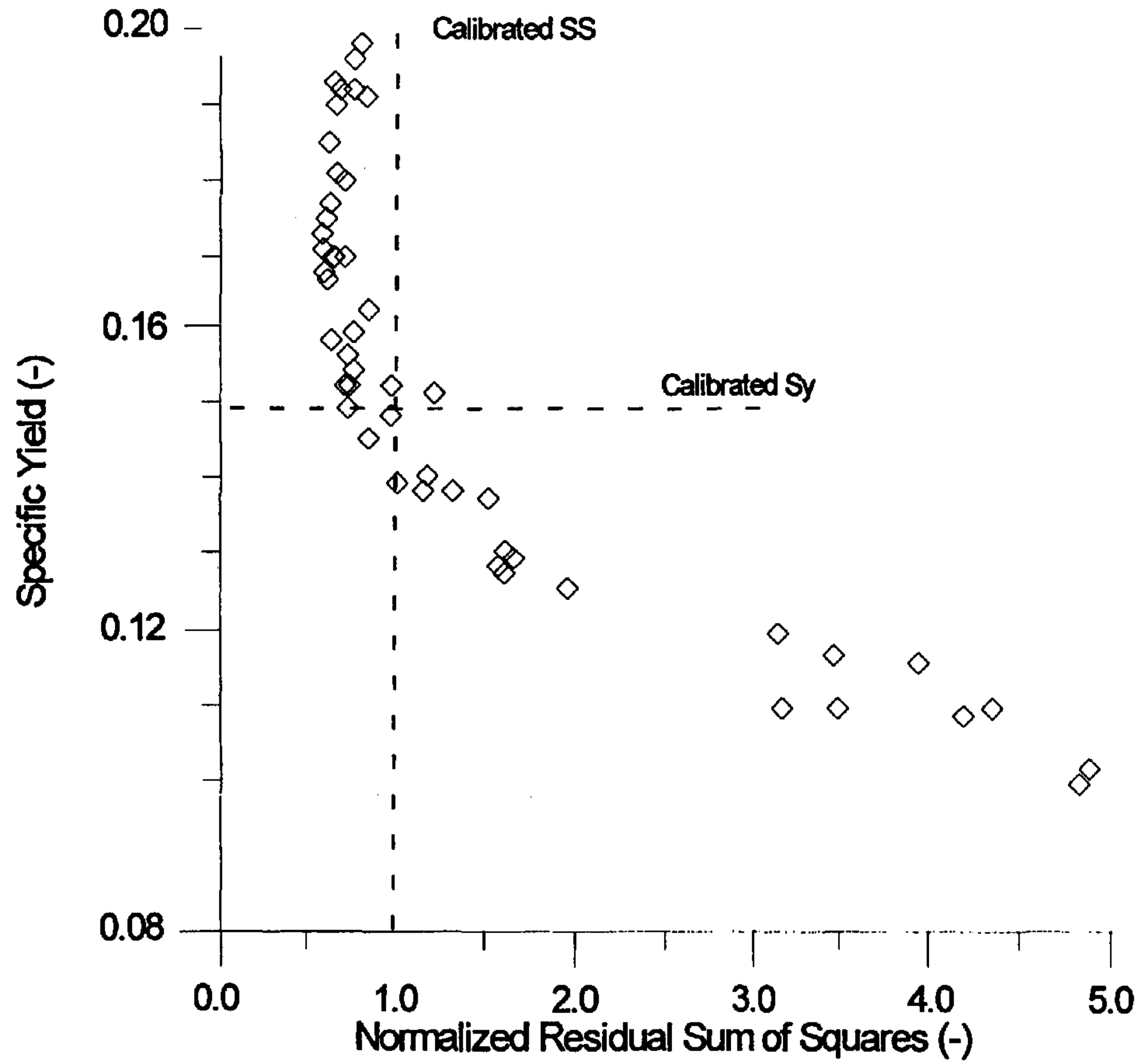

Figure 4.13 Normalized Residual Sum of Squares versus Specific Yield

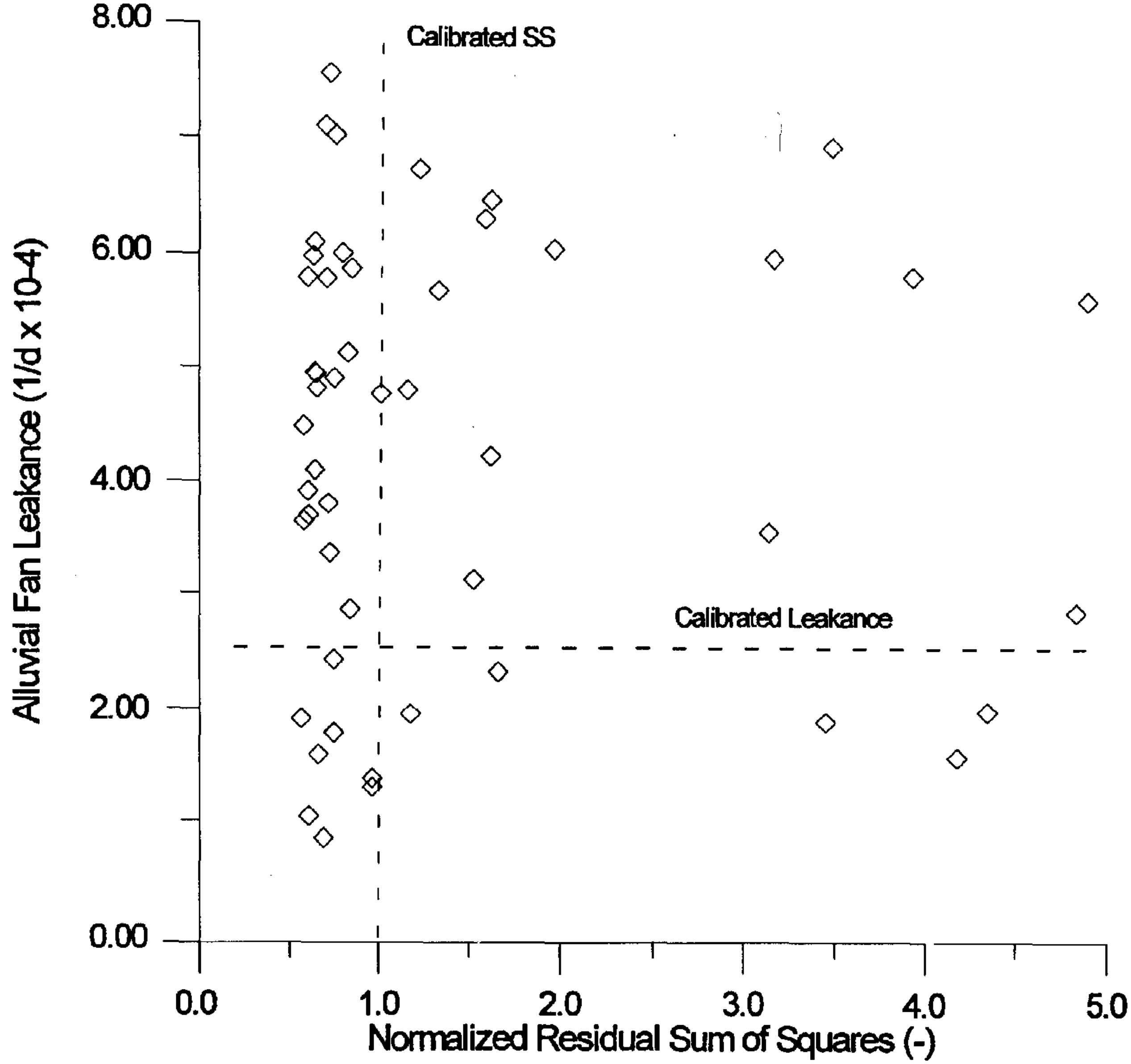

Figure 4.14 Normalized Residual Sum of Squares versus Alluvial Fan Leakance

This page intentionally left blank.

APPENDIX A

Hydrographs from Calibrated Model

This page intentionally left blank.

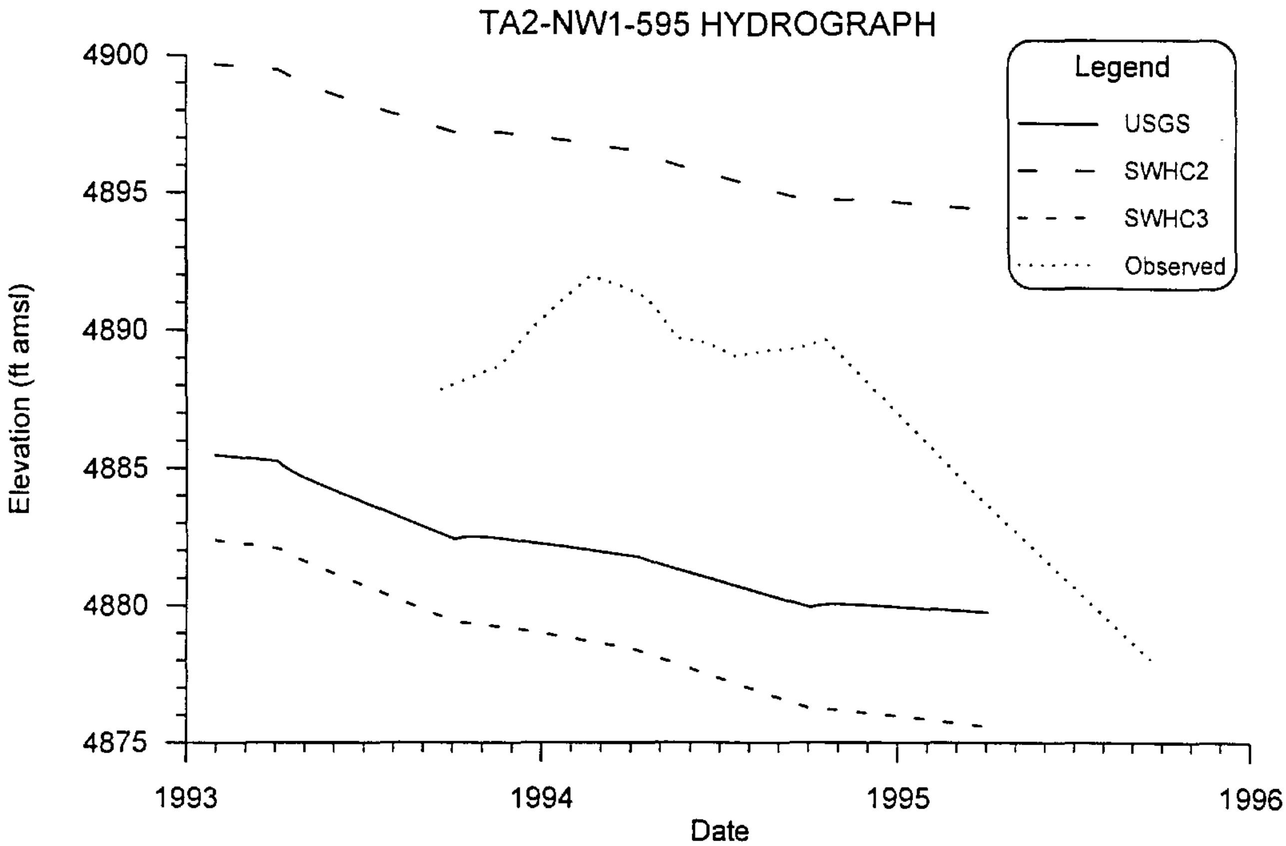
TA2-NW1-595 HYDROGRAPH
Legend
USGS
SWHC2
SWHC3
Observed
Elevation (ft amsl)
4900
4895
4890
4885
4880
4875
1993
1994
1995
1996
Date

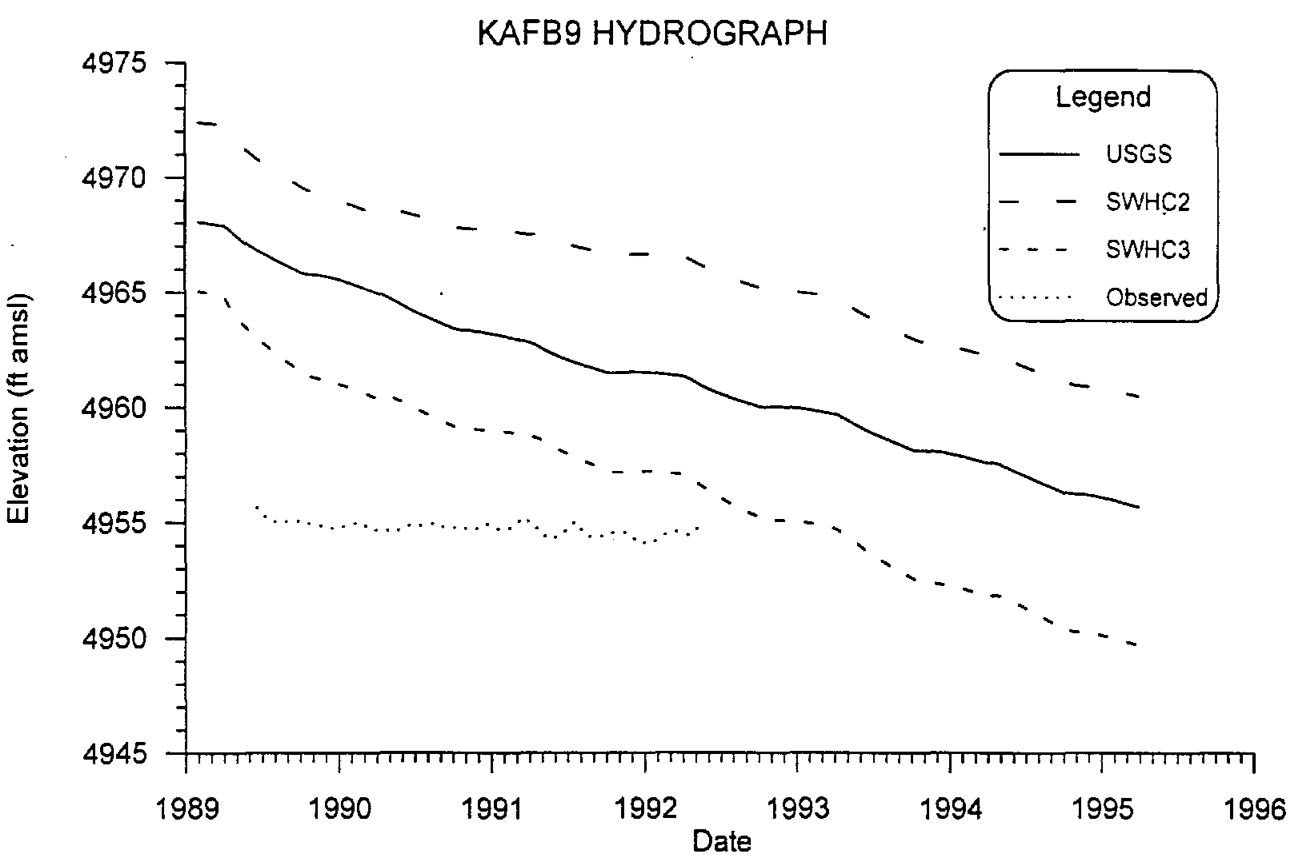
KAFB9 HYDROGRAPH
Legend
USGS
SWHC2
SWHC3
Observed
Elevation (ft amsl)
4975
4970
4965
4960
4955
4950
4945
1989
1990
1991
1992
1993
1994
1995
1996
Date

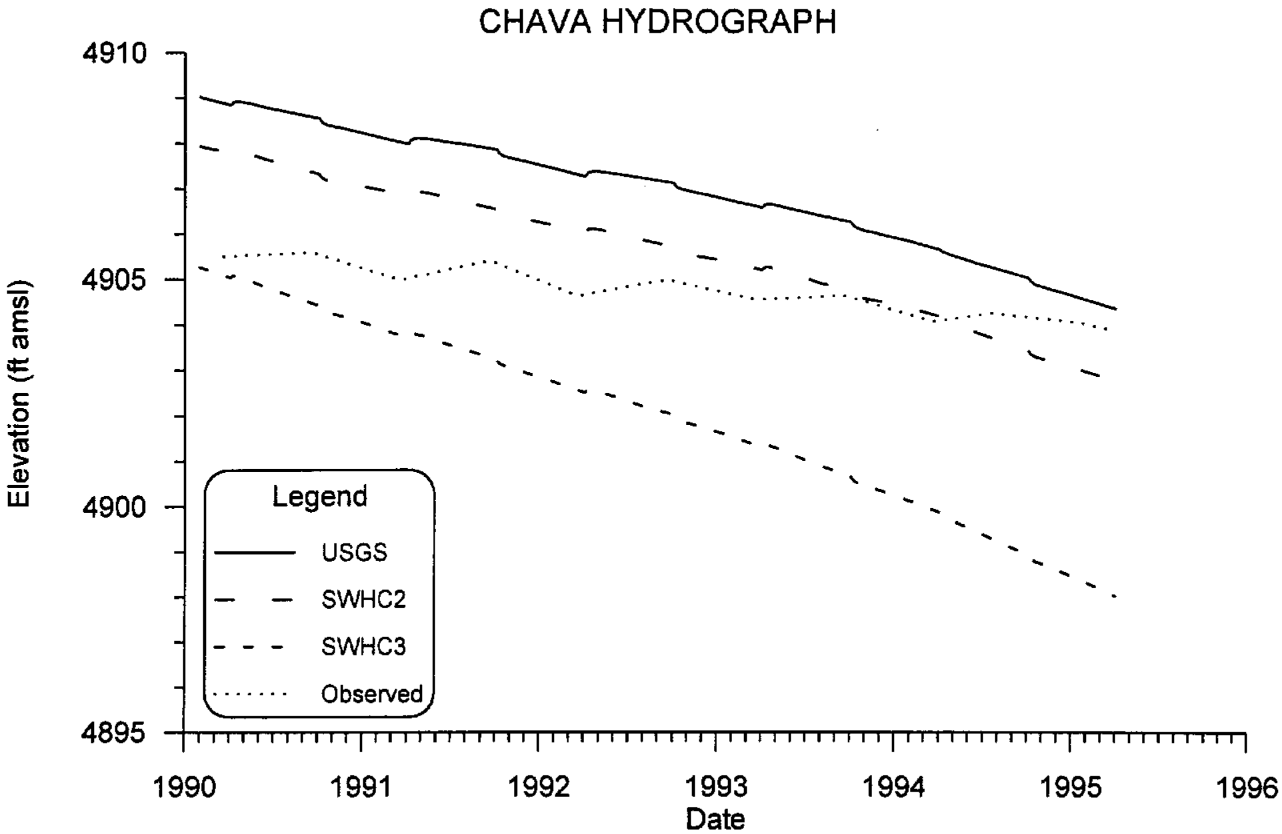
CHAVA HYDROGRAPH
4910
4905
4900
4895
Elevation (ft amsl)
Legend
USGS
SWHC2
SWHC3
Observed
1990
1991
1992
1993
1994
1995
1996
Date

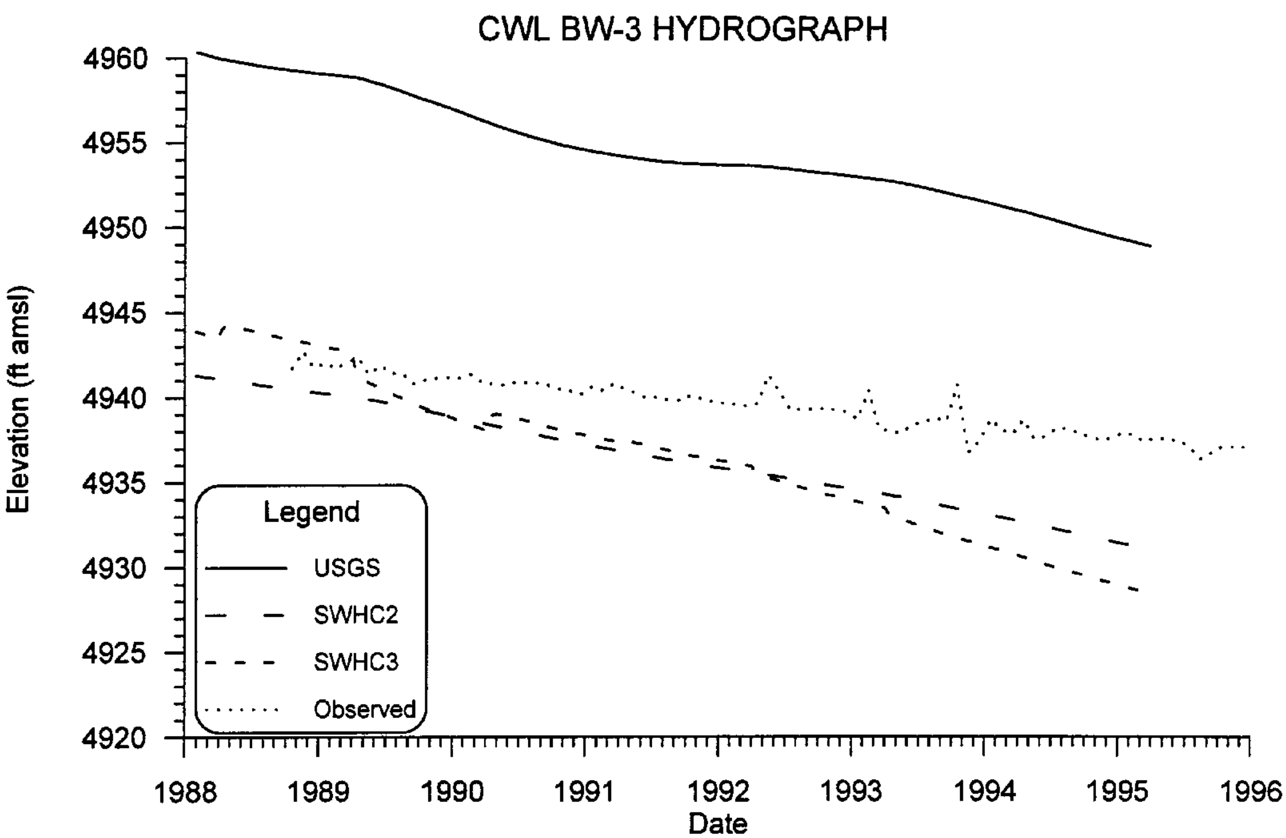
CWL BW-3 HYDROGRAPH
4960
4955
4950
4945
4940
4935
4930
4925
4920
Elevation (ft amsl)
Legend
USGS
SWHC2
SWHC3
Observed
1988
1989
1990
1991
1992
1993
1994
1995
1996
Date

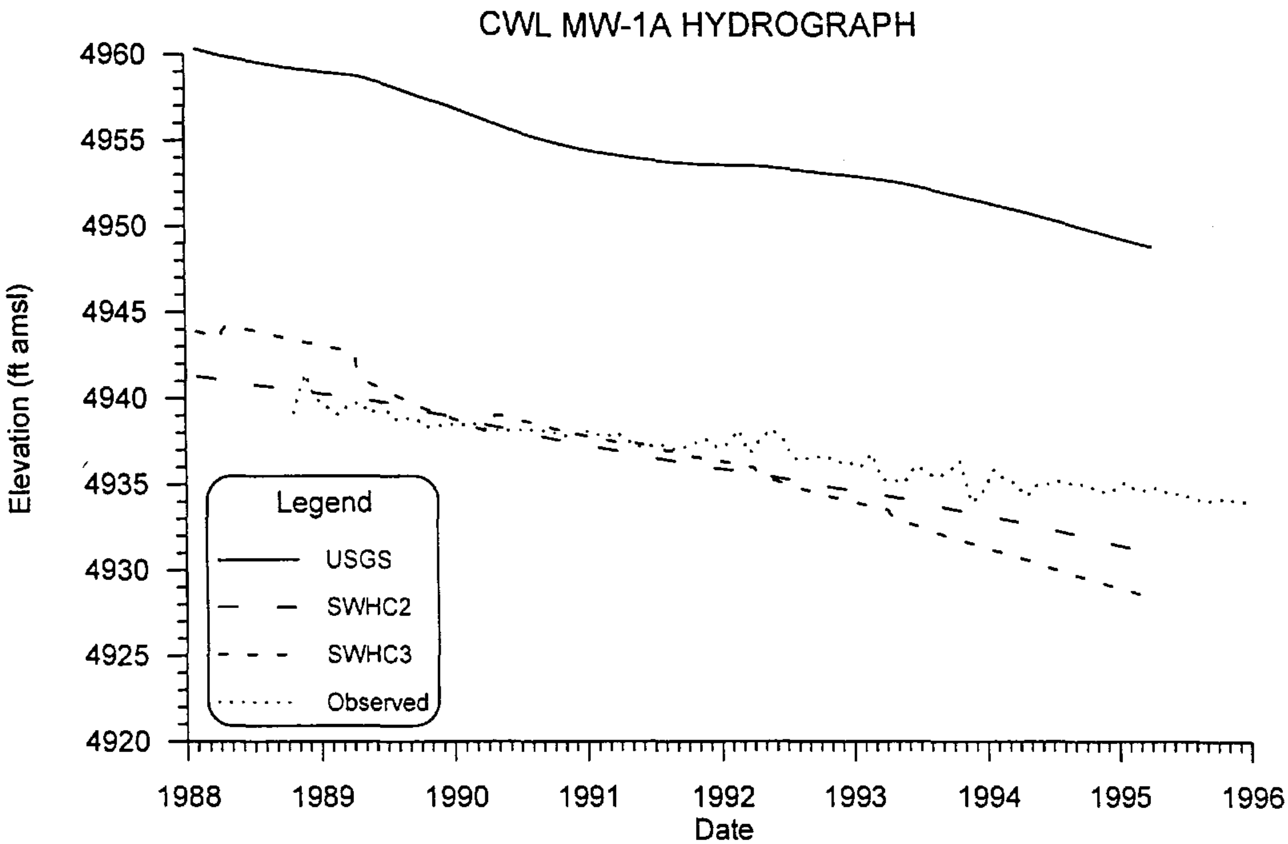
CWL MW-1A HYDROGRAPH
4960
4955
4950
4945
4940
4935
4930
4925
4920
Elevation (ft amsl)
Legend
USGS
SWHC2
SWHC3
Observed
1988
1989
1990
1991
1992
1993
1994
1995
1996
Date

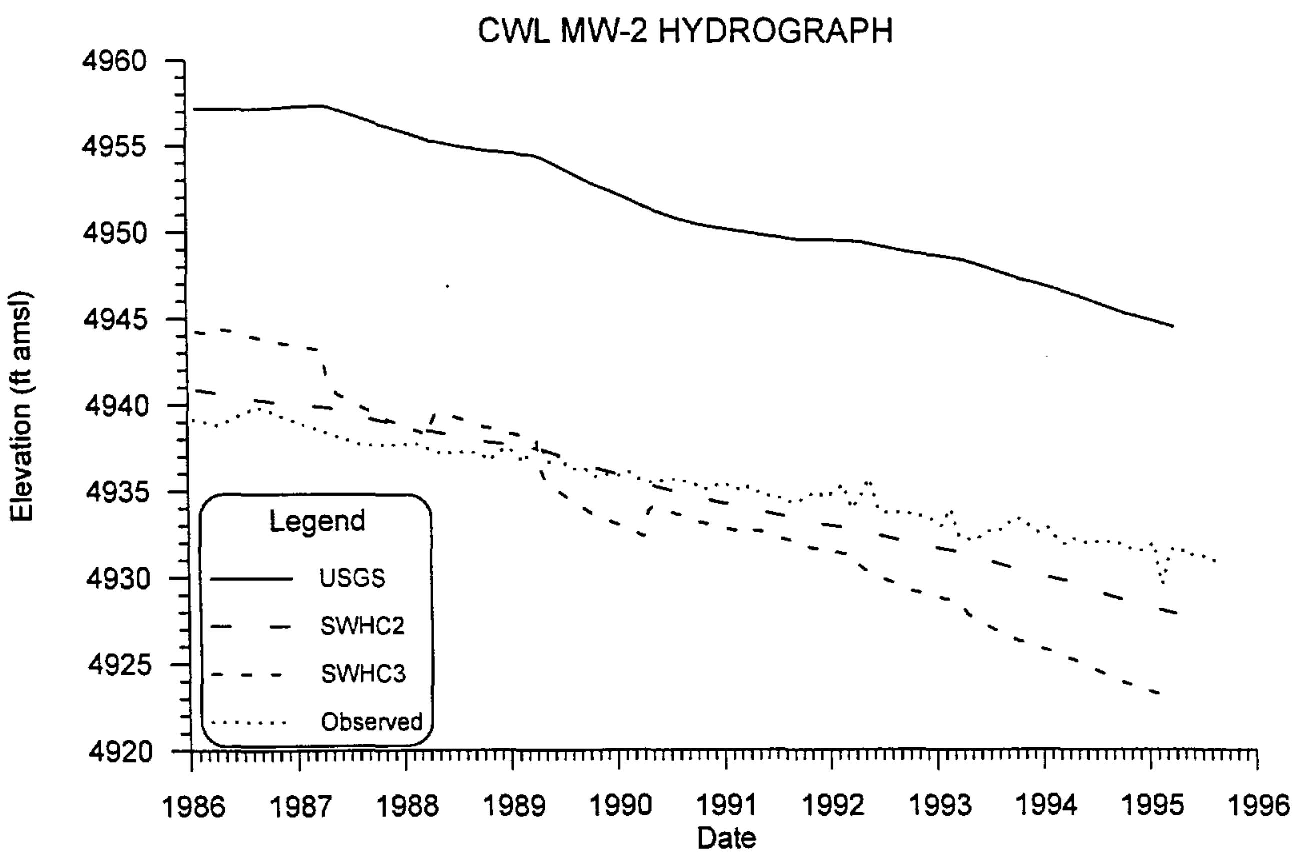
CWL MW-2 HYDROGRAPH
4960
4955
4950
4945
4940
4935
4930
4925
4920
Elevation (ft amsl)
Legend
USGS
SWHC2
SWHC3
Observed
1986
1987
1988
1989
1990
1991
1992
1993
1994
1995
1996
Date

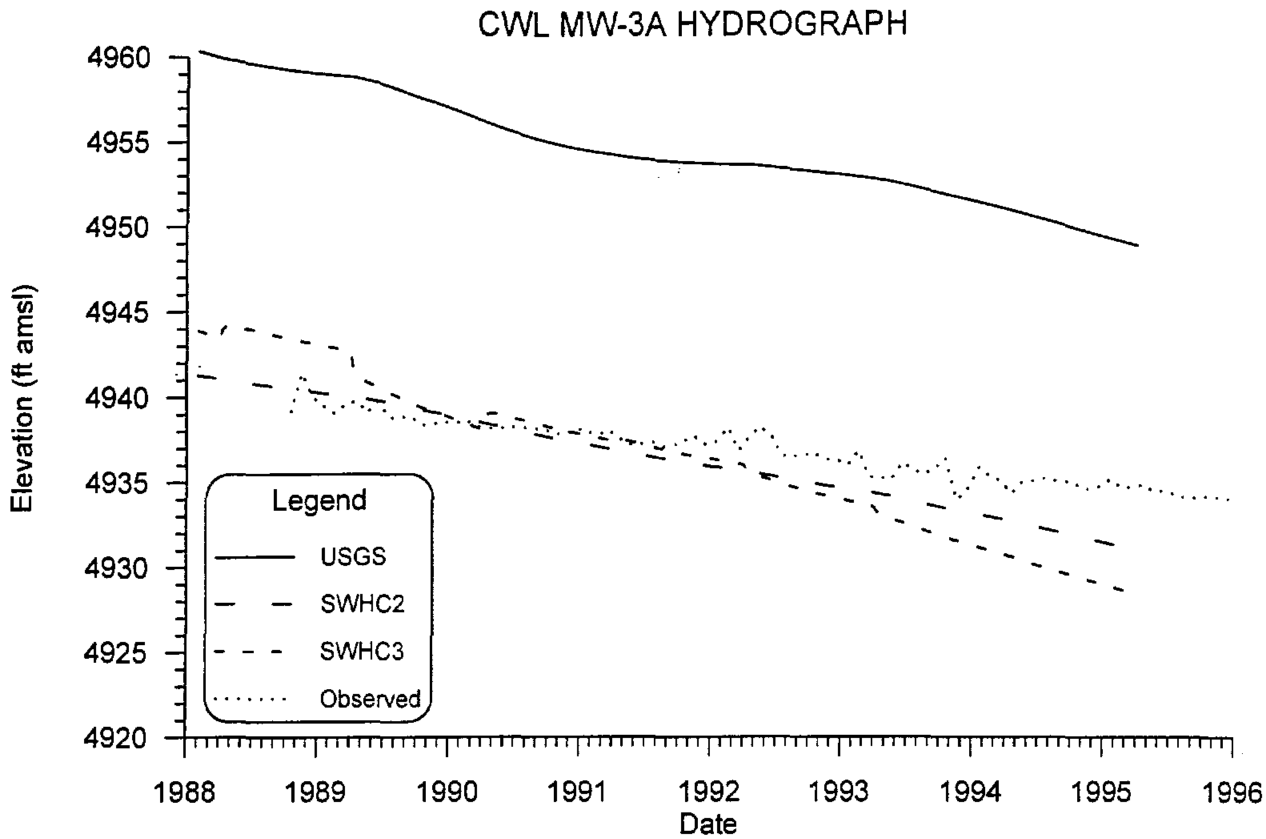
CWL MW-3A HYDROGRAPH
Elevation (ft amsl)
4960
4955
4950
4945
4940
4935
4930
4925
4920
Legend
USGS
SWHC2
SWHC3
Observed
1988
1989
1990
1991
1992
1993
1994
1995
1996
Date

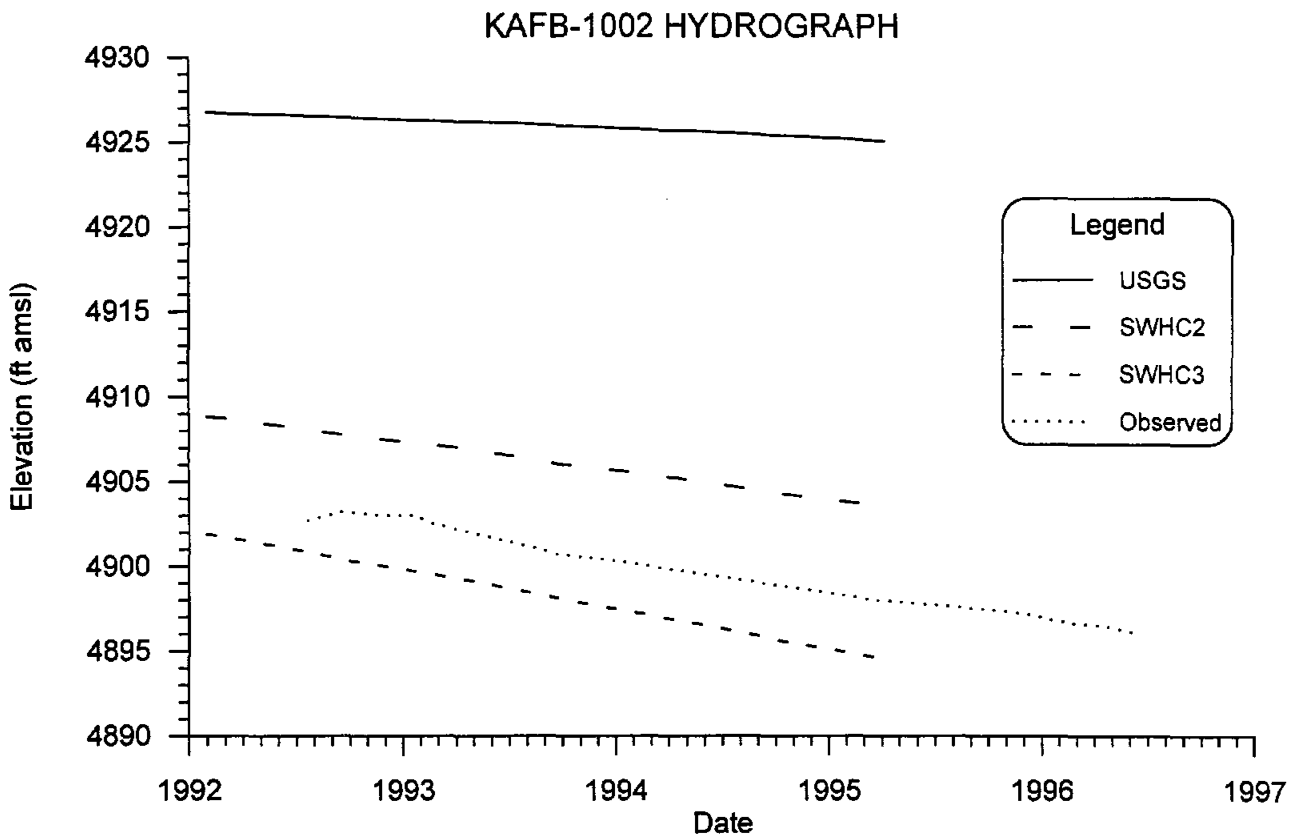
KAFB-1002 HYDROGRAPH
4930
4925
4920
4915
4910
4905
4900
4895
4890
Elevation (ft amsl)
1992
1993
1994
1995
1996
1997
Date
Legend
USGS
SWHC2
SWHC3
Observed

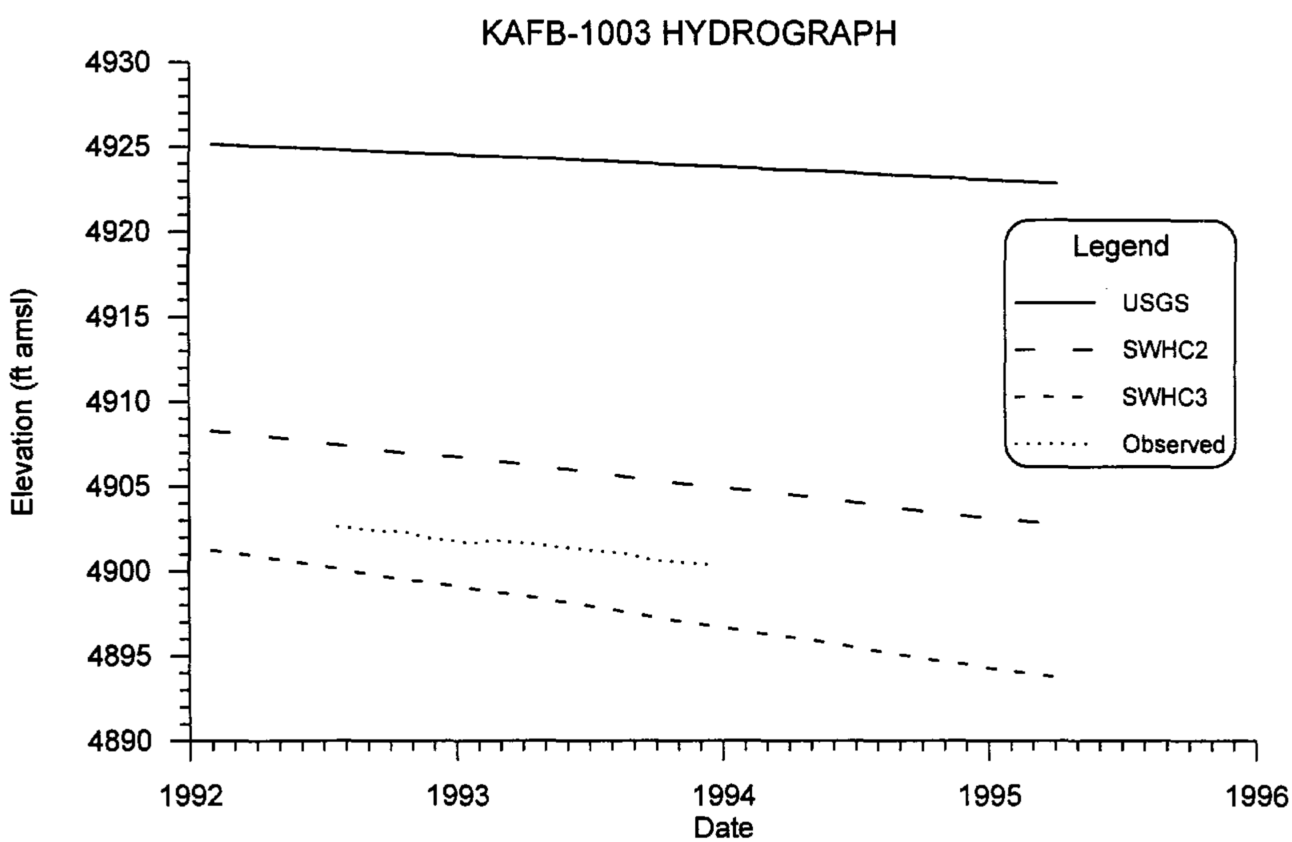
KAFB-1003 HYDROGRAPH
4930
4925
4920
4915
4910
4905
4900
4895
4890
Elevation (ft amsl)
1992
1993
1994
1995
1996
Date
Legend
USGS
SWHC2
SWHC3
Observed

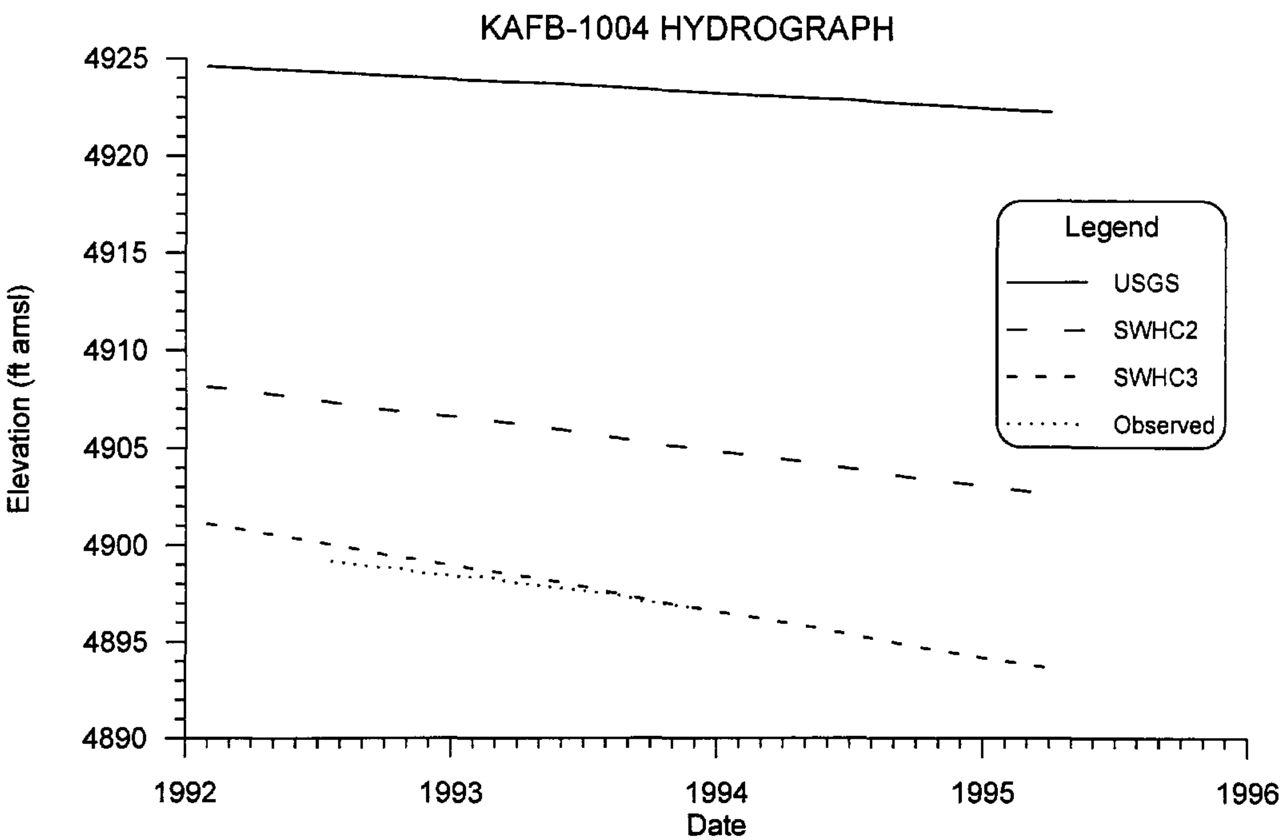
KAFB-1004 HYDROGRAPH
Elevation (ft amsl)
4925
4920
4915
4910
4905
4900
4895
4890
1992
1993
1994
1995
1996
Date
Legend
USGS
SWHC2
SWHC3
Observed

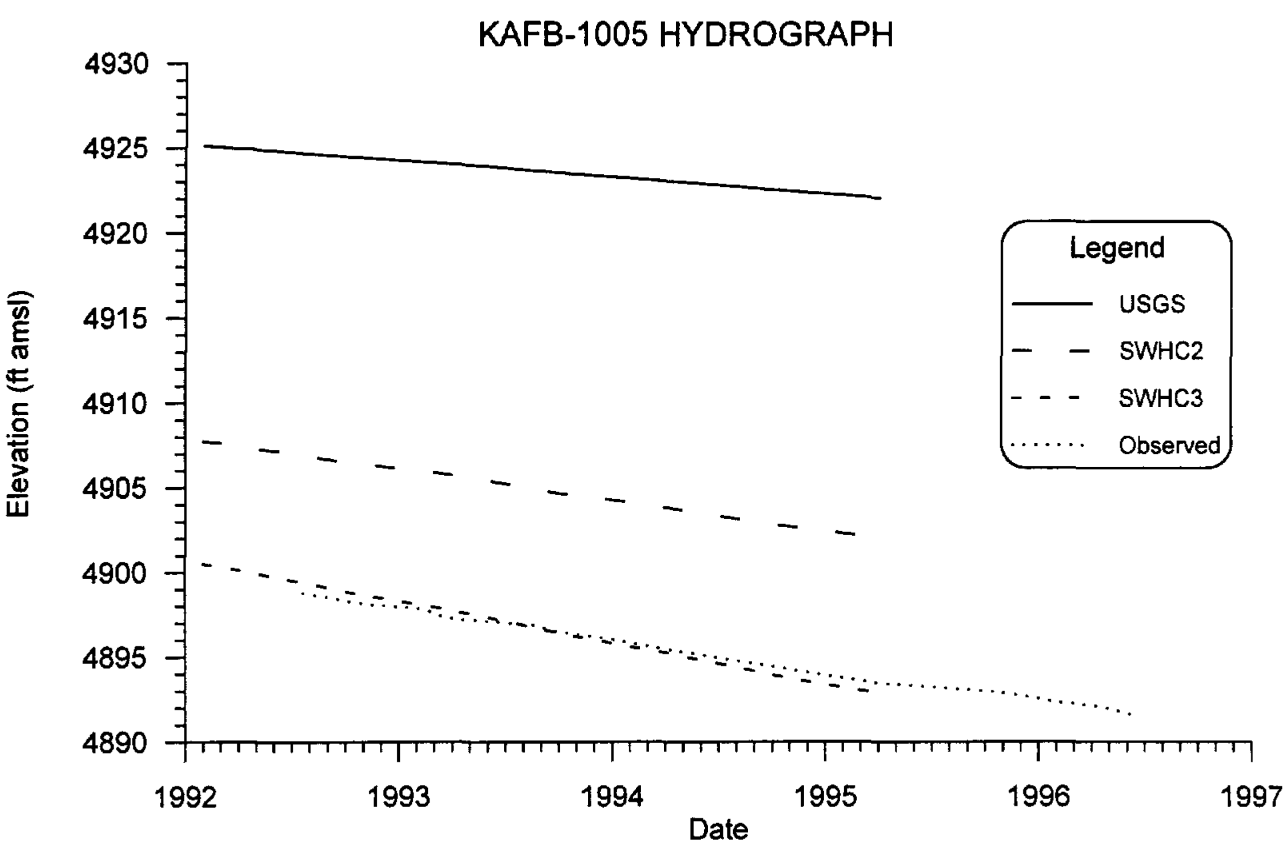
KAFB-1005 HYDROGRAPH
Elevation (ft amsl)
4930
4925
4920
4915
4910
4905
4900
4895
4890
1992
1993
1994
1995
1996
1997
Date
Legend
USGS
SWHC2
SWHC3
Observed

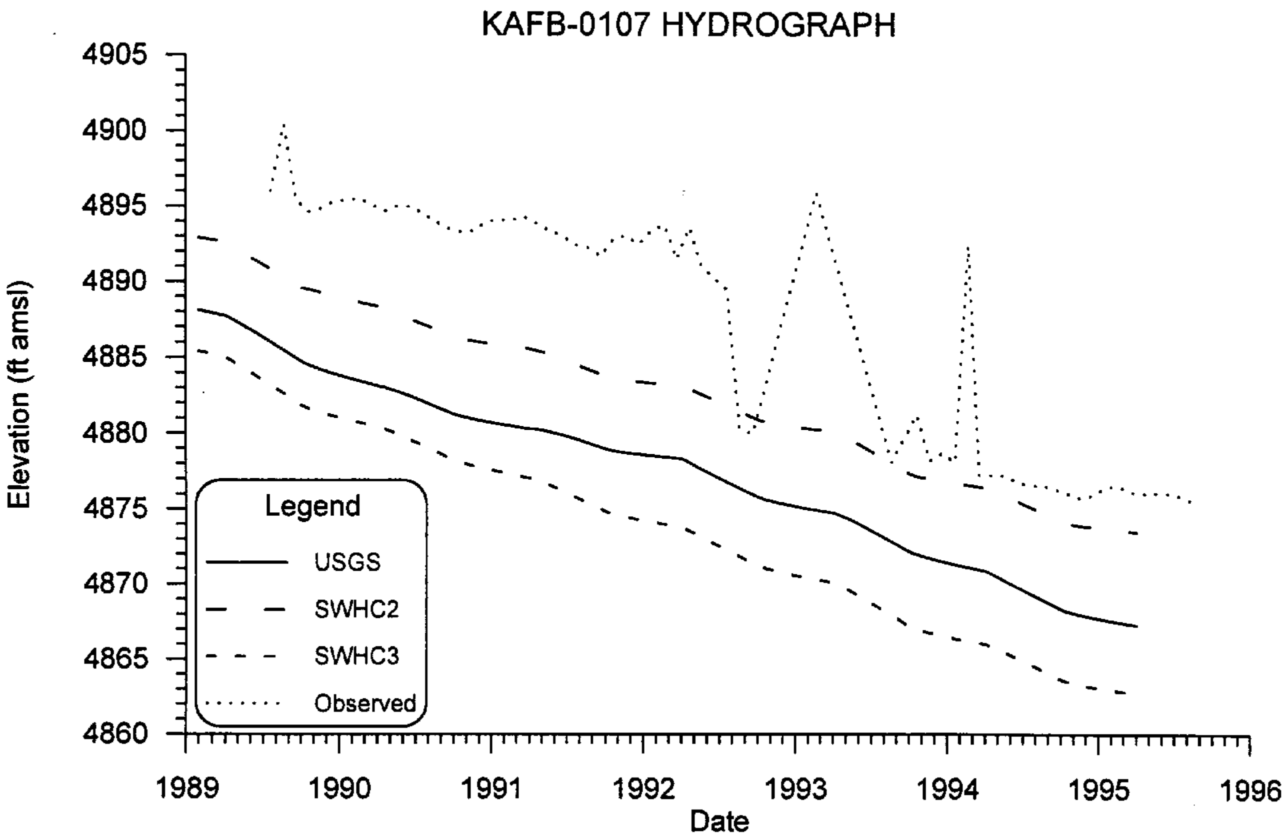
KAFB-0107 HYDROGRAPH
Elevation (ft amsl)
4905
4900
4895
4890
4885
4880
4875
4870
4865
4860
1989
1990
1991
1992
1993
1994
1995
1996
Date
Legend
USGS
SWHC2
SWHC3
Observed

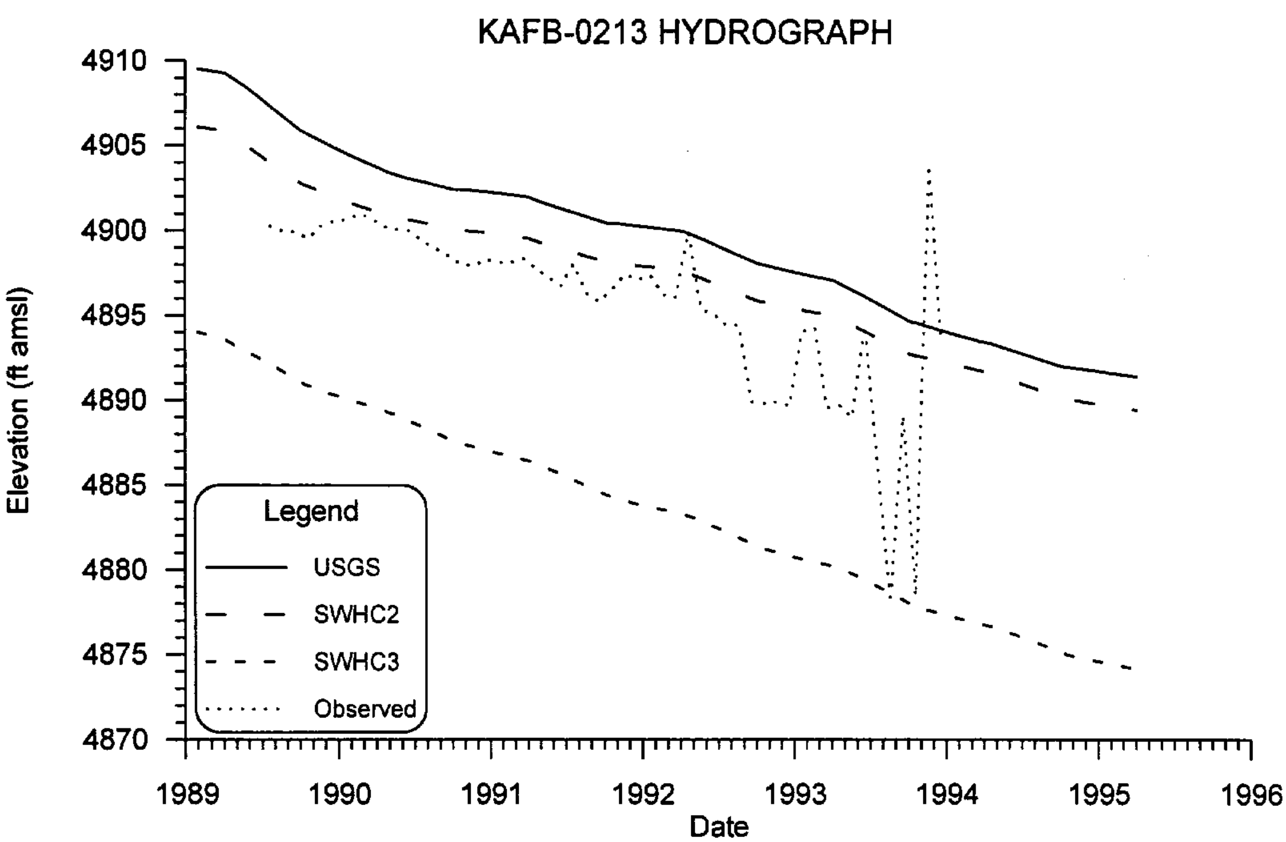
KAFB-0213 HYDROGRAPH
Elevation (ft amsl)
4910
4905
4900
4895
4890
4885
4880
4875
4870
1989
1990
1991
1992
1993
1994
1995
1996
Date
Legend
USGS
SWHC2
SWHC3
Observed

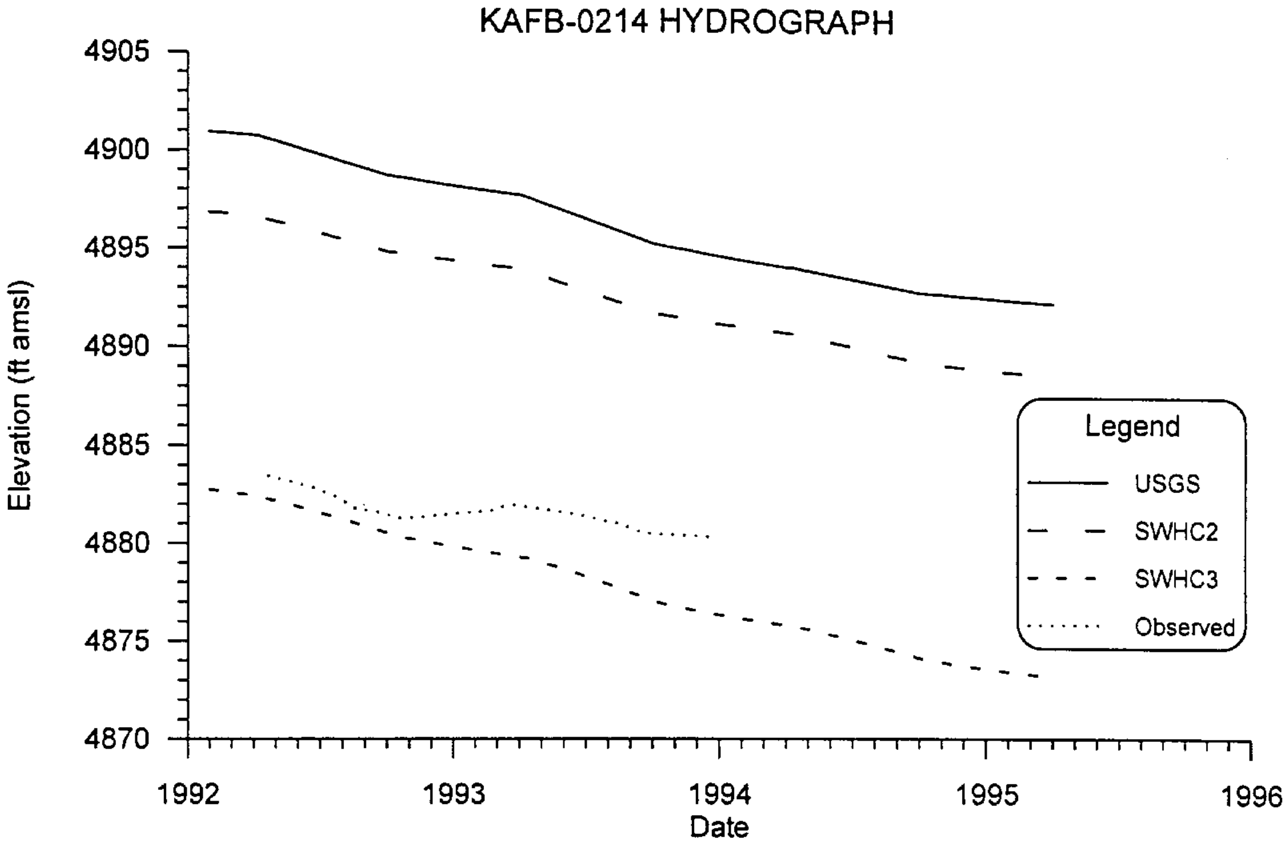
KAFB-0214 HYDROGRAPH
Elevation (ft amsl)
4905
4900
4895
4890
4885
4880
4875
4870
1992
1993
1994
1995
1996
Date
Legend
USGS
SWHC2
SWHC3
Observed

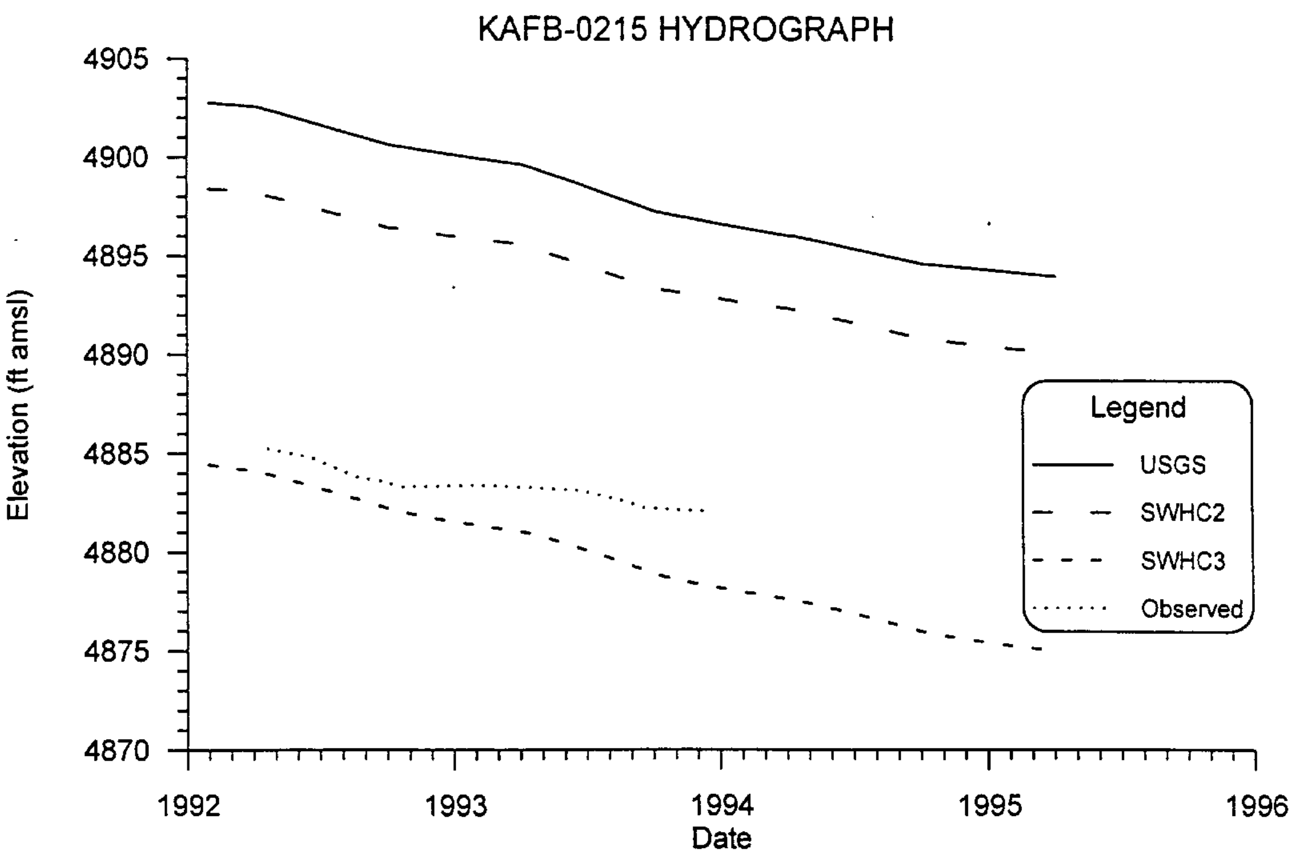
KAFB-0215 HYDROGRAPH
Elevation (ft amsl)
4905
4900
4895
4890
4885
4880
4875
4870
1992
1993
1994
1995
1996
Date
Legend
USGS
SWHC2
SWHC3
Observed

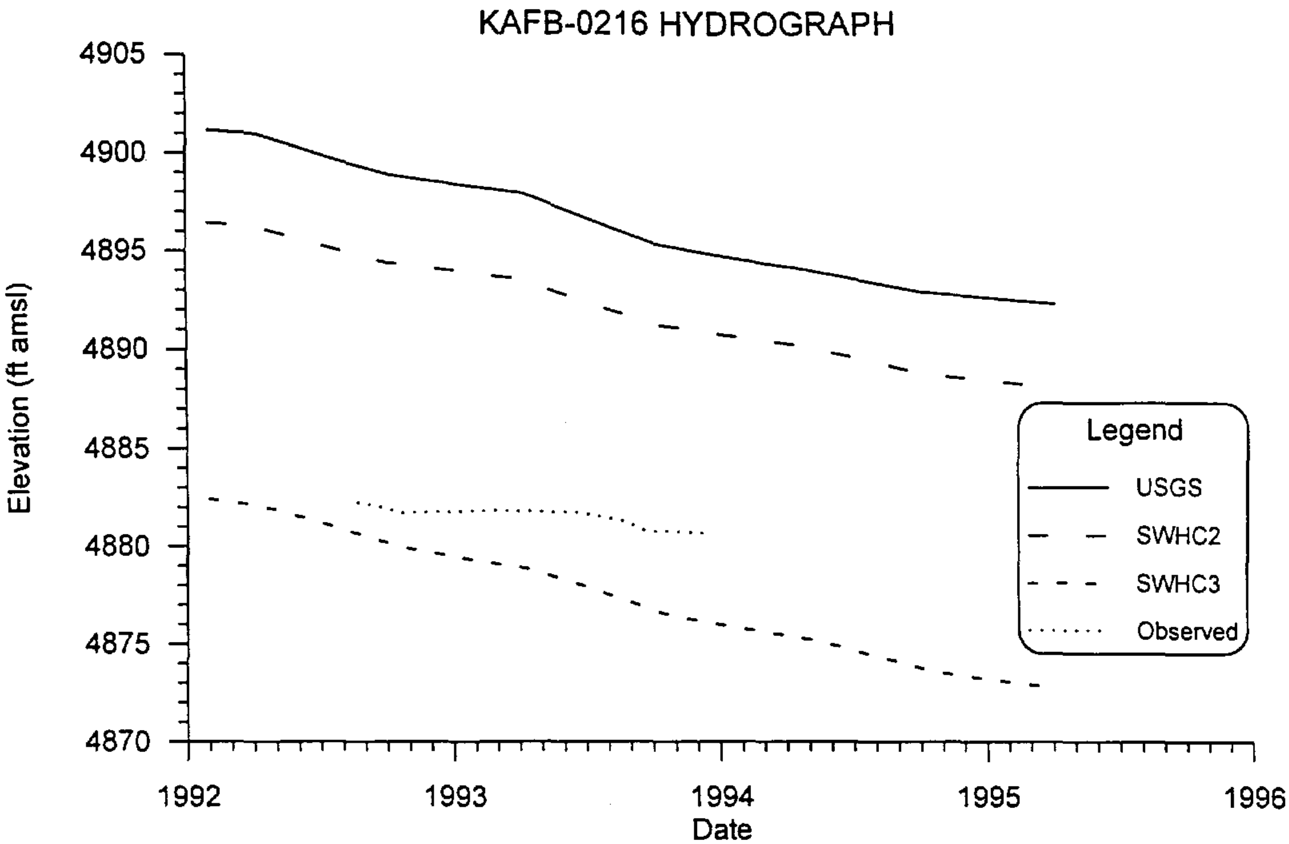
KAFB-0216 HYDROGRAPH
4905
4900
4895
4890
4885
4880
4875
4870
Elevation (ft amsl)
1992
1993
1994
1995
1996
Date
Legend
USGS
SWHC2
SWHC3
Observed

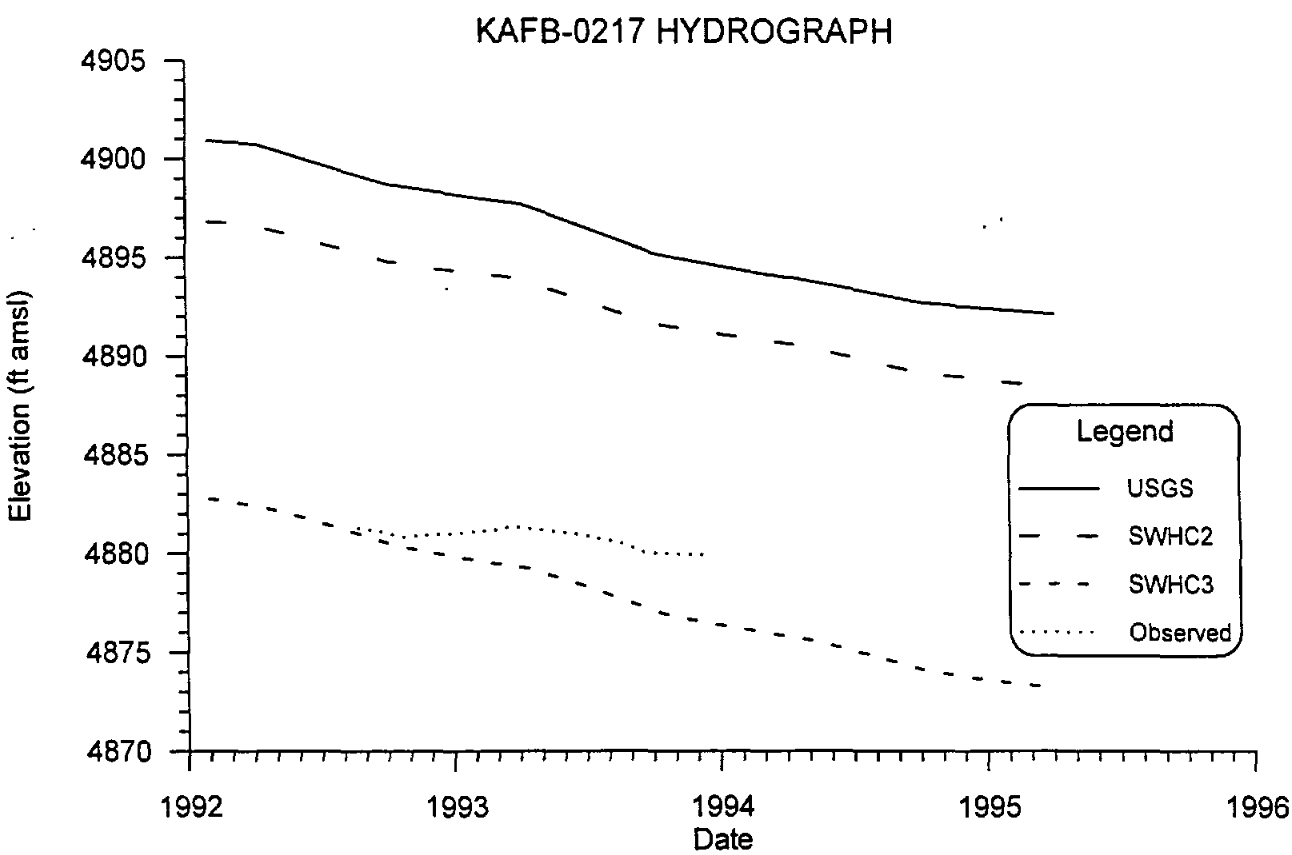
KAFB-0217 HYDROGRAPH
4905
4900
4895
4890
4885
4880
4875
4870
Elevation (ft amsl)
1992
1993
1994
1995
1996
Date
Legend
USGS
SWHC2
SWHC3
Observed

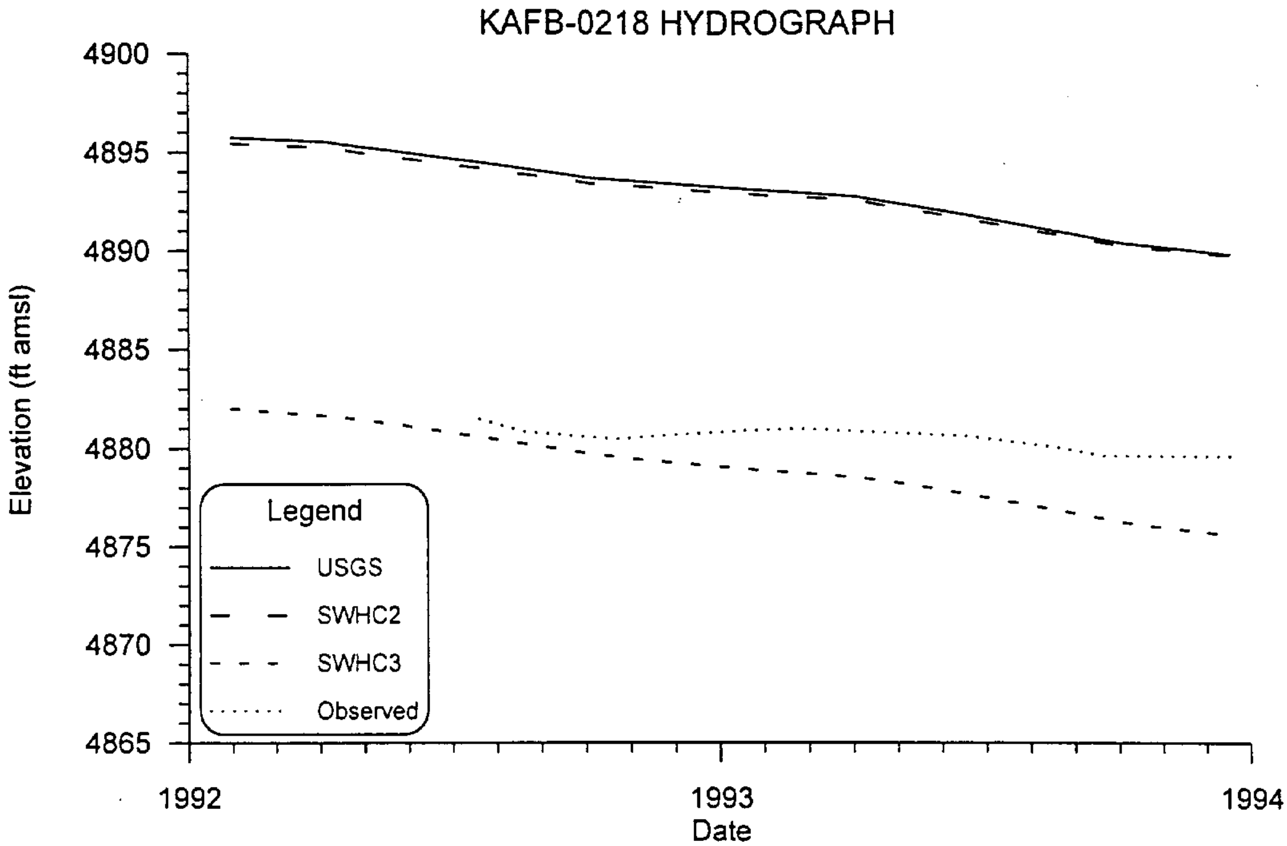

KAFB-0218 HYDROGRAPH
4900
4895
4890
4885
4880
4875
4870
4865
Elevation (ft amsl)
Legend
USGS
SWHC2
SWHC3
Observed
1992
1993
1994
Date

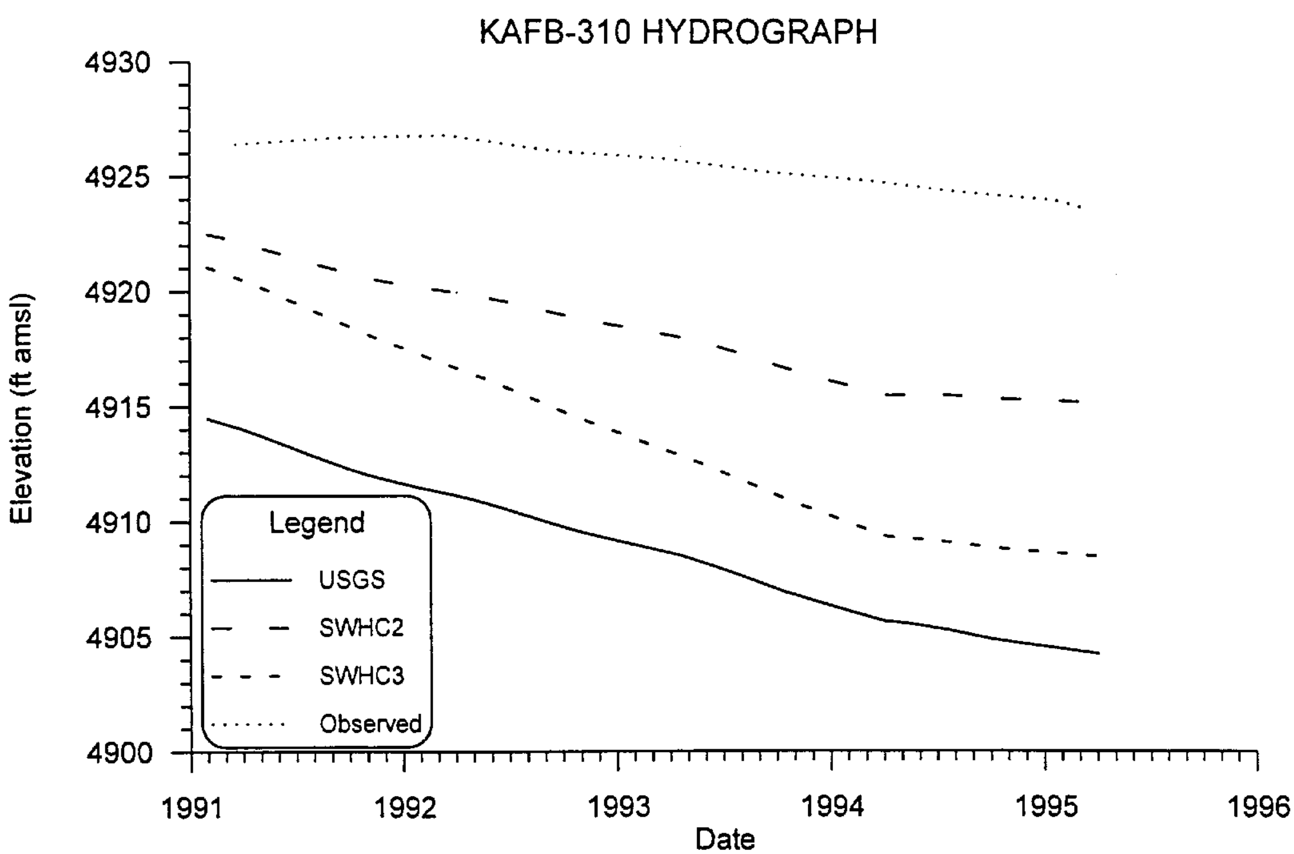

KAFB-310 HYDROGRAPH
4930
4925
4920
4915
4910
4905
4900
Elevation (ft amsl)
Legend
USGS
SWHC2
SWHC3
Observed
1991
1992
1993
1994
1995
1996
Date

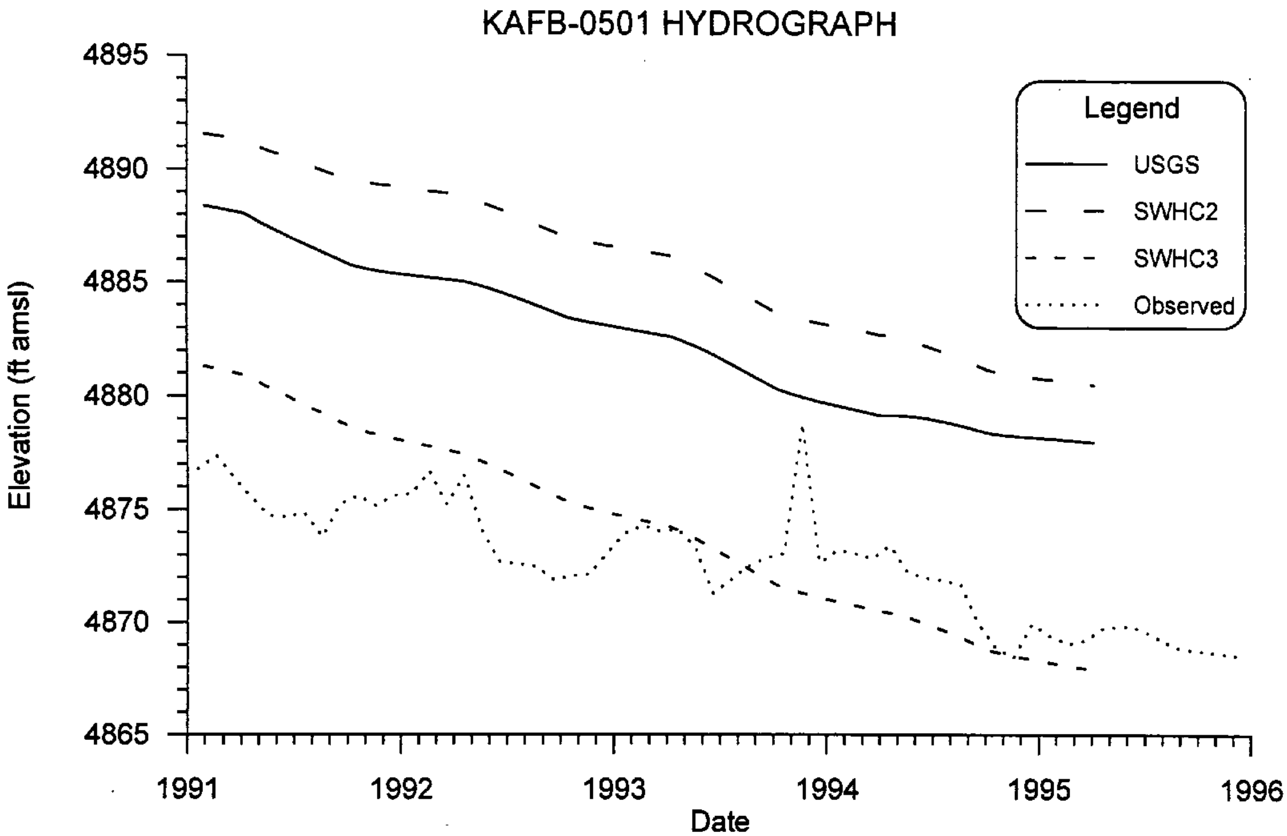
KAFB-0501 HYDROGRAPH
Legend
USGS
SWHC2
SWHC3
Observed
Elevation (ft amsl)
4895
4890
4885
4880
4875
4870
4865
1991
1992
1993
1994
1995
1996
Date

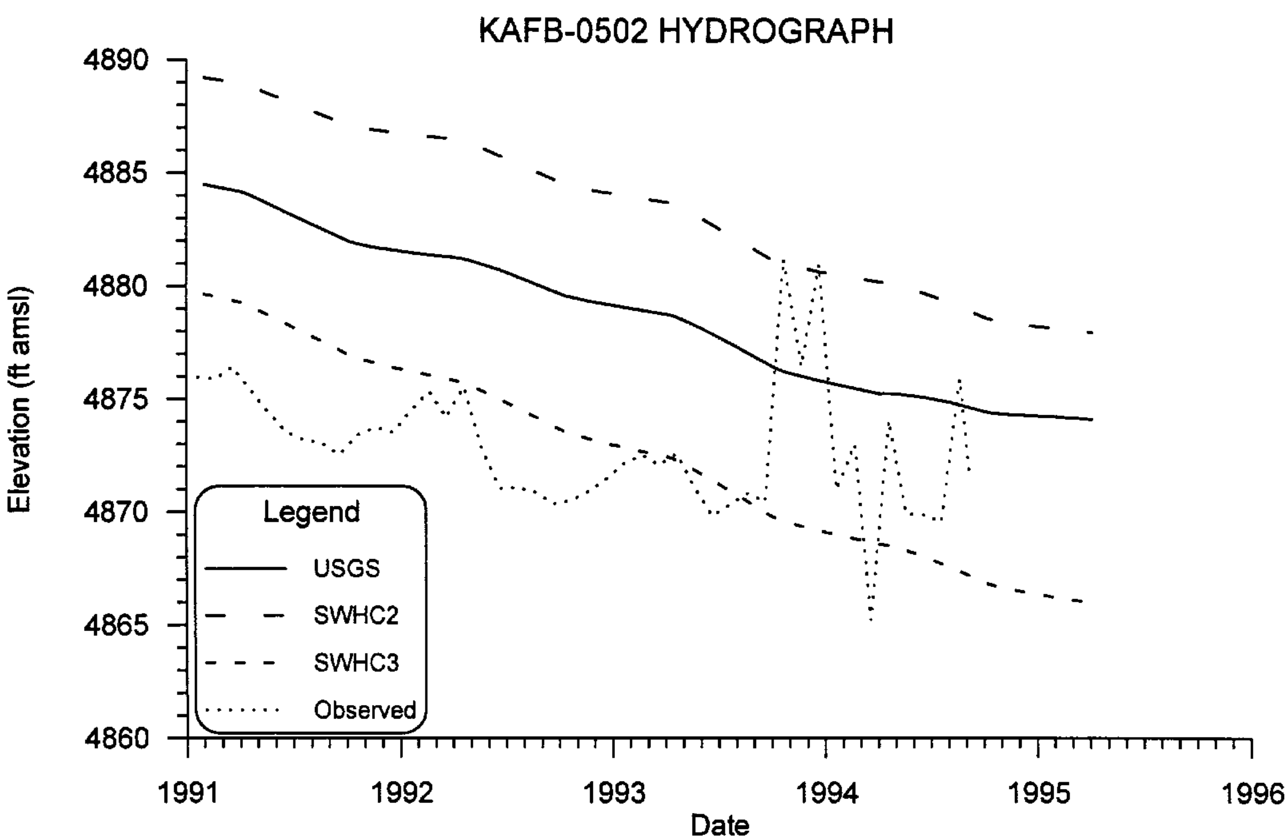
KAFB-0502 HYDROGRAPH
Legend
USGS
SWHC2
SWHC3
Observed
Elevation (ft amsl)
4890
4885
4880
4875
4870
4865
4860
1991
1992
1993
1994
1995
1996
Date

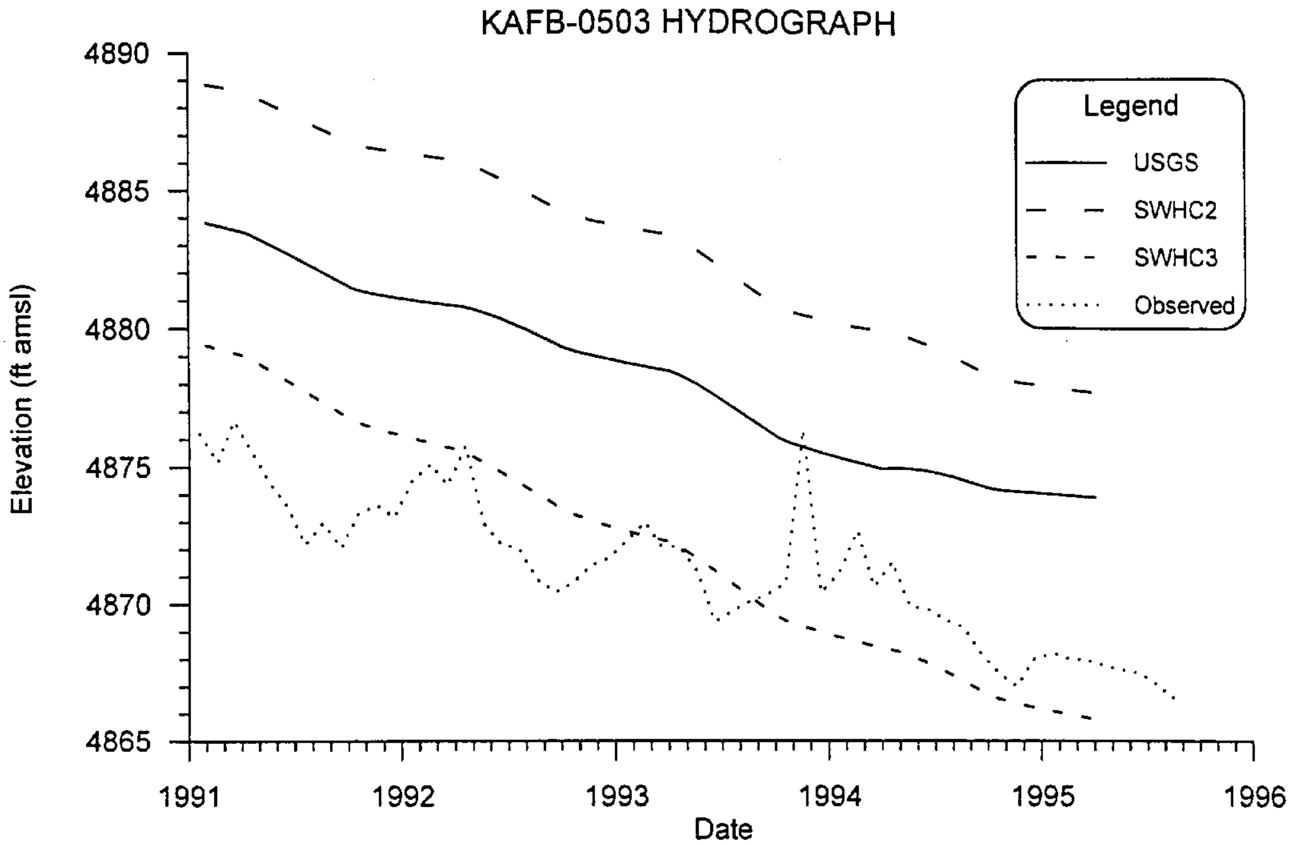
KAFB-0503 HYDROGRAPH
Legend
USGS
SWHC2
SWHC3
Observed
Elevation (ft amsl)
4890
4885
4880
4875
4870
4865
1991
1992
1993
1994
1995
1996
Date

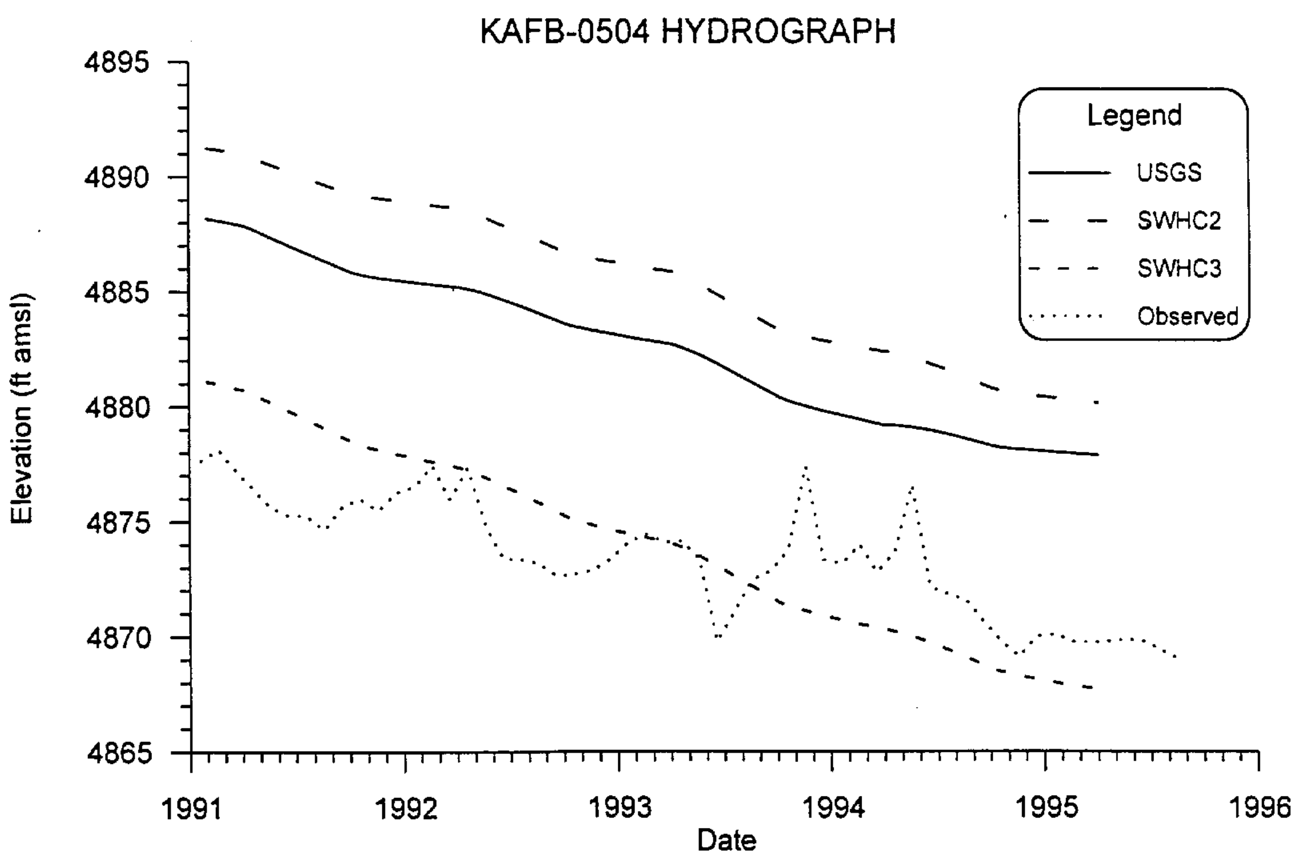
KAFB-0504 HYDROGRAPH
Legend
USGS
SWHC2
SWHC3
Observed
Elevation (ft amsl)
4895
4890
4885
4880
4875
4870
4865
1991
1992
1993
1994
1995
1996
Date

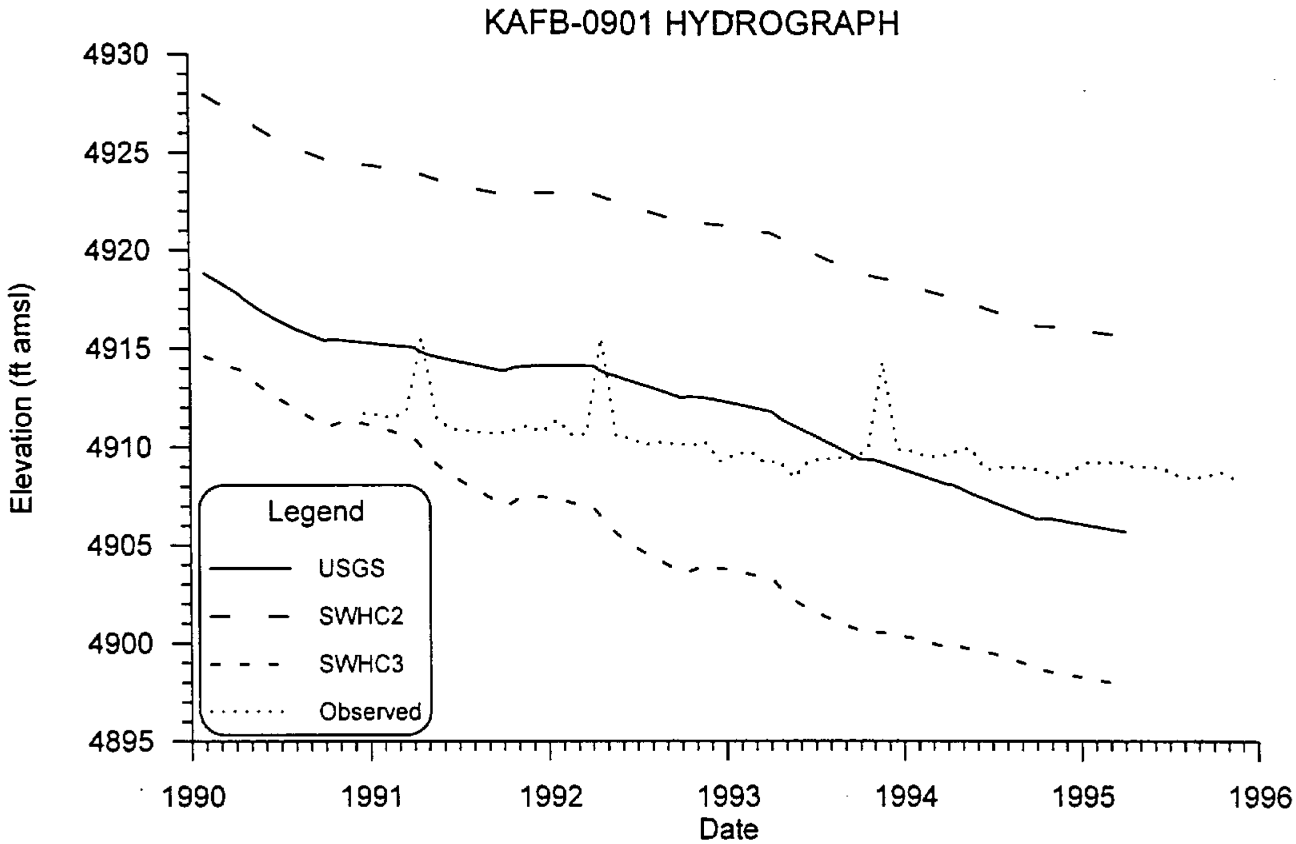
KAFB-0901 HYDROGRAPH
Elevation (ft amsl)
4930
4925
4920
4915
4910
4905
4900
4895
1990
1991
1992
1993
1994
1995
1996
Date
Legend
USGS
SWHC2
SWHC3
Observed

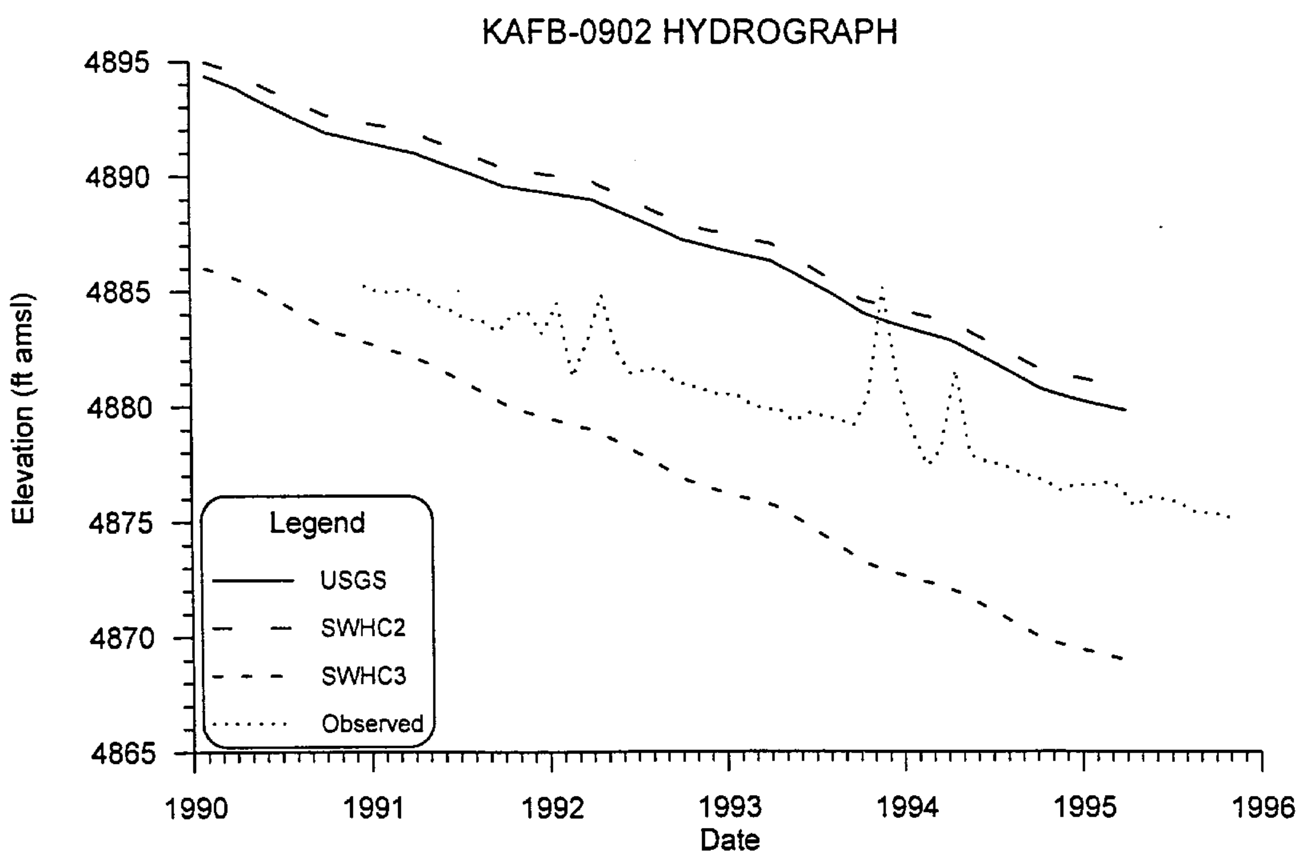
KAFB-0902 HYDROGRAPH
Elevation (ft amsl)
4895
4890
4885
4880
4875
4870
4865
1990
1991
1992
1993
1994
1995
1996
Date
Legend
USGS
SWHC2
SWHC3
Observed

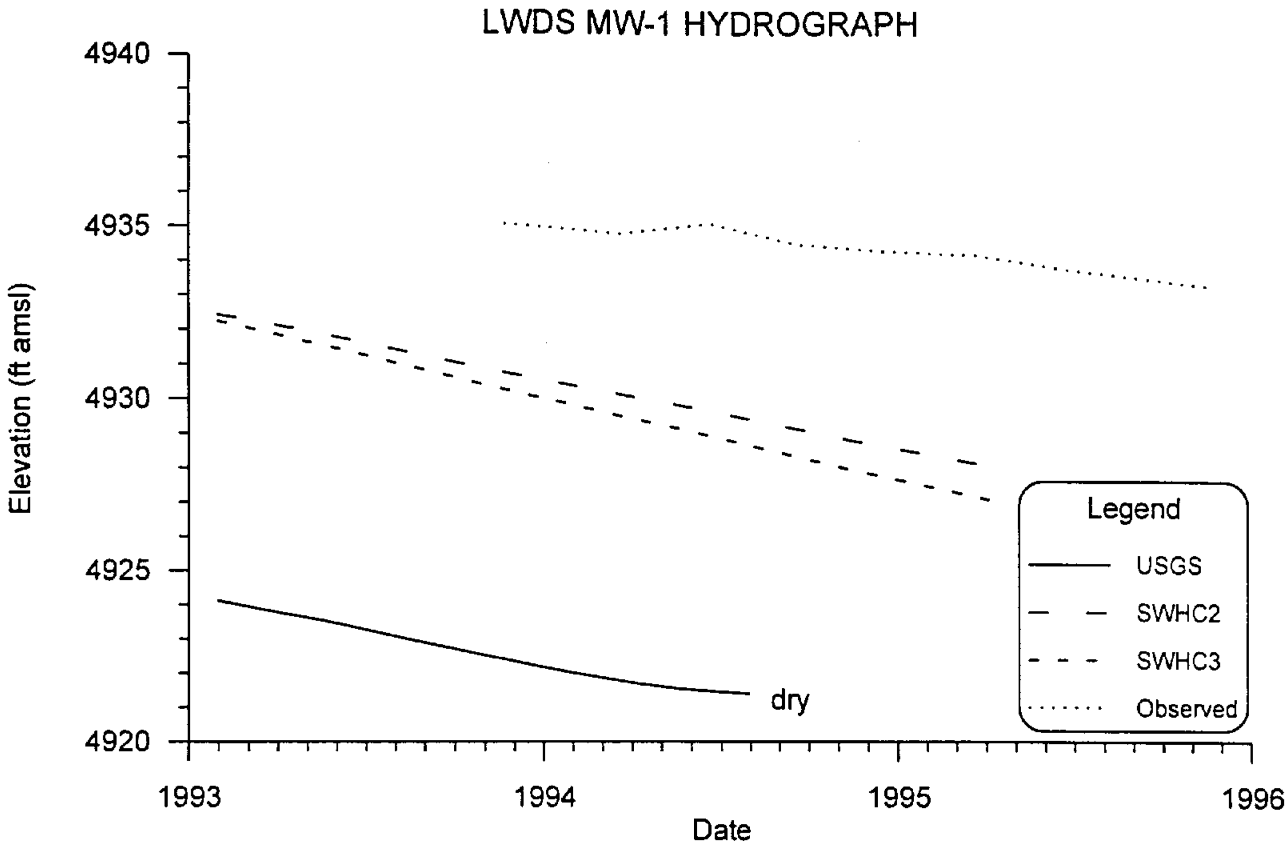
LWDS MW-1 HYDROGRAPH
4940
4935
4930
4925
4920
Elevation (ft amsl)
dry
Legend
USGS
SWHC2
SWHC3
Observed
1993
1994
1995
1996
Date

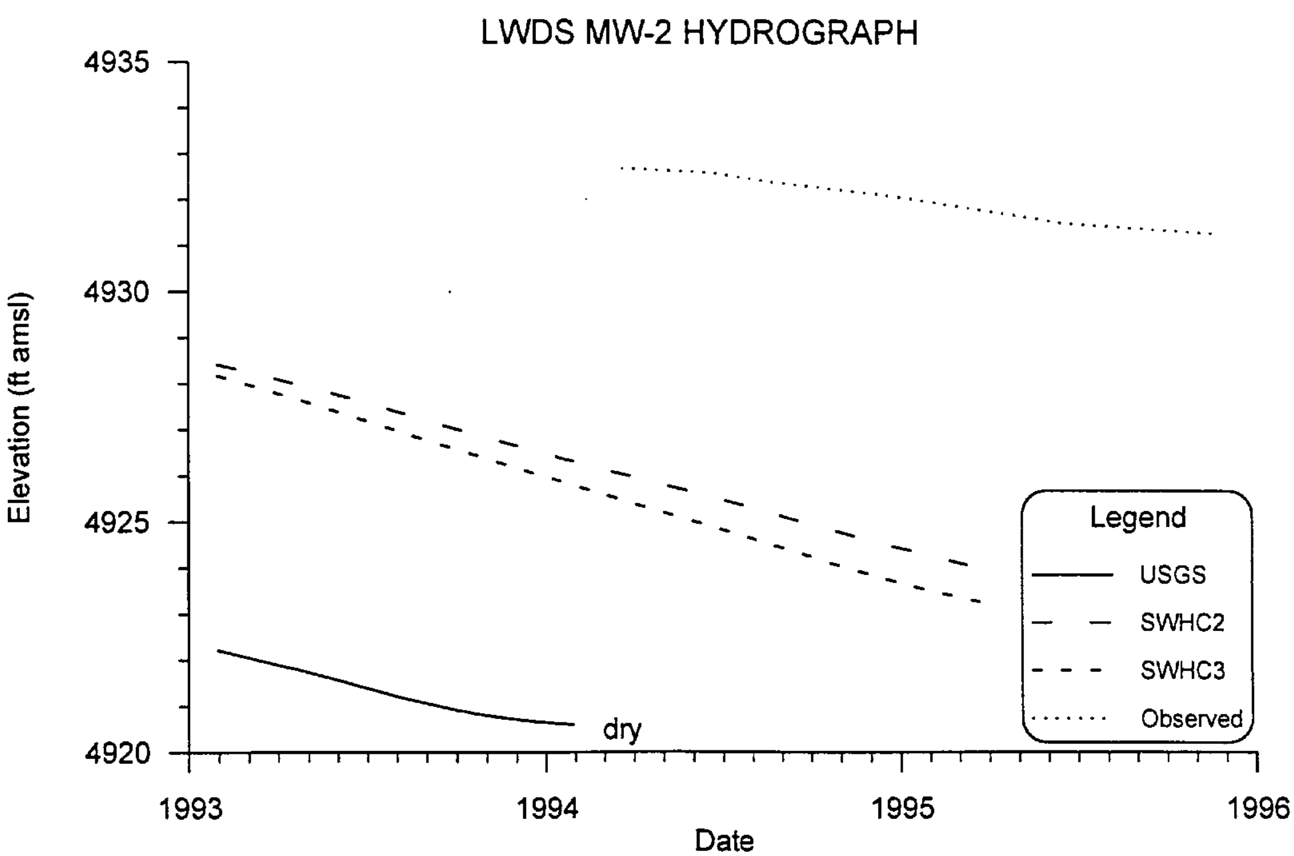
LWDS MW-2 HYDROGRAPH
4935
4930
4925
4920
Elevation (ft amsl)
dry
Legend
USGS
SWHC2
SWHC3
Observed
1993
1994
1995
1996
Date

MVMWJ HYDROGRAPH

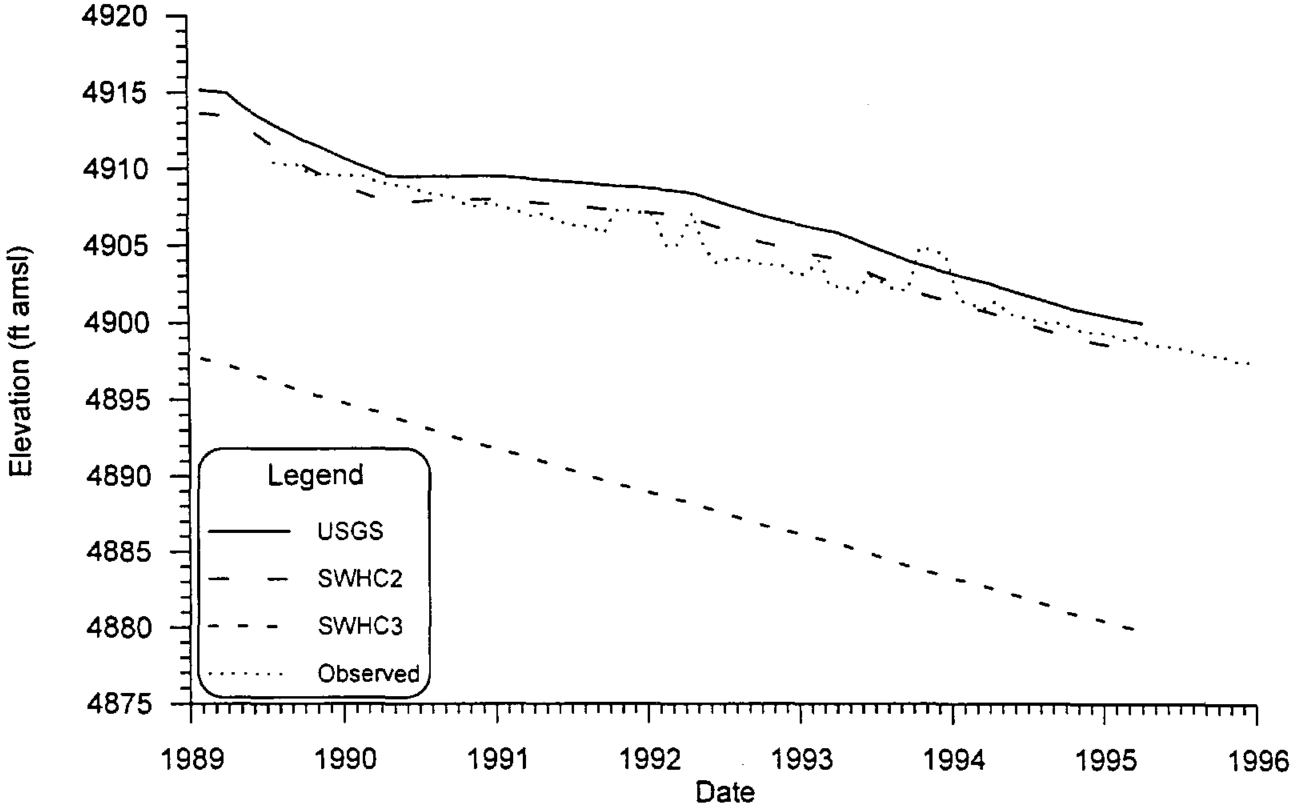

MVMWK HYDROGRAPH

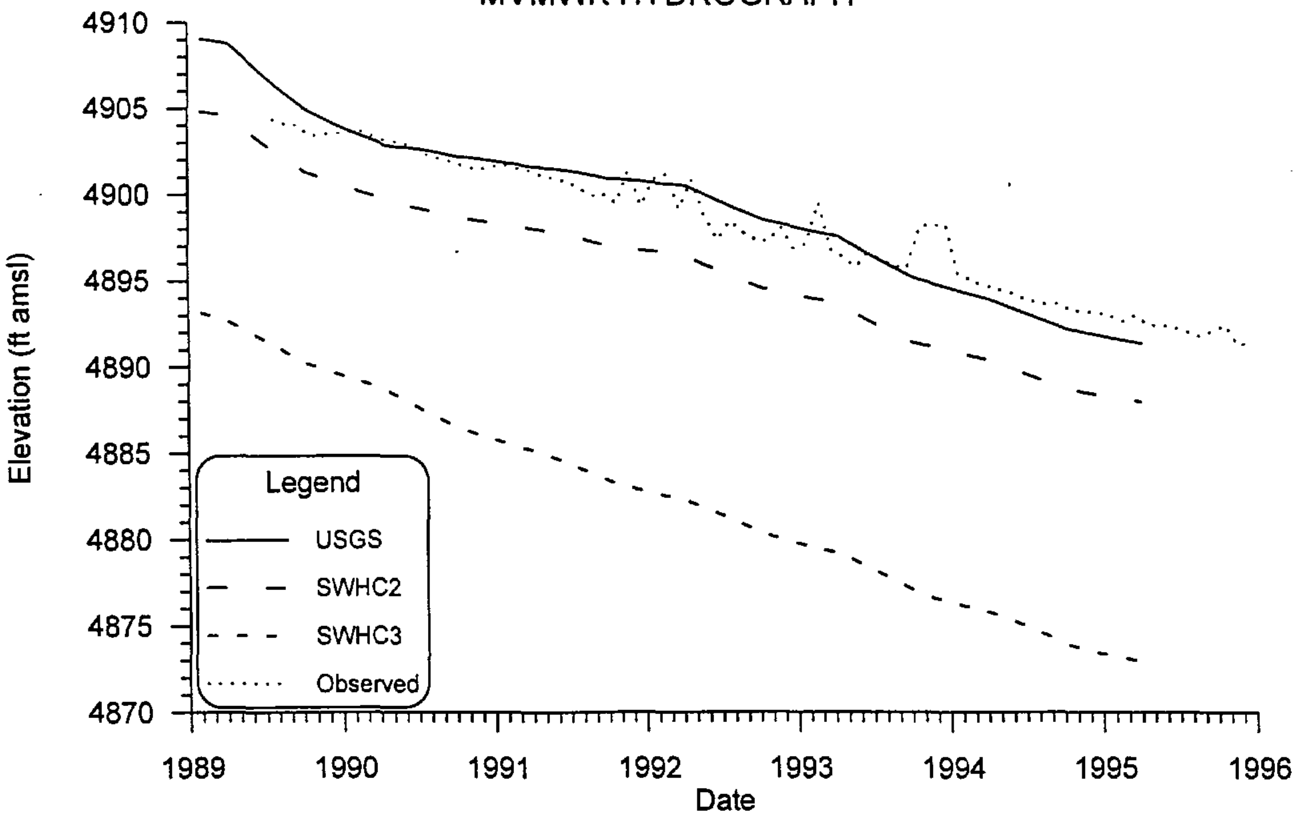

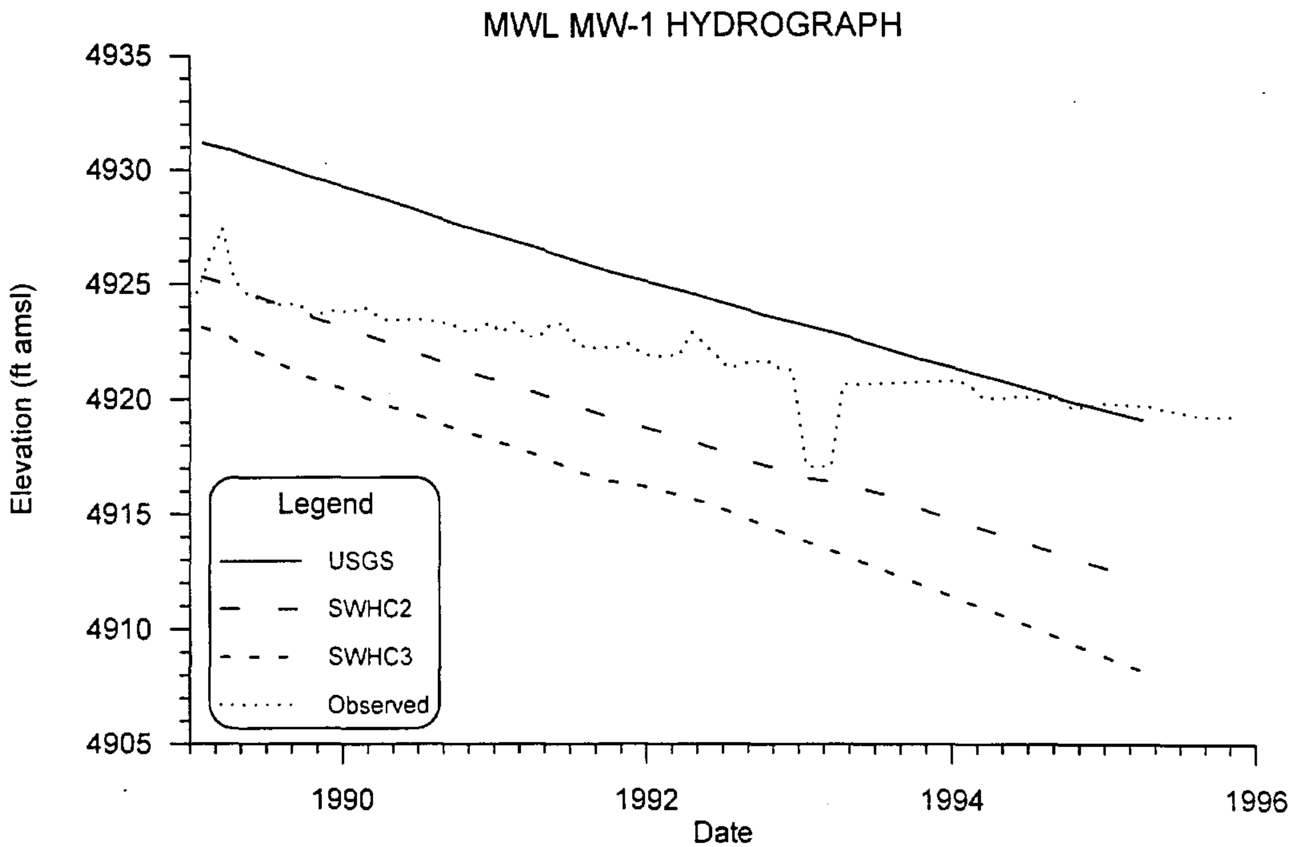
MWL MW-1 HYDROGRAPH
Elevation (ft amsl)
4935
4930
4925
4920
4915
4910
4905
1990
1992
1994
1996
Date
Legend
USGS
SWHC2
SWHC3
Observed

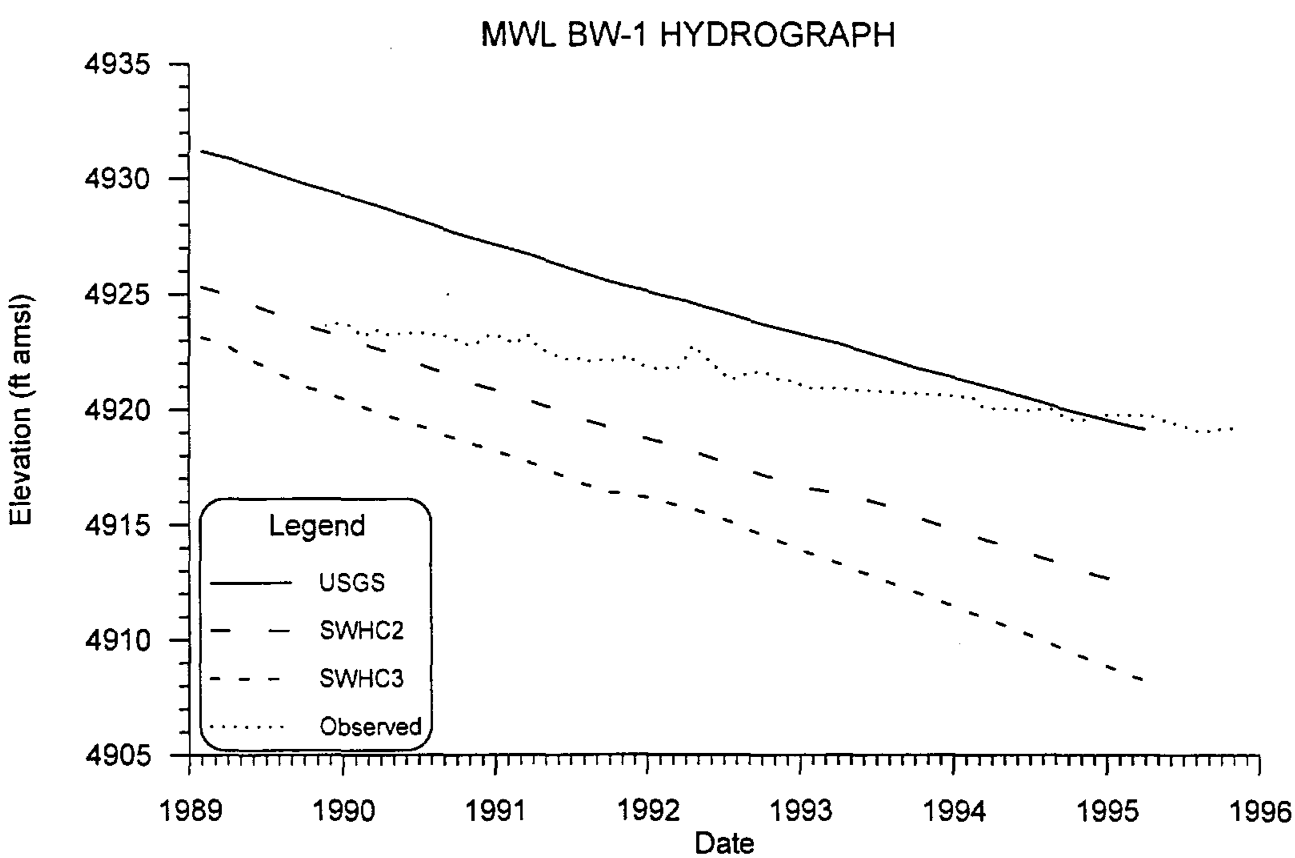
MWL BW-1 HYDROGRAPH
Elevation (ft amsl)
4935
4930
4925
4920
4915
4910
4905
1989
1990
1991
1992
1993
1994
1995
1996
Date
Legend
USGS
SWHC2
SWHC3
Observed

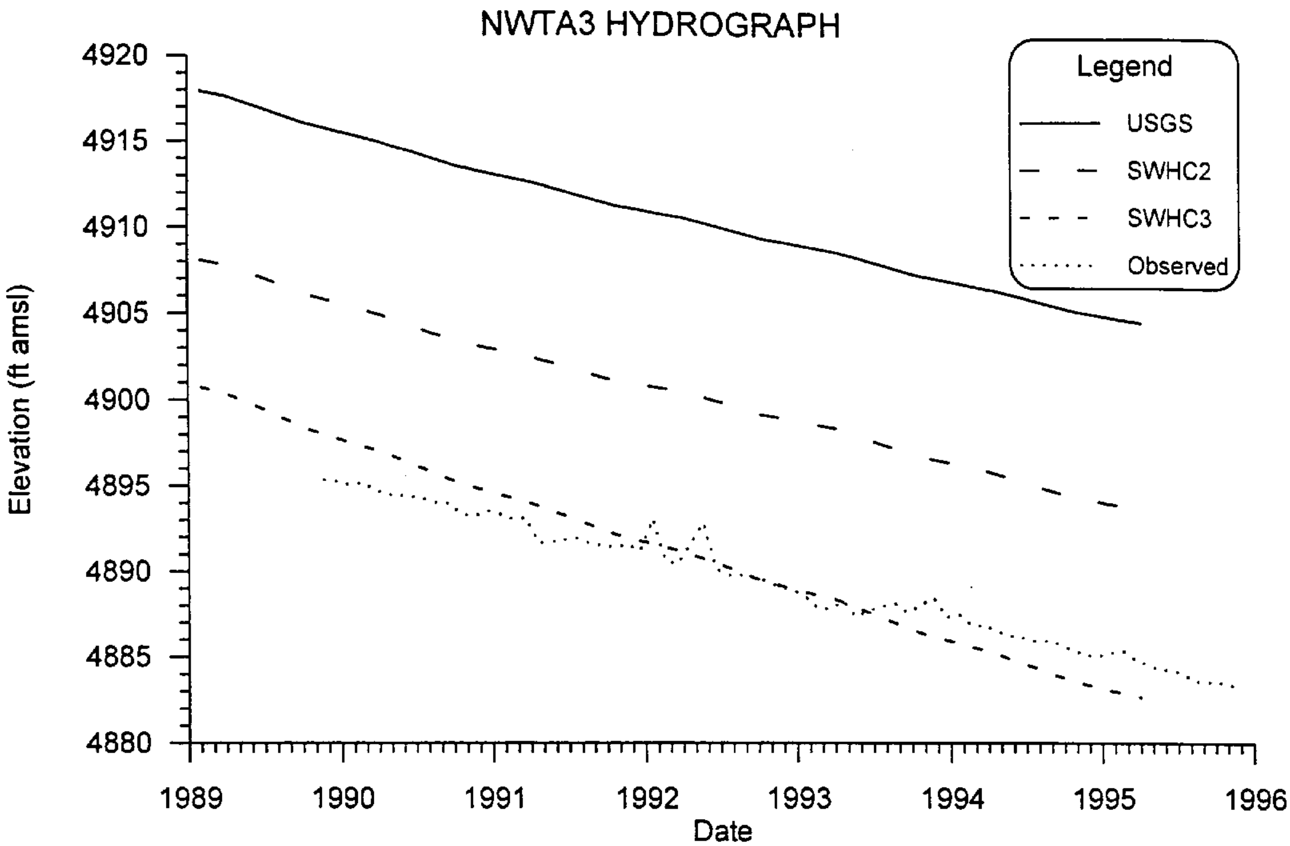
NWTA3 HYDROGRAPH
Legend
USGS
SWHC2
SWHC3
Observed
Elevation (ft amsl)
4920
4915
4910
4905
4900
4895
4890
4885
4880
1989
1990
1991
1992
1993
1994
1995
1996
Date

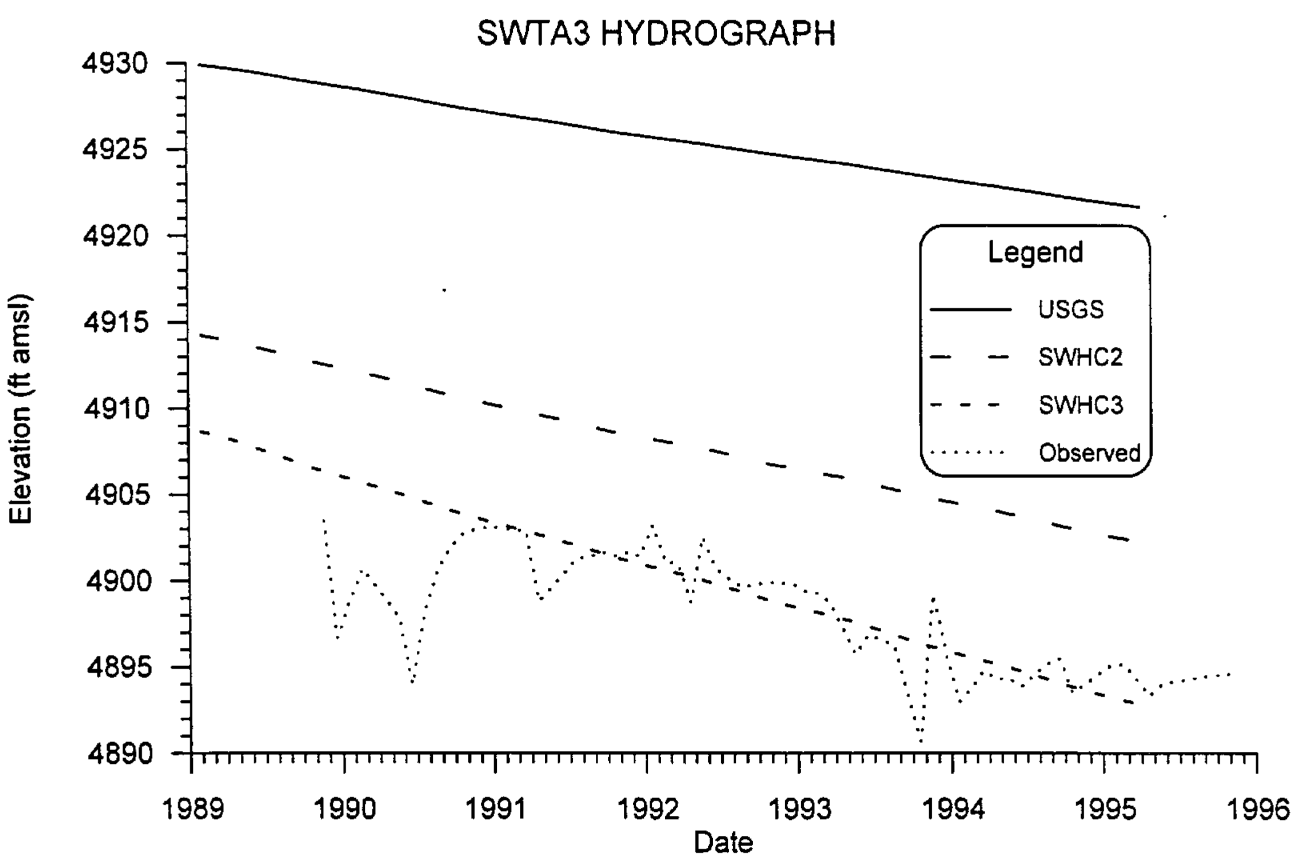
SWTA3 HYDROGRAPH
Legend
USGS
SWHC2
SWHC3
Observed
Elevation (ft amsl)
4930
4925
4920
4915
4910
4905
4900
4895
4890
1989
1990
1991
1992
1993
1994
1995
1996
Date

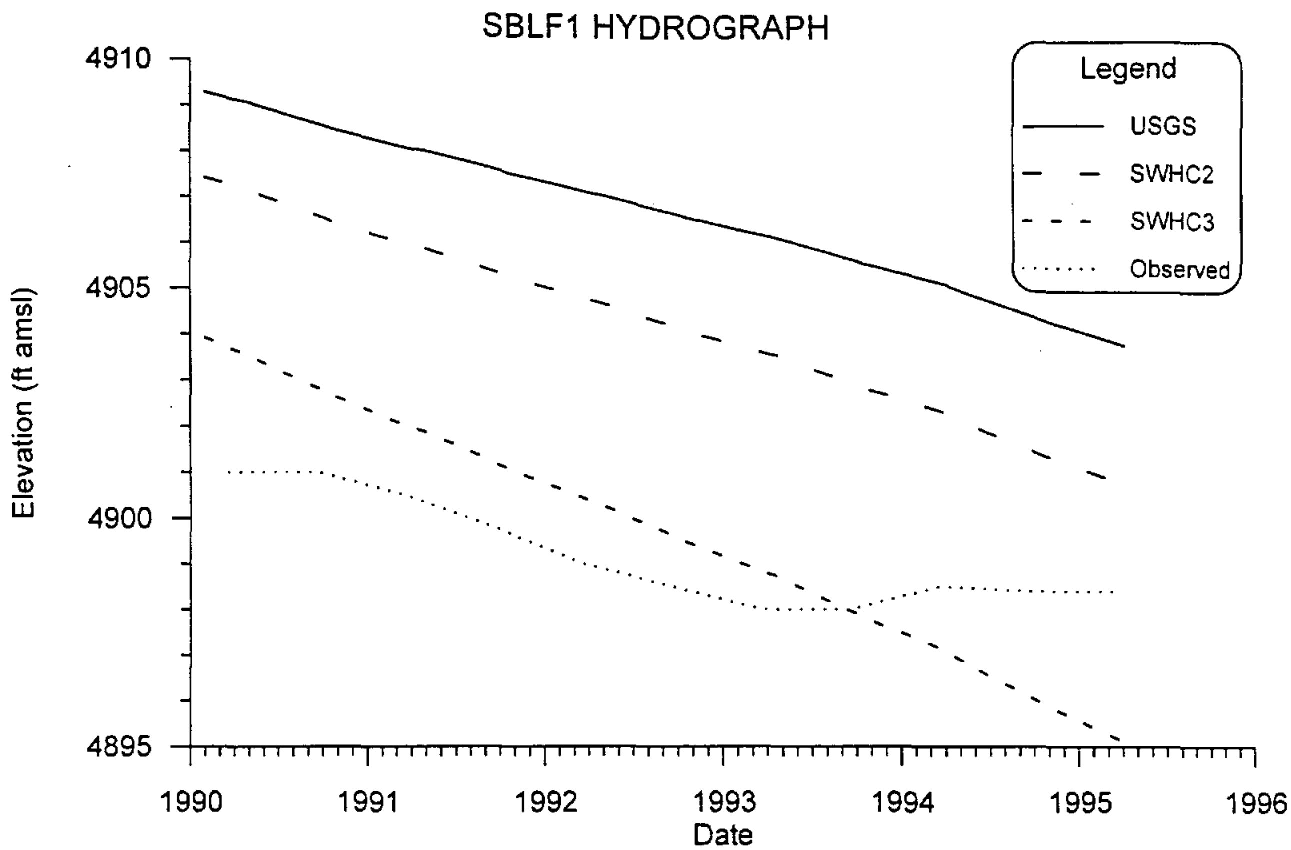
SBLF1 HYDROGRAPH
Legend
USGS
SWHC2
SWHC3
Observed
Elevation (ft amsl)
4910
4905
4900
4895
1990
1991
1992
1993
1994
1995
1996
Date

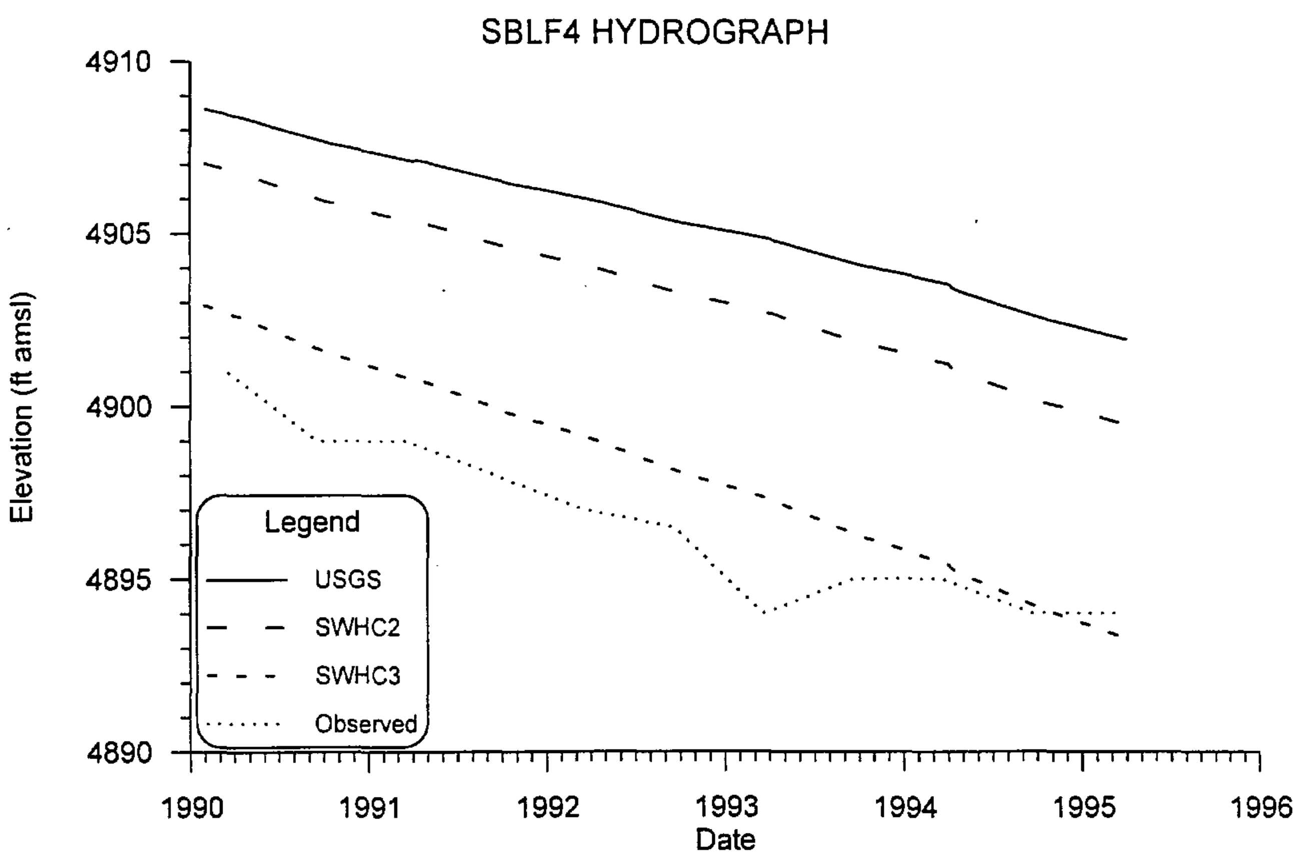
SBLF4 HYDROGRAPH
Legend
USGS
SWHC2
SWHC3
Observed
Elevation (ft amsl)
4910
4905
4900
4895
4890
1990
1991
1992
1993
1994
1995
1996
Date

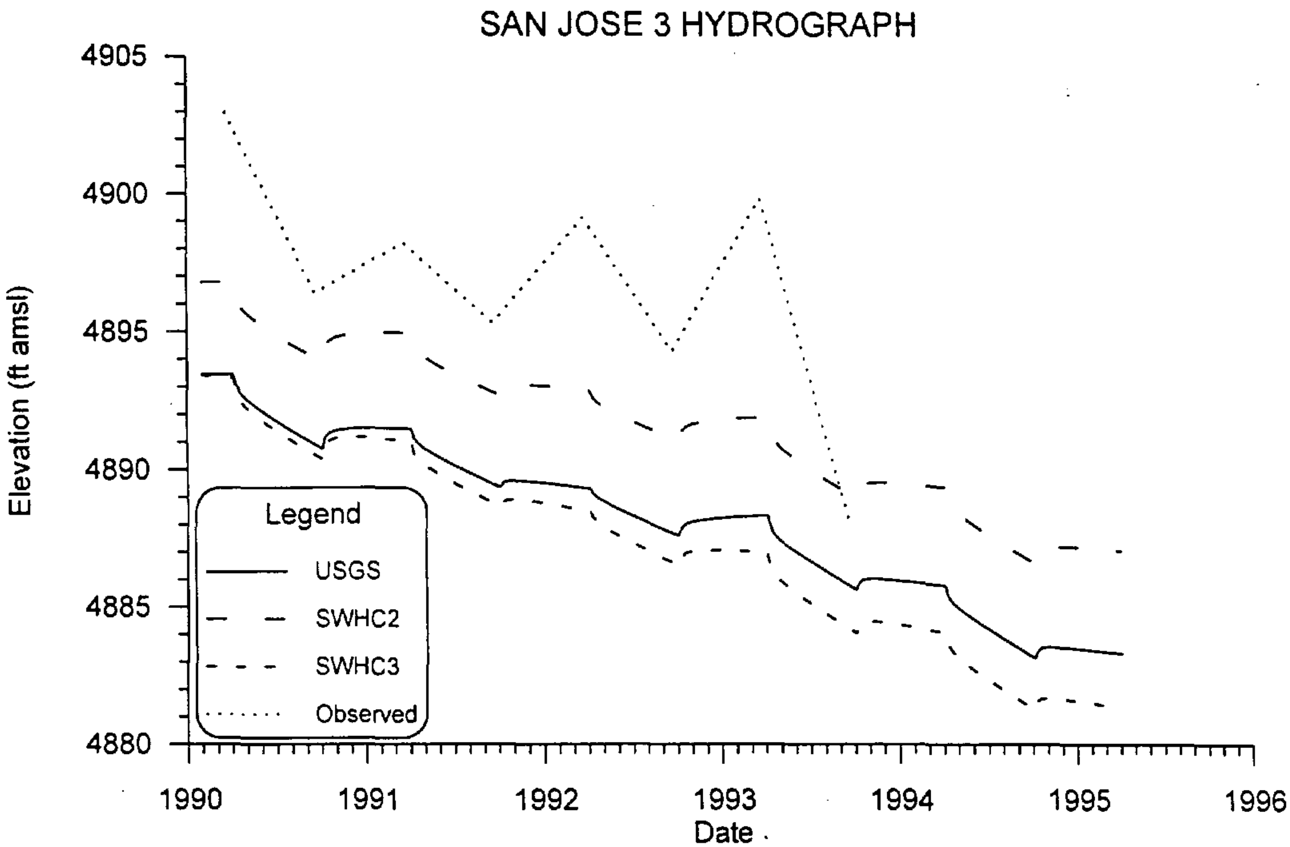
SAN JOSE 3 HYDROGRAPH
Elevation (ft amsl)
4905
4900
4895
4890
4885
4880
Legend
USGS
SWHC2
SWHC3
Observed
1990
1991
1992
1993
1994
1995
1996
Date

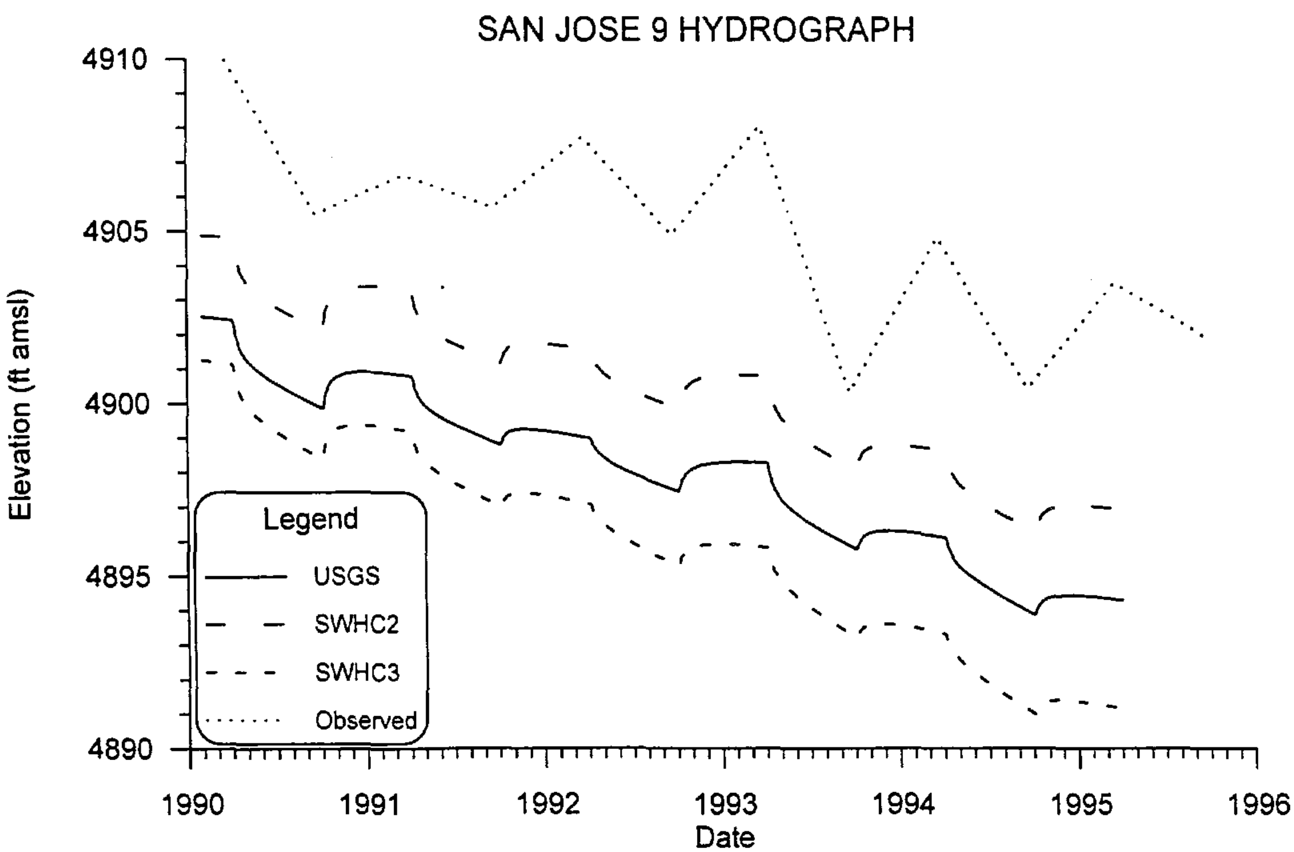
SAN JOSE 9 HYDROGRAPH
Elevation (ft amsl)
4910
4905
4900
4895
4890
Legend
USGS
SWHC2
SWHC3
Observed
1990
1991
1992
1993
1994
1995
1996
Date

PLATES

This page intentionally left blank.

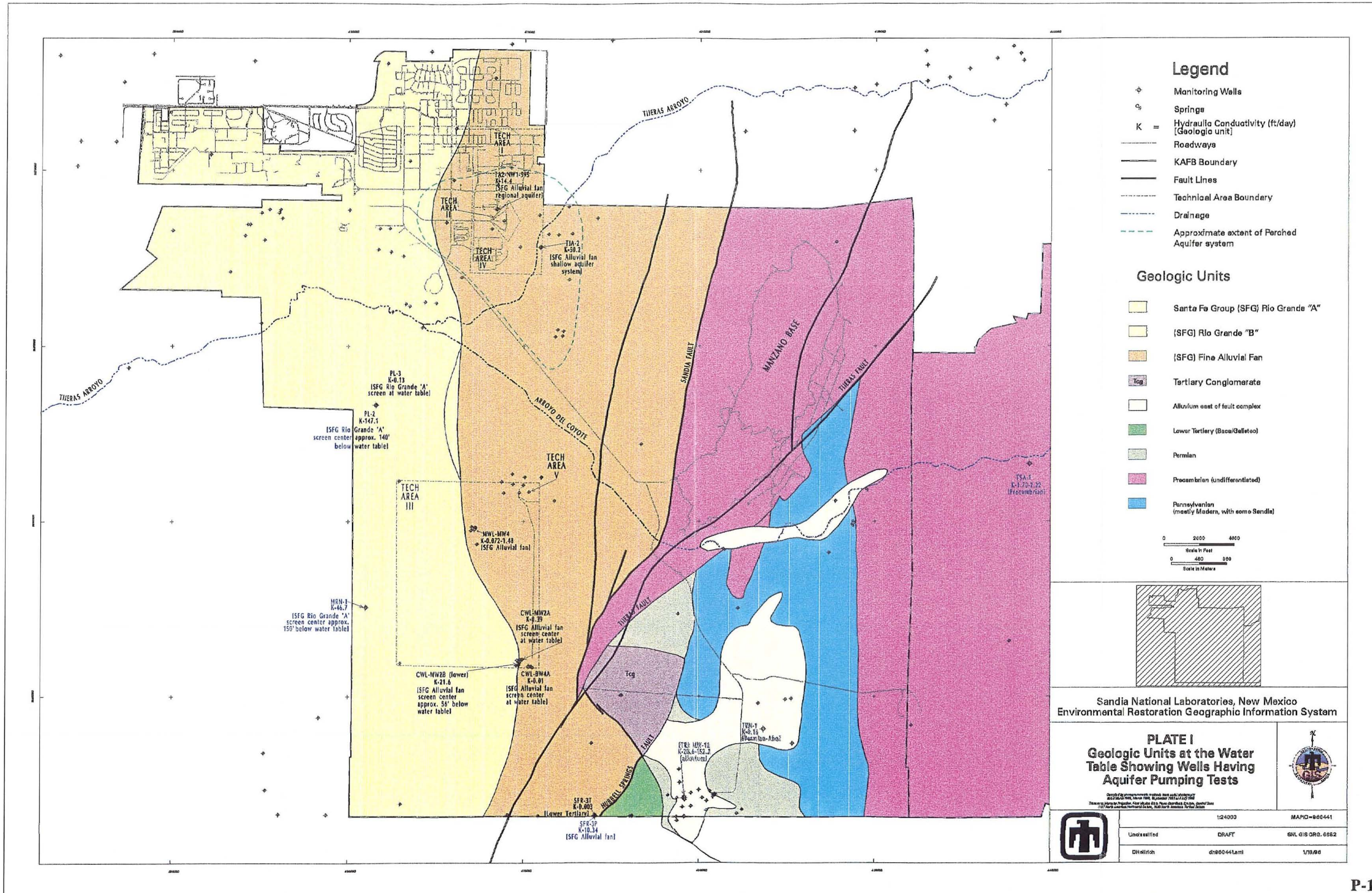

Legend
Monitoring Wells
Springs
K = Hydraulic Conductivity (ft/day) [Geologic unit]
Roadways
KAFB Boundary
Fault Lines
Technical Area Boundary
Drainage
Approximate extent of Perched Aquifer system
Geologic Units
Santa Fe Group (SFG) Rio Grande "A"
(SFG) Rio Grande "B"
(SFG) Fine Alluvial Fan
Tertiary Conglomerate
Alluvium east of fault complex
Lower Tertiary (Baca/Galisteo)
Permian
Precambrian (undifferentiated)
Pennsylvanian (mostly Madera, with some Sandia)
Tcg
TIJERAS ARROYO
ARROYO DEL COYOTE
SANDIA FAULT
MANZANO BASE
TIJERAS FAULT
HUBBELL SPRINGS FAULT
TECH AREA I
TECH AREA II
TECH AREA III
TECH AREA IV
TECH AREA V
TA2-NW1-595 K-14.4 [SFG Alluvial fan regional aquifer]
TJA-2 K-30.2 [SFG Alluvial fan shallow aquifer system]
PL-3 K-0.13 [SFG Rio Grande 'A' screen at water table]
PL-2 K-147.1 [SFG Rio Grande 'A' screen center approx. 140' below water table]
MWL-MW4 K-0.072-1.48 [SFG Alluvial fan]
MRN-1 K-46.7 [SFG Rio Grande 'A' screen center approx. 150' below water table]
CWL-MW2A K-0.39 [SFG Alluvial fan screen center at water table]
CWL-MW2B (lower) K-21.6 [SFG Alluvial fan screen center approx. 56' below water table]
CWL-BW4A K-0.01 [SFG Alluvial fan screen center at water table]
SFR-3T K-0.003 [Lower Tertiary]
SFR-3P K-10.34 [SFG Alluvial fan]
Sandia National Laboratories, New Mexico
Environmental Restoration Geographic Information System
PLATE I
Geologic Units at the Water Table Showing Wells Having Aquifer Pumping Tests
1:24000
MAPID=960441
Unclassified
DRAFT
DHeilrich
1/19/96

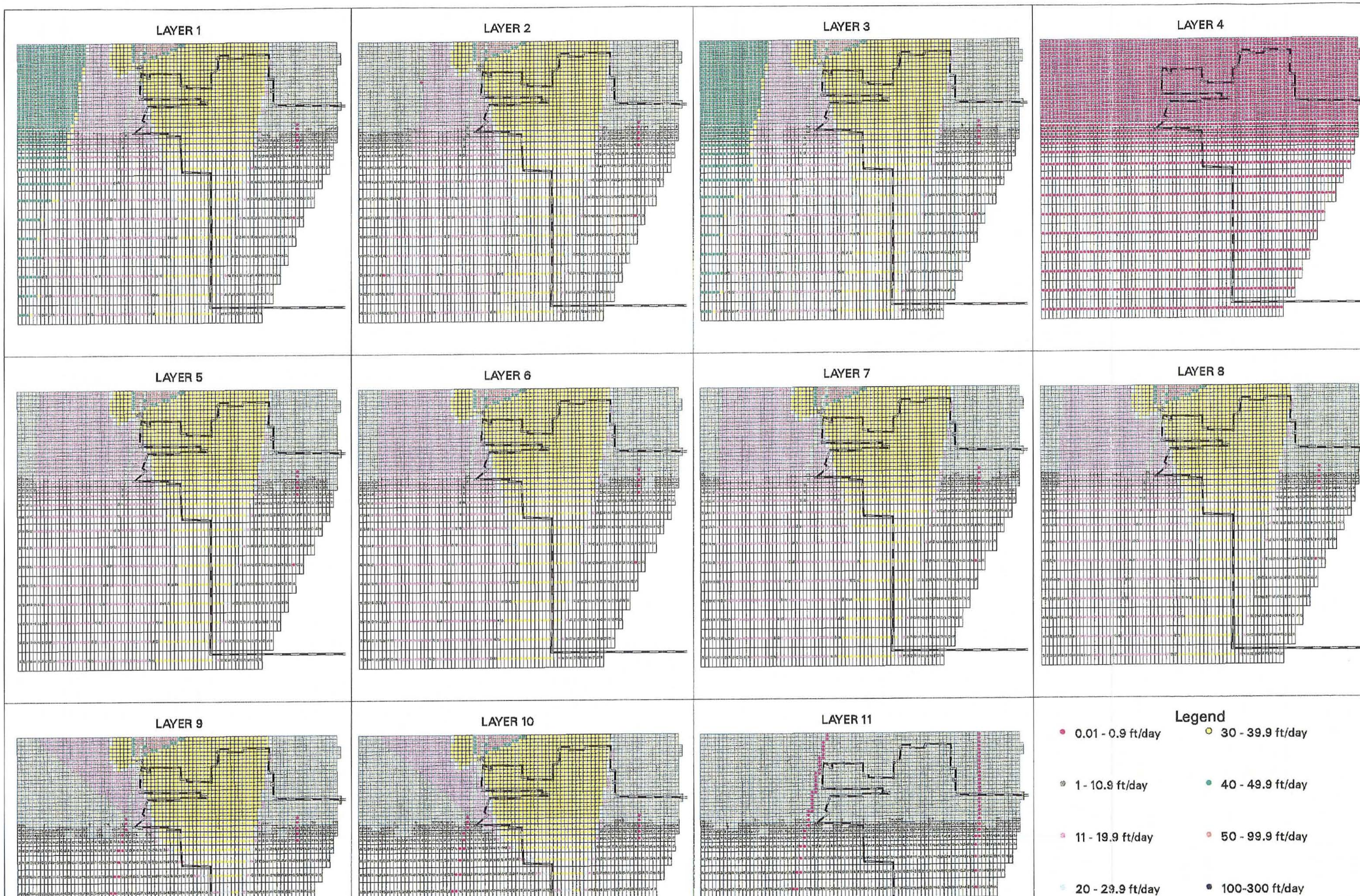

Plate 2
Horizontal Hydraulic
Conductivity Zonation
USGS Model

1"=2000'	1:24000	MAPID=970799
Unclassified	DRAFT	SNL GIS ORG. 6682
D Helfrich	ulik-ul1k.aml	10/30/97

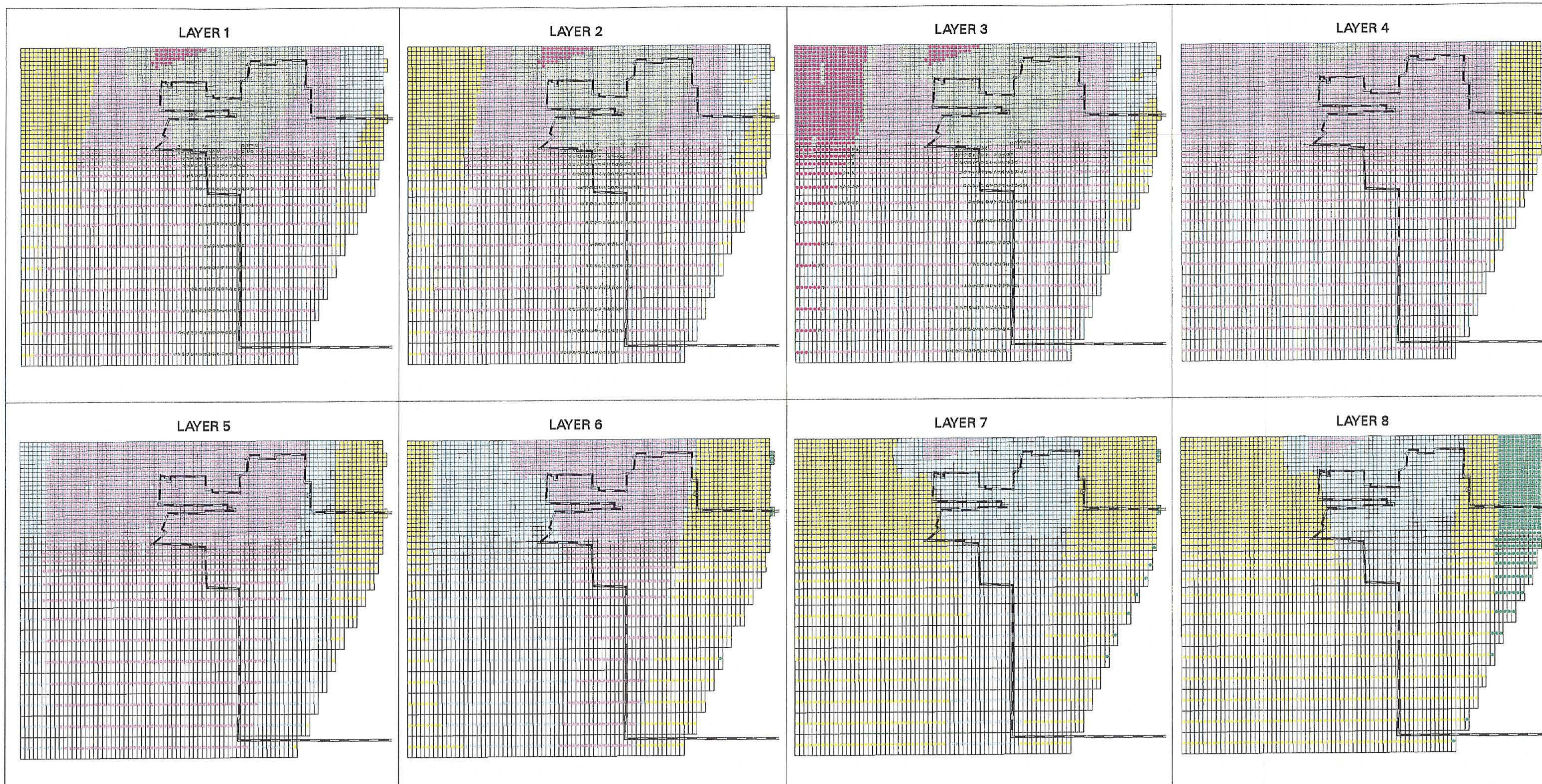

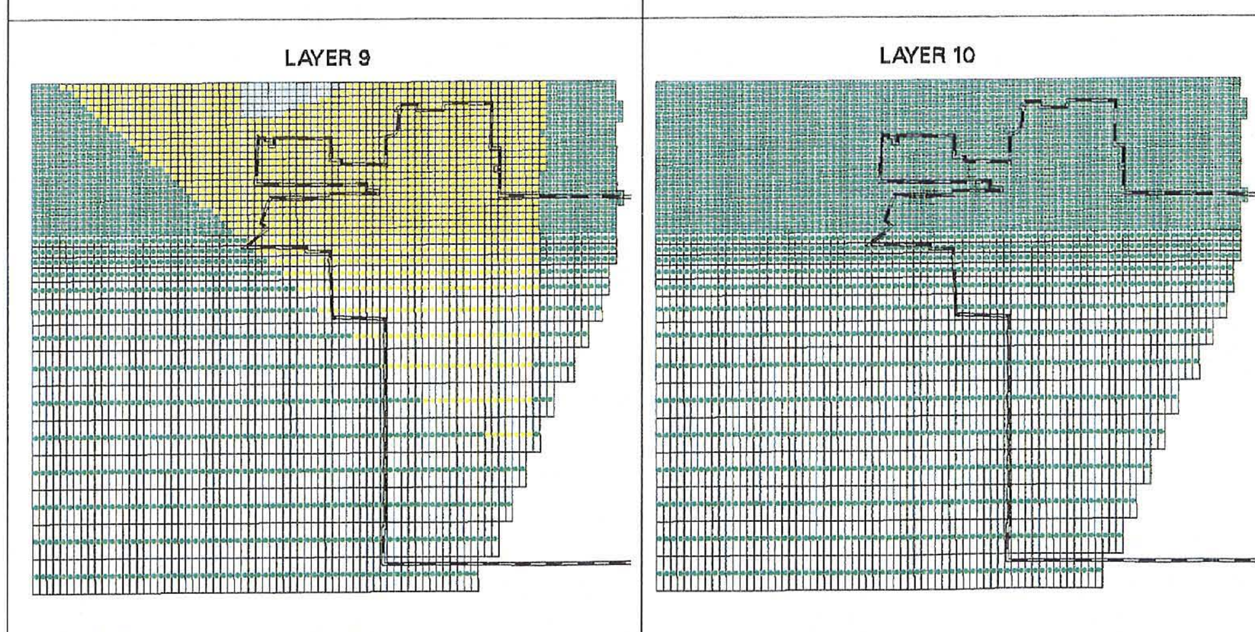

Legend

- 0.01 - .1 1/day
- 0.0001 - 0.0005 1/day
- 0.005 - 0.01 1/day
- 0.00001 - 0.0001 1/day
- 0.001 - 0.005 1/day
- 0.0005 - 0.001 1/day
- Less Than 0.00001 1/day

Plate 3
Leakance Zonation
USGS Model

1"=2000'	1:24000	MAPID=970800
Unclassified	DRAFT	SNL GIS ORG. 6682
D Helfrich	ul1l-ul10l.aml	2/12/97

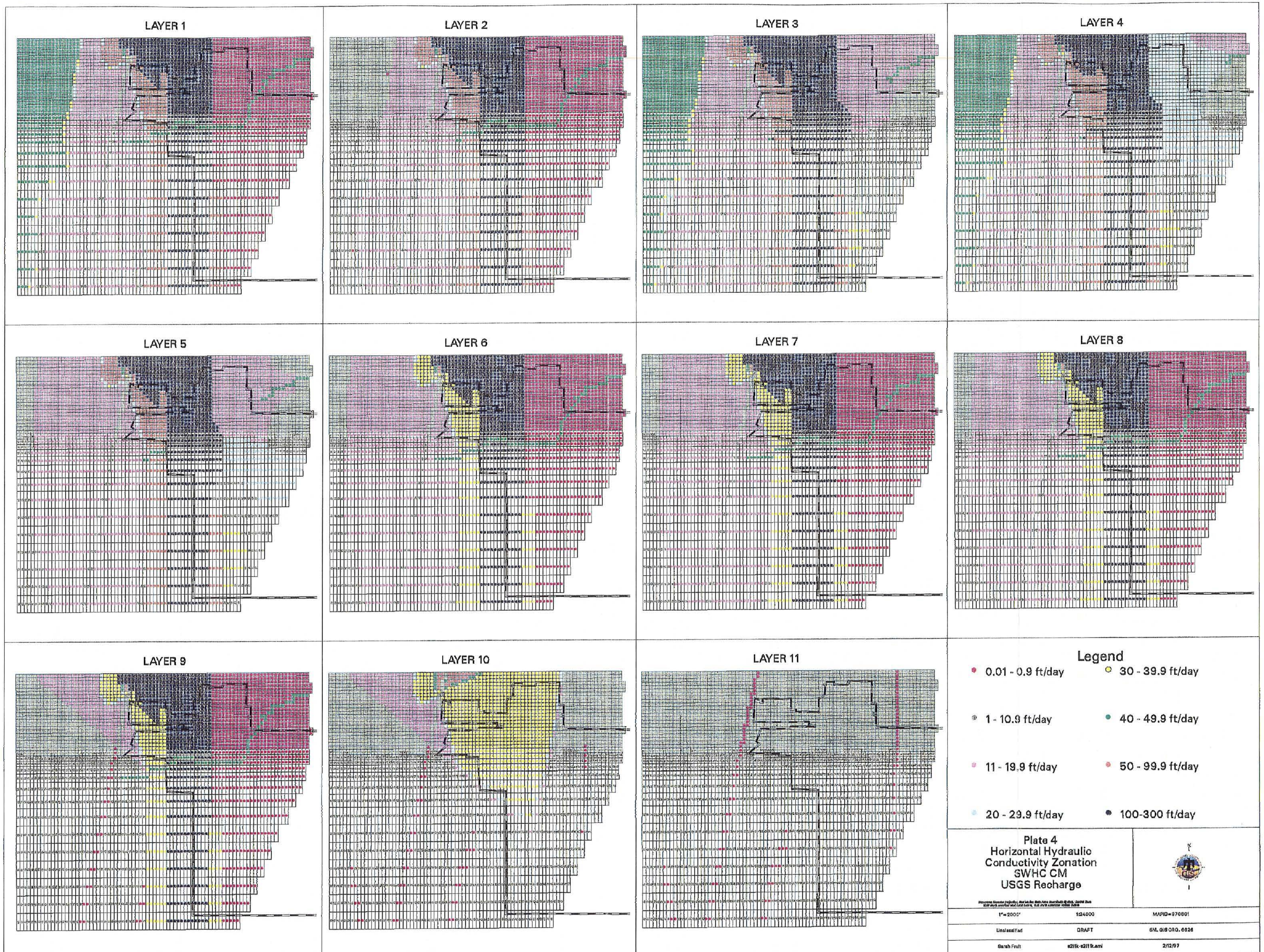

LAYER 1
LAYER 2
LAYER 3
LAYER 4
LAYER 5
LAYER 6
LAYER 7
LAYER 8
LAYER 9
LAYER 10
LAYER 11
Legend
0.01 - 0.9 ft/day
30 - 39.9 ft/day
1 - 10.9 ft/day
40 - 49.9 ft/day
11 - 19.9 ft/day
50 - 99.9 ft/day
20 - 29.9 ft/day
100-300 ft/day
Plate 4
Horizontal Hydraulic
Conductivity Zonation
SWHC CM
USGS Recharge
1"=2000'
1:24000
MAPID=970601
Unclassified
DRAFT
SNL GIS ORG. 6626
Sarah Fruit
s2l5k-s2l11k.aml
2/12/97

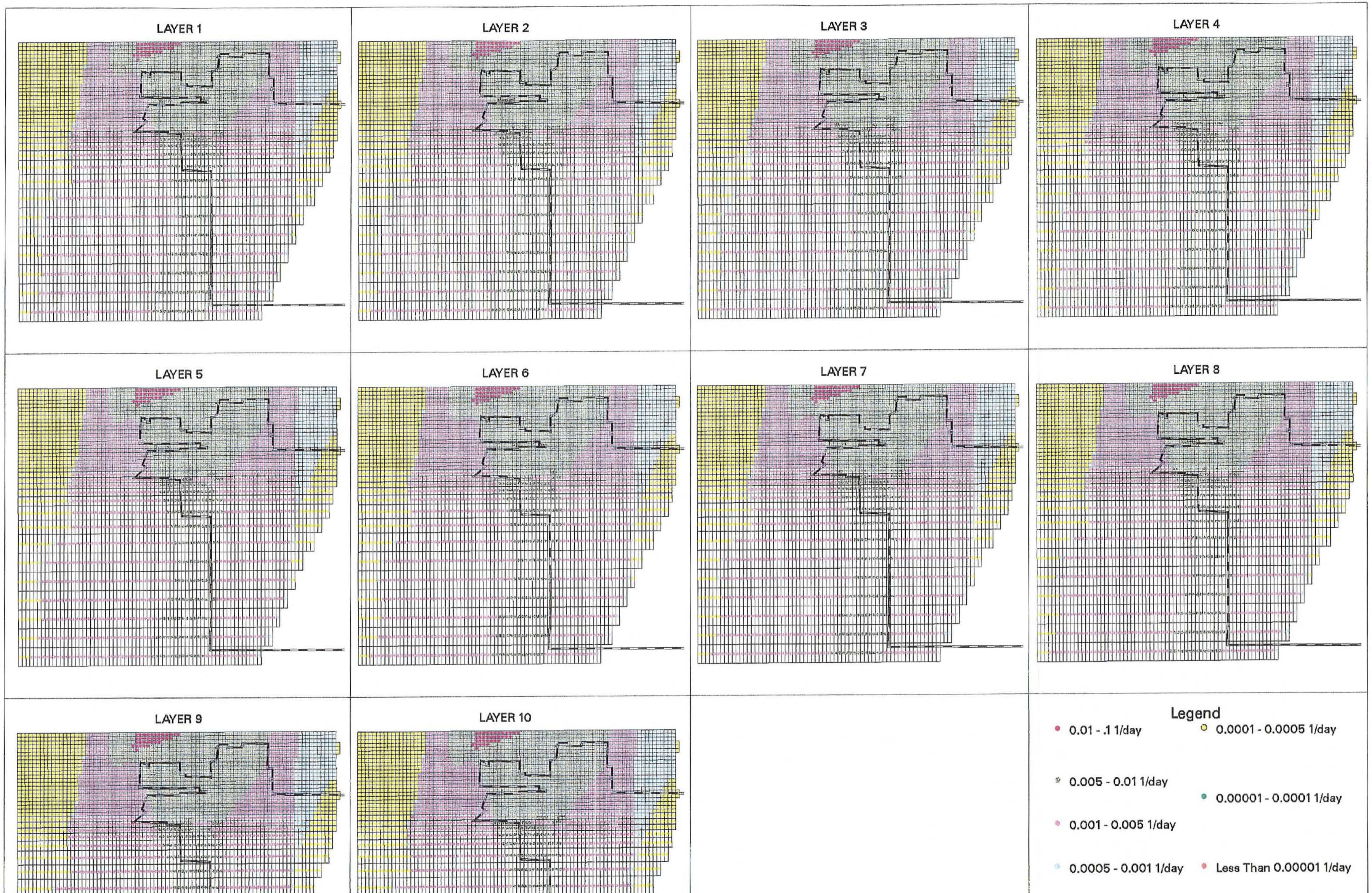

Plate 5
Leakance Zonation
SWHC CM
USGS Recharge

1" = 2000'	1:24000	MAPID=970802
Unclassified	DRAFT	SNL GIS ORG. 6682
D Helfrich	s2lll-s2l10l.aml	2/13/97

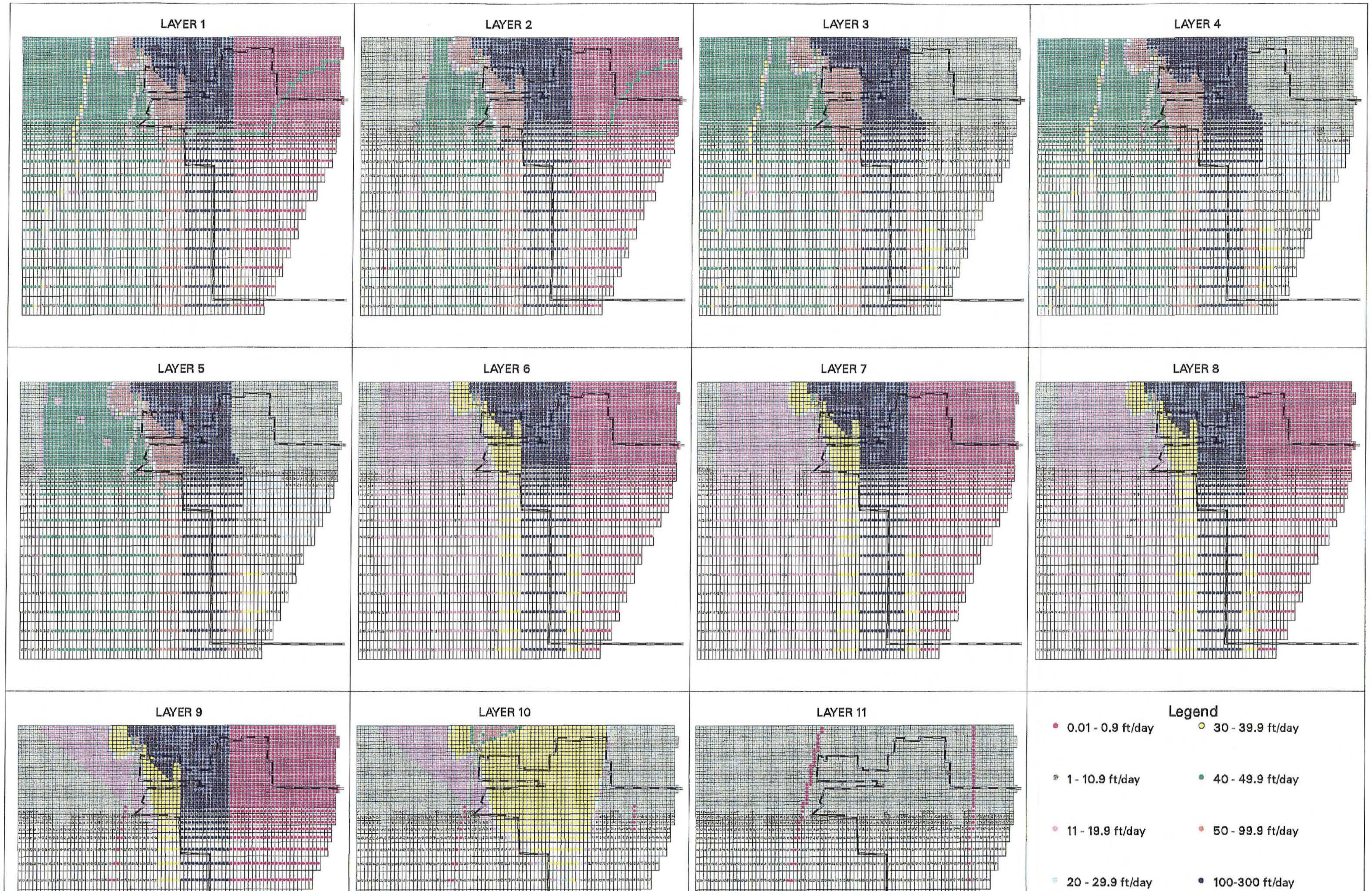

Plate 6
Horizontal Hydraulic
Conductivity Zonation
SWHC CM
SWHC Recharge

1"=2000'	1:24000	MAPID=970803
Unclassified	DRAFT	SNL GIS ORG. 6682
D Helfrich	s3l1k-s3l1k.aml	2/14/97

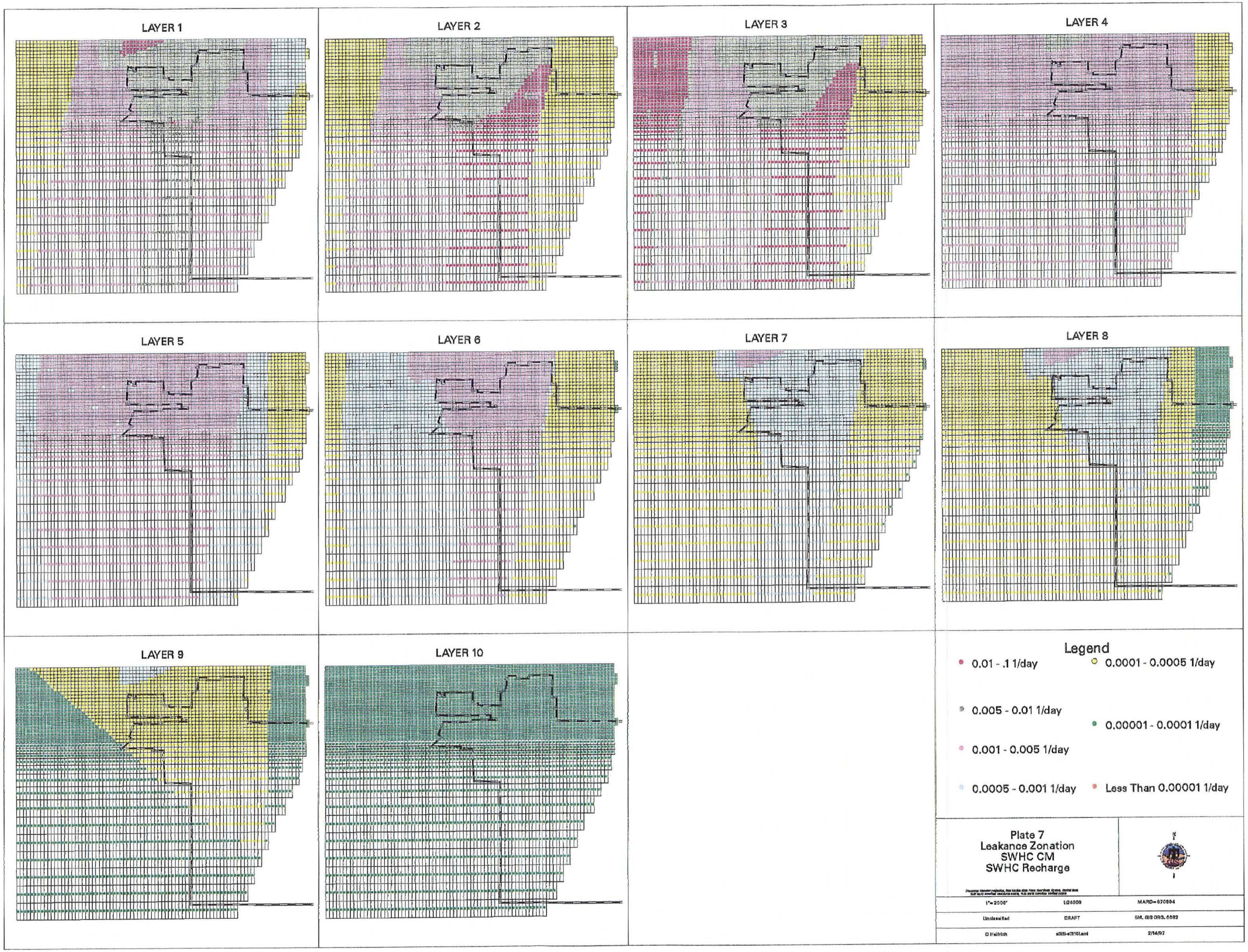
LAYER 1
LAYER 2
LAYER 3
LAYER 4
LAYER 5
LAYER 6
LAYER 7
LAYER 8
LAYER 9
LAYER 10
Legend
0.01 - .1 1/day
0.0001 - 0.0005 1/day
0.005 - 0.01 1/day
0.00001 - 0.0001 1/day
0.001 - 0.005 1/day
0.0005 - 0.001 1/day
Less Than 0.00001 1/day
Plate 7
Leakance Zonation
SWHC CM
SWHC Recharge
1"=2000'
1:24000
MAPID=970804
Unclassified
DRAFT
SML GIS ORG. 6882
D Helfrich
2/14/97

THE EFFECTS OF FAULT REPRESENTATION ON THE SNL/KAFB GROUNDWATER FLOW MODEL

Letter Report

prepared by

Greg Ruskauff, CGWP, P.Hg.
INTERA Inc.
1650 University Blvd. Ste. 300
Albuquerque, NM 87102

for

Sue Collins
Sandia National Laboratories
P.O. Box 5800, MS 1147
Albuquerque, NM 87185

AUG 15 1997

Introduction

The Sitewide Hydrogeologic Characterization Project (SWHC) constructed a three-dimensional numerical groundwater flow model in the area of Kirtland Air Force Base (KAFB) and Sandia National Laboratories (SNL) near Albuquerque, New Mexico. The purpose of the analysis was to develop a determinstic, numerical groundwater flow model of the KAFB area. The model was used to explore and test, in a quantitative fashion, the conceptual model of the hydrogeology of the area developed by the Site-Wide Hydrogeologic Characterization Project (SWHC). This model is documented in the Sitewide Hydrogeologic Characterization Project Calender Year 1995 Annual Report.

The results of the SWHC model, while acceptable given the amount of data and complexity of the groundwater flow system, did not show as pronounced a trough in water levels as the data suggested. It was postulated that the faults, which were crudely implemented in the original Albuquerque Basin model (ABM) by Kernodle et al. (1995), may have lower hydraulic conductivity than that and may be acting to compartalize the flow system and so focus drawdown from municipal pumping as to produce the trough. This letter report investigates this issue further. In addition, in the original model specific yield was noted to be an extremely sensitive parameter, the impact of which was further investigated in this analysis.

Background

The Albuquerque basin is located in the Rio Grande valley (Figure 1). Low topographic relief characterizes the floor of the basin (elevation 4,900 ft msl), with the Sandia and Manzano Mountains (elevation 10,000 ft) for the eastern basin boundary, and a gentle rise to the plains forming the western boudary (elevation 6,500 ft). The Albuquerque Basin has no distinct north and south boundaries, rather the northern limit is generally established where the Sandia and Jemez Mountains created a narrowing of the alluvial deposits. Over the last 30 million years the deep valley created by the rift has been filled in by erosion of the mountains around the basin and by sediment brought into the basin and deposited by rivers. These deposits are comprised, in part, of the late Oligocene to middle Pleistocene Age Santa Fe Group sediments, which range in thickness from 2,400 to 13,800 ft in the Albuquerque area (Hawley and Haase, 1992). The Santa Fe Group (SFG) is subdivided into Lower, Middle, and Upper units (Hawley and Haase, 1992). The Upper Santa Fe Group (USF) is the formation used almost exclusively for groundwater supply in the Albuquerque basin.

Barriers to groundwater flow exist within the SFG. Barriers include pinch out of productive material, for instance, as channel deposits grade and abut into distal alluvial deposits. Faults are also barriers to groundwater flow within the basin. Faulting within the basin can juxatapose productive aquifer units against unproductive units, abruptly terminating high hydraulic conductivity material and creating a barrier to groundwater flow. It is believed that cementation of faults has further restricted flow (Thorn et al., 1993). Preferential flow paths occur within the braided-stream deposits associated with channel deposits, and as gravel and sand deposits within alluvial fan deposits.

One issue is whether the faults on SNL/KAFB are low- or high-permeability features. Available regional data do not strongly support either interpretation. Haneberg (1995) reported on modeling results that he suggested were indicative that these faults are low-permeability features. However, the generic aquifer system Haneberg considered was for confined aquifers with head differences across faults being piezometric, rather than elevational (free surface) heads. While the SNL/KAFB-area aquifers do behave as though they are confined, most often free water is present in the aquifer materials at the height of the peizometric surface, suggesting that the aquifers are only partially confined. Sensitivity analysis (SWHC, 1997) showed that, at least with the current representation, the conceptual model is not sensitive to the faults. The faults are represented by 1 to 3 blocks of lower hydraulic conductivity material embedded in an area where hydraulic conductivity is order of magnitude or more greater. The horizontal flow barrier (HFB) package (Hsieh and Freckleton, 1992) was designed to represent features such as faults more efficiently than previously described.

Sigda (1997) performed detailed permeability measurements near and on faults in eolian sands exposed in an excavation on the western side of the Albuquerque Basin with an air minipermeameter. Even in relatively clean sands with only a few meters of slip along the fault permeability near and on the fault was reduced 3 orders of magnitude. Once the faults have been created their properties may be modified by groundwater and associated geochemical changes, but initially at least the permeability along the faults is greatly reduced.

The initial model (SWHC, 1997) was very sensitive to specific yield and specific storativity, which confirms the conceptual model which has large amounts of flow from storage (i.e., dewatering the basin) as the primary source of water pumped from the SFG. Specific yield and specific storativity were asssumed by the USGS. Comparison of SWHC Project pumping tests with the assumed value of specific storage suggests that it is reasonable. However, the model is more sensitive to specific yield than specific storage (which is reasonable since more water is released from storage per unit decline of the potentiometric surface under water table than confined conditions), which is not well characterized on SNL/KAFB or in the basin in general. A plausible range of values is 0.1 to 0.25 (Johnson, 1967) for sediments such as the SFG. Thorn et al. (1993) suggest that the true value of specific yield is closer to 0.20 than 0.10. McAda (personal communication, 1997) suggests that 0.17 is a more representative value. The ABM currently uses a specific yield of 0.15.

Approach

Vertical faults that act as barriers to flow are relatively thin compared with the typical dimensions (hundreds of feet) of a finite-difference grid block used in groundwater flow simulation. These features can be simulated in MODFLOW (McDonald and Harbaugh, 1988) by reducing model grid spacing appropriately over the domain or by using variable grid spacing in the region of the faults. An alternate approach was developed by Hsieh and Freckleton (1992) which circumvents some of the difficulties with the previous two approaches. In their approach the faults are considered to be barriers located on the boundaries of finite-difference grid blocks. The key assumption is that the width of the barrier is negligible. The sole function of the barrier is to lower the horizontal "branch conductance" (or conductance) between the two cells that it separates.

The "branch conductance" is the equivalent conductance between nodes of adjacent cells rather than conductance defined within individual cells. The horizontal conductance terms, CR along the row direction for instance, are calculated between adjacent horizontal nodes (McDonald and Harbaugh, 1988) as follows:

$$CR_{i,j+1/2,k} = 2DELC_i \frac{TR_{i,j,k}\, TR_{i,j+1,k}}{TR_{i,j,k}\, DELR_{j+1} + TR_{i,j+1,k}\, DELR_j} \qquad (1)$$

where:

TR is transmissivity in the row direction (L^2/T);
DELR is the grid width along a row (L); and
DELC is the grid width along a column (L).

Some sample calculations illustrate how the conductance calculation works. In the northern half of the model the column and row spacings are equal (not necessary for this example, but convenient) at 656.2 ft. Near the area of the Rio Grande fault aquifer transmissivity is 1,500 ft^2/d, with the block that represents the fault assigned a value of 300 ft^2/d. The conductance between an aquifer and a fault grid block is 500 ft^2/d, versus 1,500 ft^2/d between two aquifer blocks. Thus, the full effect of the fault is not achieved because of averaging although the average transmissivity is more representative of the fault.

The HFB package modifies the conductance calculation as follows:

$$CR_{i,j+1/2,k} = \frac{CR^*_{i,j+1/2,k}\, TDW_{i,j+1/2,k}\, DELC_i}{CR^*_{i,j+1/2,k} + TDW_{i,j+1/2,k}\, DELC_i} \qquad (2)$$

where:

TDW is the barrier transmissivity (or hydraulic conductivity) divided by the width of the barrier between block *i,j,k* and *i,j+1,k* (L/T), or "hydraulic characteristic",
CR* is the conductance if the barrier did not exist (L^2/T) computed from (1).
If the hydraulic characteristic is 1, 0.35, and 0.035 the conductance is reduced from 1,500 to 447, 200, and 23, respectively.

The representation of the Rio Grande and Sandia Faults was modified from discrete changes in grid block hydraulic properties to representation with the HFB package (Hsieh and Freckleton, 1992).

$$CR_{i,j+1/2,k} = 2DELC_i \frac{TR_{i,j,k}\,TR_{i,j+1,k}}{TR_{i,j,k}\,DELR_{j+1} + TR_{i,j+1,k}\,DELR_j} \tag{1}$$

where:

TR is transmissivity in the row direction (L^2/T);
DELR is the grid width along a row (L); and
DELC is the grid width along a column (L).

Some sample calculations illustrate how the conductance calculation works. In the northern half of the model the column and row spacings are equal (not necessary for this example, but convenient) at 656.2 ft. Near the area of the Rio Grande fault aquifer transmissivity is 1,500 ft^2/d, with the block that represents the fault assigned a value of 300 ft^2/d. The conductance between an aquifer and a fault grid block is 500 ft^2/d, versus 1,500 ft^2/d between two aquifer blocks. Thus, the full effect of the fault is not achieved because of averaging although the average transmissivity is more representative of the fault.

The HFB package modifies the conductance calculation as follows:

$$CR_{i,j+1/2,k} = \frac{CR^*_{i,j+1/2,k}\,TDW_{i,j+1/2,k}\,DELC_i}{CR^*_{i,j+1/2,k} + TDW_{i,j+1/2,k}\,DELC_i} \tag{2}$$

where:

TDW is the barrier transmissivity (or hydraulic conductivity) divided by the width of the barrier between block *i,j,k* and *i,j+1,k* (L/T), or "hydraulic characteristic",
CR* is the conductance if the barrier did not exist (L^2/T) computed from (1).
If the hydraulic characteristic is 1, 0.35, and 0.035 the conductance is reduced from 1,500 to 447, 200, and 23, respectively.

The representation of the Rio Grande and Sandia Faults was modified from discrete changes in grid block hydraulic properties to representation with the HFB package (Hsieh and Freckleton, 1992).

The PEST (for **P**arameter **EST**imation) code by Watermark Computing, Inc. version 1.08 was used in conjunction with MODFLOW to perform parameter estimation. For more details see the PEST User's Guide (Watermark, 1994).

The model parameters that were estimated included mountain front recharge near Manzano Base, HFB hydraulic characteristic, and specific yield. Mountain front recharge was added since a branch of the Sandia Fault separates the near mountain front region from the rest of the area, and it would not be correct to leave recharge fixed at the original value since the fault representation was being changed. The few observation wells in this area (mainly KAFB-09) were overpredicted by the original model and poorly fit. Recharge was originally represented as changing with each stress period (basically winter and summer). This was simplified to a single constant representation. This is justified by the fact that the groundwater potentiometric data in the area show little seasonal trends.

Results and Conclusions

A variety of simulations were conducted, but only a limited number are presented here. For the first simulation specific yield was set at 0.15 (the ABM base value), mountain-front recharge at 4.5×10^{-3} ft/d, leakance of the area representing axial channel deposits was doubled from the ABM value to 7×10^{-3} d^{-1}, and HFB hydraulic characteristics were 3.6, 0.23, 0.36, for HFB groups 1, 2, and 3 (see Figure 2), respectively. Leakance had remained unchanged from the ABM value in the original SWHC model even though the hydraulic conductivity of the axial channel deposits increased from 30 (in the ABM) to 210 ft/day (in the SWHC model). Leakance was increased to compensate for the change in vertical flow properties implied by this change. Another simulation with the same input parameters but specific yield of 0.18 was used. Figure 3 shows the original and the revised simulation results.

The sensitivity of the model to HFB hydraulic characteristics was tested by reducing fault hydraulic conductivity 2 orders of magnitude (Figure 4). The basic shape of the flow field remains about the same, although very near the faults sharp changes in simulated potentials can be seen by the sudden bending, or kinking, in the contour lines. An additional sensitivity run was made where the hydraulic conductivity of the ancestral Rio Grande axial channel deposits was increased from 210 to 420 ft/day (Figure 4). This change did amplify the trough somewhat, but is still insufficient to replicate it very well.

Overall the effects of changing the fault representation and lowering fault hydraulic conductivity are minor, and consist of somewhat elongating the flow field in the north-south direction. These results do not necessarily refute the possibility that the faults have much lower hydraulic conductivity than previously used in the model by Kernodle et al. (1995), and influence the flow field more. There are two reasons for this. The first reason is that Pine (1995) (in a synthetic analysis of the effects of faults on groundwater flow) showed that the ability to identify the effects of faults is compromised by inadequate well coverage. In particular, observation wells need to be located very close to faults, and Pine suggested that as much independent geologic information as possible be used when locating observation wells near faults. The second reason is related to how the SWHC submodel area was removed from the Albuquerque Basin Model of Kernodle et al. (1995). The northern, southern, and western boundaries of the SWHC model are artificial, that is, they are not the natural hydrologic boundaries. Given the scale of the basin and its model this was a necessary compromise for the model to be cost-effectively applied to the area. The northern, southern, and western boundaries are specified-flow boundaries, which are very "active" boundaries in that the specified amount of water *must* be taken from or put into the model regardless of the flow field (see Franke and Reilly [1987] for further discussion). Thus, to some extent, the flow field is artificially controlled by the boundary conditions, which were derived from the ABM which does not have as high a hydraulic conductivity for the axial channel deposits as the SWHC model.

References

Franke, O.L. and T.E. Reilly, 1987. The effects of boundary conditions on the steady-state response of three hypothetical ground-water systems-results and implications of numerical experiments, U.S. Geological Survey Water-Supply Paper 2315, Denver, CO.

Haneberg, W.C., 1995, Steady state groundwater flow across idealized faults, Water Resources Research, Vol. 31, No. 7, pp. 1815-1820, July 1995.

Hawley, J.W., and C.S. Hasse (eds.), 1992. Hydrogeologic Framework of the Northern Albuquerque Basin, New Mexico Bureau of Mines and Mineral Resources Open-File Report 387.

Hsieh, P.A. and J.R. Freckleton, 1992. Documentation of a Computer Program to Simulate Horizontal-Flow Barriers using the U.S. Geological Survey's Modular Three-Dimensional Finite-Difference Ground-Water Flow Model, U.S. Geological Survey Open-File Report 92-477, Sacramento, California.

Kernodle, J.M., McAda, D.P., and C.R. Thorn, 1995. "Simulation of ground-water flow in the Albuquerque Basin, Central New Mexico, 1901-1994, with projections to 2020", U.S. Geological Survey, Water-Resources Investigations Report 94-4251.

McDonald, M. and A. Harbaugh, 1988. A modular three-dimensional finite-difference ground water flow model, Techniques of Water-Resources Investigations 06-A1, U.S. Geological Survey, Reston, VA.

Pine, Robert A., 1995. Modeling Groundwater Flow in the Vicinity of Dip-Slip Faults, Master's Thesis, New Mexico Institute of Mining and Technology, Socorro, New Mexico.

Sigda, John. 1997. Master's Thesis, New Mexico Institute of Mining and Technology, Socorro, New Mexico.

SWHC, 1997. Evaluation of groundwater flow and hydrogeologic conceptual model Kirtland Air Force Base, Albuquerque Basin, New Mexico, Sandia National Laboratories.

Watermark Computing, Inc., 1994. PEST User's Guide, version 1.08.

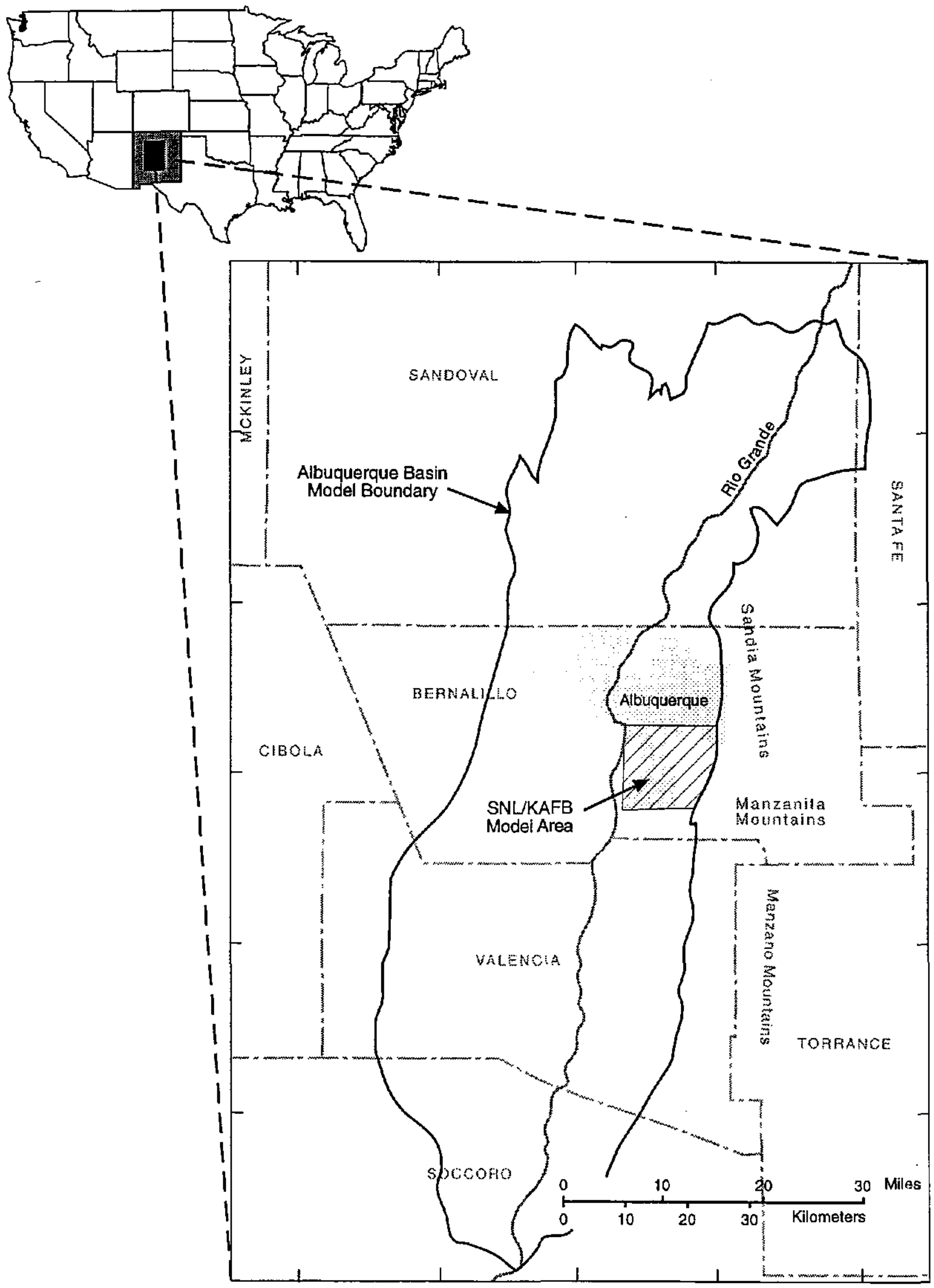

Figure 1. Albuquerque basin map with SNL/KAFB area.

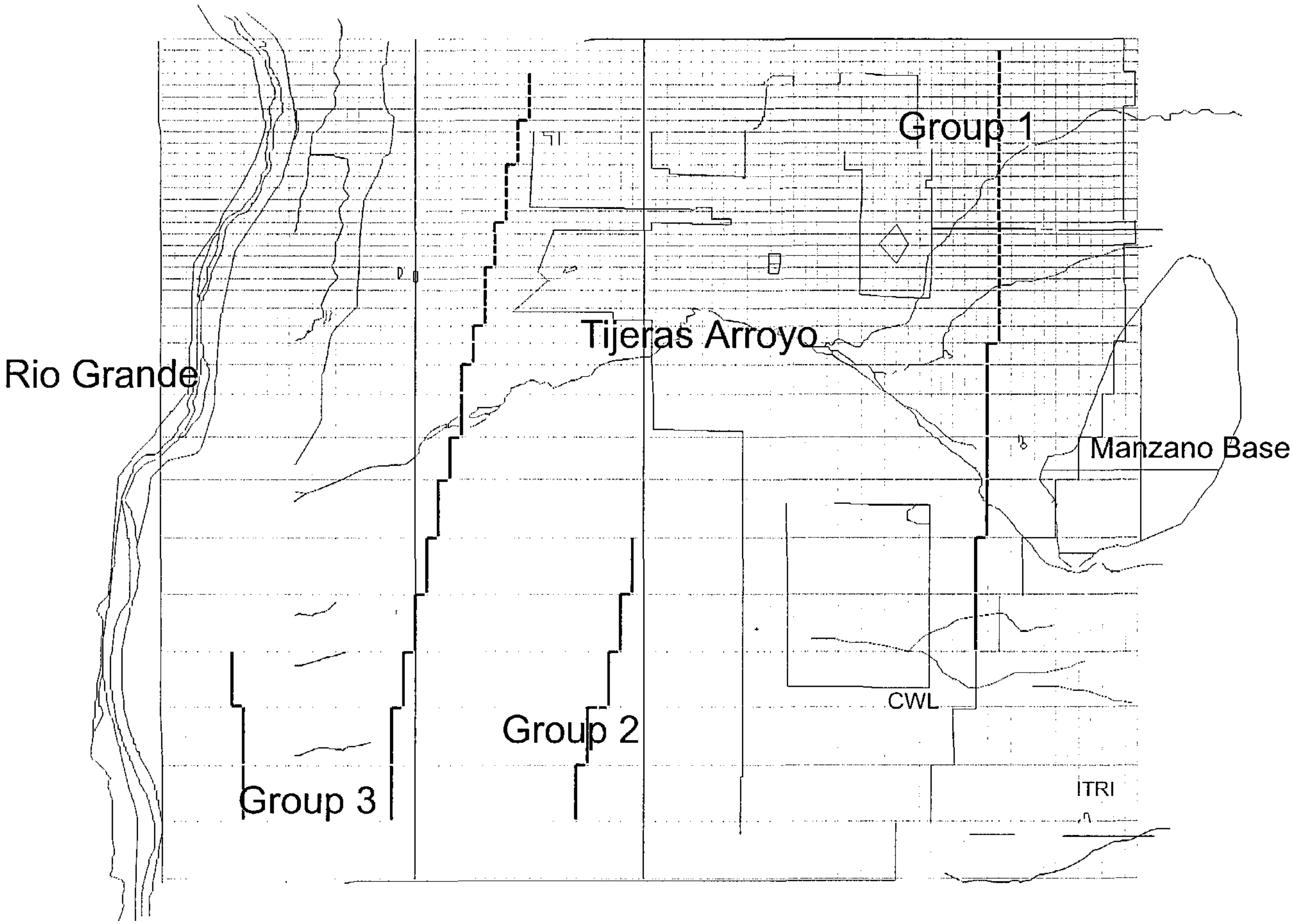

Figure 2. Grid and Location of HFBs

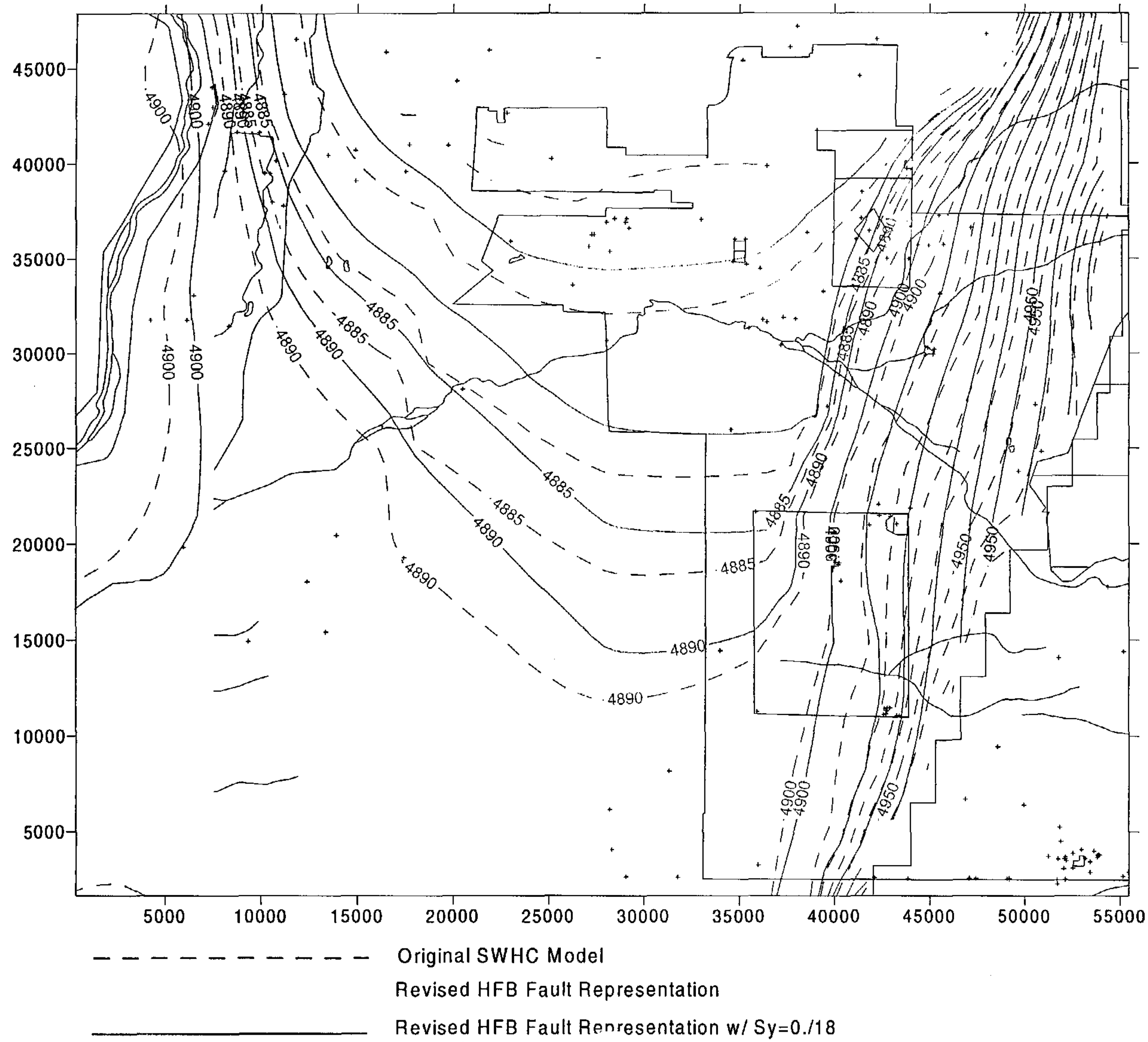

Figure 3. Comparsion of Simulaιed Flow Fields, March 1995, Layer 4

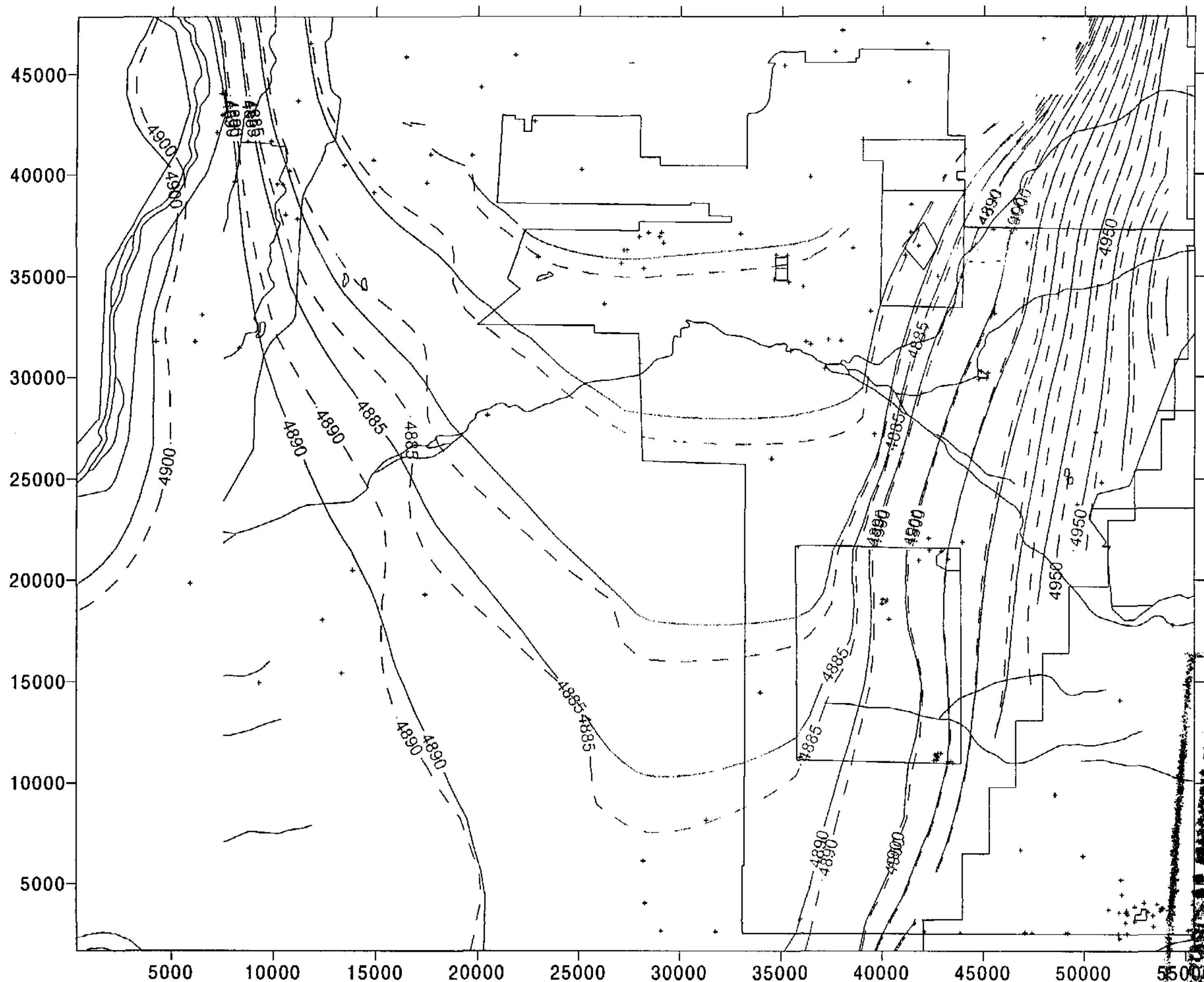

Revised HFB Fault Representation

Revised HFB Fault Representation, 2 order magnitude reduction in Fault Permeability

Revised HFB Fault Representation, 2x Increase in ARG Hydraulic Conductivity

Figure 4. Comparison of Simulated Flow Fie. ., March 1995, Layer 4, Sensitivity Analysis